Holography and thermodynamics of 5D dilaton-gravity

Published by IOP Publishing for SISSA

Received: *March 3, 2009*
Accepted: *April 20, 2009*
Published: *May 8, 2009*

Holography and thermodynamics of 5D dilaton-gravity

U. Gürsoy,[a] **E. Kiritsis,**[b,1] **L. Mazzanti**[c] **and F. Nitti**[d]

[a] *Institute for Theoretical Physics, Utrecht University, Leuvenlaan 4, 3584 CE Utrecht, The Netherlands*
[b] *Department of Physics, University of Crete, 71003 Heraklion, Greece*
[c] *CPHT, Ecole Polytechnique, CNRS, 91128, Palaiseau, France*
[d] *APC, Université Paris 7, Bâtiment Condorcet, F-75205, Paris Cedex 13, France*

E-mail: U.Gursoy@uu.n, kiritsis@physics.uoc.gr, liuba.mazzanti@cpht.polytechnique.fr, nitti@apc.univ-paris7.fr

Abstract: The asymptotically-logarithmically-AdS black-hole solutions of 5D dilaton gravity with a monotonic dilaton potential are analyzed in detail. Such theories are holographically very close to pure Yang-Mills theory in four dimensions. The existence and uniqueness of black-hole solutions is shown. It is also shown that a Hawking-Page transition exists at finite temperature if and only if the potential corresponds to a confining theory. The physics of the transition matches in detail with that of deconfinement of the Yang-Mills theory. The high-temperature phase asymptotes to a free gluon gas at high temperature matching the expected behavior from asymptotic freedom. The thermal gluon condensate is calculated and shown to be crucial for the existence of a non-trivial deconfining transition. The condensate of the topological charge is shown to vanish in the deconfined phase.

Keywords: Gauge-gravity correspondence, Black Holes

ArXiv ePrint: 0812.0792

[1] http://hep.physics.uoc.gr/~kiritsis/

doi:10.1088/1126-6708/2009/05/033

JHEP05(2009)033

Contents

JHEP05(2009)033

JHEP05(2009)033

1 Introduction and summary

In the past decade we have witnessed a rebirth of theoretical efforts to address the strong coupling problem in gauge theories. The tool has been the large-N_c expansion but a new twist has emerged, whereby the relevant dual string theories live in an appropriately curved higher dimensional space-time.

The prototype example has been the AdS/CFT correspondence as exemplified by the (well studied by now) duality of $\mathcal{N} = 4$ super Yang-Mills theory and IIB string theory on $AdS_5 \times S^5$ [1–3]. Further studies focused on providing examples that are closer to real world QCD, [4, 5]. It is fair to say that we now have a good holographic understanding of phenomena like confinement, chiral symmetry and its breaking as well as several related issues. The finite temperature dynamics of gauge theories, has a natural holographic counterpart in the thermodynamics of black-holes on the gravity side, and the thermal properties of various holographic constructions have been widely studied, [4, 6–10], exhibiting the holographic version of deconfinement and chiral restoration transitions.

The simplest top-down string theory model of QCD involves D_4 branes with supersymmetry breaking boundary conditions for fermions [4], as well as a flavor sector that involves pairs of $D_8 - \overline{D}_8$ probe branes inserted in the bulk, [11]. The qualitative thermal properties of this model closely mimic what we expect in QCD, [7]. Although such theories reproduced the qualitative features of IR QCD dynamics, they contain Kaluza-Klein modes, not expected in QCD, with KK masses of the same order as the dynamical scale of the gauge theory. Above this scale the theories deviate from QCD. Therefore, although the qualitative features of the relevant phenomena are correct, a quantitative matching to real QCD is difficult.

Despite the hostile environment of non-critical theory, several attempts have been made to understand holographic physics in lower dimensions in order to avoid the KK contamination, based on two-derivative gravitational actions, [12]. Indeed, large N QCD is expected to be described by a 5-dimensional theory. The alternative problem in non-critical theories is that curvatures are of string scale size and the truncation of the theory to the zero mode sector is subtle and may be misleading.

A different and more phenomenological bottom-up approach was developed and is now known as AdS/QCD. The original idea described in [13] was successfully applied to the meson sector in [14], and its thermodynamics was analyzed in [8, 15]. The bulk

JHEP05(2009)033

gravitational background consists of a slice of AdS_5, and a constant dilaton. There is a UV and an IR cutoff. The confining IR physics is imposed by boundary conditions at the IR boundary. This approach, although crude, has been partly successful in studying meson physics, despite the fact that the dynamics driving chiral symmetry breaking must be imposed by hand via IR boundary conditions. Its shortcomings however include a glueball spectrum that does not fit very well the lattice data, the fact that magnetic quarks are confined instead of screened, and asymptotic Regge trajectories for glueballs and mesons that are quadratic instead of linear.

A phenomenological fix of the last problem was suggested by introducing a soft IR wall, [16]. Although this fixes the asymptotic spectrum of mesons and meson dynamics is in principle self-consistent, it does not allow a consistent treatment of the glue sector both at zero and finite temperature. In particular, neither dilaton nor metric equations of motion are solved. Therefore the "on-shell" action is not really on-shell. The entropy computed from the BH horizon does not match the entropy calculated using standard thermodynamics from the free energy computed from the action, etc. Phenomenological metrics for the deconfined phase were also suggested, [17, 18] capturing some aspects of the expected thermodynamics.

The theoretical advances were paralleled by a very successful experimental effort at RHIC, [19]. The consensus on the existing data is that shortly after the collision a ball of quark-gluon plasma (QGP) forms that is at thermal equilibrium, and subsequently expands until its temperature falls below the QCD transition (or crossover) where it finally hadronizes. Relativistic hydrodynamics describes very well the QGP [20], with a shear-viscosity to entropy density ratio close to that of $\mathcal{N} = 4$ SYM, [21]. The QGP is at strong coupling, and it necessitates a treatment beyond perturbative QCD approaches, [22]. Moreover, although the shear viscosity from $\mathcal{N} = 4$ seems to be close to that "measured" by experiment, lattice data indicate that in the relevant RHIC range $1 \leq \frac{T}{T_c} \leq 3$ the QGP seems not to be a fully conformal fluid. Therefore the bulk viscosity is expected to play a role near the phase transition [23, 24]. The lattice techniques have been successfully used to study the thermal behavior of QCD, however they are not easily extended to the computation of hydrodynamic quantities. They can be used however, together with parametrizations of correlators in order to pin down parameters [24]. To date it seems that the holographic approach is a promising one in this direction.

In the bottom-up holographic model of AdS/QCD, the bulk viscosity is zero as conformal invariance is essentially not broken (the stress tensor is traceless). In the soft-wall model, no reliable calculation can be done for glue correlators and therefore transport coefficients are ill-defined. Similar remarks hold for other phenomenologically interesting observables as the drag force and the jet quenching parameter [25–27].

In order to go beyond the inadequacies of existing bottom-up holographic models, input has been put together both from string theory and QCD in order to craft an improved holographic QCD model, [28]. It is a five-dimensional Einstein dilaton system, with an appropriately chosen dilaton potential.

The vacuum solution involves an asymptotically logarithmically AdS solution near the boundary. The bulk field λ, dual to the 't Hooft coupling, is vanishing logarithmically

JHEP05(2009)033

near the boundary in order to match the expected QCD behavior. This implies that the potential must have a regular Taylor expansion as $\lambda \to 0$, and that $\lambda = 0$ is not an extremum. This is unlike almost all asymptotically AdS solutions discussed so far in the literature. In particular the canonically normalized scalar (the dilaton) is diverging at the boundary $r \to 0$ as $\phi \sim -\log(-\log r)$. The coefficients of the UV Taylor expansion of the potential are in one-to-one correspondence with the holographic β-function.

In the IR, the potential must have an appropriate behavior so that the theory is confined, has a mass gap and a discrete spectrum. This selects a narrow range of asymptotics that roughly obey

$$V(\lambda) \sim \lambda^{2Q} \quad , \quad \lambda \to \infty \qquad \text{with} \qquad \frac{2}{3} \leq Q < \frac{4}{3}. \tag{1.1}$$

The vacuum solution always ends in a naked singularity in the bulk. Demanding that this is a "good" singularity in the classification of Gubser [29] implies $Q < 4/3$. However, here we use a narrower notion of what we mean by "good" singularity: we accept only singularities that are *repulsive* to physical fluctuations, i.e. such that no extra boundary conditions are needed there. This requirement further restricts $Q < \frac{2\sqrt{2}}{3}$ in (1.1). Simple interpolations between the UV and IR asymptotics reproduce very well the low-lying glueball spectrum as well as the perturbative running of the 't Hooft coupling [28].

Five-dimensional Einstein dilaton systems with a monotonic dilaton potential (no extrema) provide an interesting class of gravitational theories that display diverse behaviors as a function of the IR asymptotics of the potential. Potentials with asymptotics growing slower than (1.1) with $Q = 2/3$ do not exhibit confinement. Potentials with asymptotics growing faster than (1.1) with $Q = 2\sqrt{2}/3$ do exhibit confinement but the naked singularity is too strong and extra boundary conditions are needed at the singularity in order to study the spectrum of fluctuations.

In this paper we will analyze the existence and structure of black-hole solutions, and their thermodynamics, in the class of gravitational theories described above. We will take the horizon to be a flat three-dimensional torus, but our techniques extend to the case where the horizon is a three-sphere. Our preliminary results in this direction have been published in [30]. The thermodynamics of similar systems has also been analyzed in [31]. Our aim is to eventually describe the finite-temperature structure of a holographic model closely resembling pure large-N_c Yang Mills theory. The latter is widely analyzed using lattice techniques (see e.g. [32, 33]), which indicate that the theory exhibits a first order confinement-deconfinement phase transition at a non-zero critical temperature of the order of the strong coupling scale Λ. While one of the main motivations for having a realistic holographic description of finite-temperature QCD is the computation of transport coefficients and other quantities relevant for heavy ion collision experiments, in this paper we will only be concerned with equilibrium thermodynamics, as this is already a daunting task. We leave the hydrodynamics for the very near future [34].

As we show in this paper, the correspondence between the 5D Einstein-dilaton setup advocated in [28] and 4D large N_c pure Yang-Mills extends to the finite temperature regime in a remarkable way. One of the main results of this work is *the proof of the the existence,*

JHEP05(2009)033

in the case of confining theories, of a first order Hawking-Page phase transition between the thermal gas and black-hole solutions. Moreover, the 5D black-holes in confining theories provide a realistic holographic description of the thermodynamics of the deconfined phase of 4D, large N_c pure Yang-Mills, that emerges from lattice studies.

The black-holes that we discuss obey the same UV asymptotics as the zero-temperature solution, namely they are asymptotically-logarithmically AdS with a logarithmically vanishing dilaton. Close to the AdS boundary the metric is that of a 5D AdS-Schwarzschild black-hole in Poincaré coordinates (i.e. with flat horizon), up to logarithmic corrections. Although asymptotically AdS black holes in Einstein-dilaton theories have received considerable attention (see e.g. [35]), these examples were always associated with the existence of an exactly AdS solution with constant dilaton, corresponding to an extremum of the dilaton potential. In contrast, the 5D black-holes we discuss here are of a new type, since the dilaton potential in our model is always monotonic. The AdS point is at infinity in field space, therefore the models we discuss *do not have a pure AdS solution*.

In this paper we derive a series of general results about the thermodynamics of the 5D system, that do not depend on the specific form of the potential but only on its small λ and large λ asymptotics. All these results point to the remarkable similarity between the thermodynamics of 5D models in the confining class, and the thermodynamics of 4D large N_c Yang-Mills. While the detailed quantitative comparison between a specific model and the lattice results for thermal Yang-Mills will appear elsewhere [36], these general results are the main focus of this paper. Below we briefly summarize them.

Parameters of the solutions. The parameters of the action are the 5D Planck mass M_p, and the various parameters that determine the shape of the dilaton potential $V(\lambda)$. In particular, the value $V(0)$ sets the AdS length scale ℓ. In addition, every black hole solution is characterized by the five integration constants of the 5th order dilaton-gravity system of equations.

We show how to identify these parameters in the dual gauge theory and eventually how to fix them.

- We keep the form of the potential generic, except that it should be a monotonic function of λ and it should obey the small and large λ asymptotics we mentioned above. A specific potential can be fixed by requiring that the zero-T spectrum agrees with the lattice data, as was done in [28].

- The specific value of the AdS length ℓ is irrelevant for any physical observable, and sets the overall units of the 5D solution.

- The 5D Planck scale (in AdS units) is fixed by matching the free field asymptotics of the QCD free energy in the high-temperature limit. This universally fixes $M_p\ell = 1/(45\pi^2)$. The physical Planck mass, that determines the strength of gravitational interactions (and of the interactions between glueballs in the dual theory) includes an extra factor of $N_c^{2/3}$, that guarantees the suppression of quantum corrections in the large N_c limit in our setup.

JHEP05(2009)033

- Among the 5 integration constants of the equations of motion, only two are physical and independent: the value of the dilaton at the horizon, and an overall scale Λ, related to the dilaton asymptotics near the UV boundary. The former determines the black hole temperature and entropy; the latter is also present in the vacuum solution, and it is dual to $\Lambda_{\rm QCD}$. Fixing the UV asymptotics is equivalent to selecting a specific value for Λ.

Since our model should be thought of as coming from a non-critical string theory, an additional parameter is the string scale ℓ_s. This is invisible in the 5D Einstein-dilaton setup we assume throughout this paper, and we will not discuss it any further. It can be fixed by comparing the effective string tension (calculated from the linear part of the static quark potential) to the lattice data, as was done in [28].

Existence and uniqueness of the black-hole solutions. The $T = 0$ solution defines a vacuum background. Once we specify the UV asymptotics of a black-hole solution to be the same as for the vacuum background, there is only one additional parameter that characterizes the solution, that we take to be the value of the dilaton at the horizon, λ_h. For any *monotonic* dilaton potential $V(\lambda)$ we show that, for each λ_h, ranging between zero and infinity, there exists a unique black-hole solution, with a temperature T, entropy S (horizon area) and free energy $\mathcal{F}$ functions of λ_h only. Thus, the thermodynamics is encoded in the functions $T(\lambda_h)$, $S(\lambda_h)$ and $\mathcal{F}(\lambda_h)$, namely the temperature, entropy and free energy. Moreover, we show that the limit $\lambda_h \to \infty$ of the black-hole solution coincides with the *unique* zero-temperature solution that, for a given potential, displays a "good" (i.e. repulsive) singularity.

Although our models allow an infinite number of black-hole solutions (each with a different value of Λ) with the same mass, this does not imply that these black-holes admit scalar hair. The reason is that each different value of Λ corresponds to a different asymptotic for the metric and dilaton. In other words, Λ plays the role of an extra "charge" that can be measured at infinity. Moreover, due to the absence of extrema in the dilaton potential, there is no pure AdS-Schwarzschild solution with a constant dilaton. Thus, our black hole solutions satisfy the no-hair theorems for asymptotically AdS gravity coupled to scalars (see [37] for a recent discussion).

Deconfinement phase transition. We show that any 5D theory, whose zero-temperature solution is dual to a UV-free and IR-confining 4D theory, also exhibits a Hawking-Page type of phase transition, dual to a deconfining phase transition in 4D. The transition is always first order, except in the special case when the IR behavior of the vacuum solution is at the borderline between confining and non-confining geometries: in this case the (string frame) solution is asymptotically a flat metric with a linear dilaton, and the phase transition is second order. Conversely, non-confining theories do not exhibit a phase transition: black-holes dominate the thermal ensemble for any non-zero temperature T.

The phase structure of black-holes in confining theories is similar to what is found in the original Hawking-Page situation [38], namely:

- Black hole solutions exist only above a certain temperature $T_{\rm min}$;

JHEP05(2009)033

- Generically, for any $T > T_{\rm min}$ there exist (at least) two different black-hole solutions with the same T and the same UV asymptotics (large and small BHs);

- Above a certain critical temperature $T_c > T_{\rm min}$, it is (one of the) large black-holes that dominate the thermal ensemble, while for $0 < T < T_c$ it is the "thermal gas" solution (with the same metric and dilaton as the zero-temperature solution) that dominates. On the other hand, the small black-holes never dominate the ensemble.

- Typically, the big black-holes have positive specific heat, and are thermodynamically stable, whereas the small black-holes have negative specific heat and are unstable. There may be however exceptions to this rule, where in a limited range of λ_h the small black-holes are also stable.

- In the borderline case (asymptotically linear dilaton), there is only a single black-hole for $T > T_{\rm min}$, and the second order transition occurs exactly at $T_{\rm min}$.

There is one important difference with the Hawking-Page case, however. There, the black-holes are global AdS-Schwarzschild with horizon topology S^3, and the theory is dual to a conformal field theory on the $S^1 \times S^3$ [4]; Here instead we are dealing with black-holes whose horizon has topology T^3, and the phase transition is associated with dynamical confinement instead of the non-trivial topology of space.

Similarities of the black-hole phase and the deconfined phase in Yang-Mills. The thermodynamics of black-holes in 5D duals of confining theories shares many features with the deconfined phase of 4D Yang-Mills at large N_c.

- The appropriately regularized free energy $\mathcal{F}/N_c^2$ acts as an order parameter for the phase transition. This is similar to the case of $\mathcal{N} = 4$ SYM on the sphere, and as expected in pure YM in flat space;

- Another order parameter is the Polyakov loop which vanishes in the confined phase and becomes non-trivial above the deconfinement transition. This is paralleled by the dual gravity computation. A string worldsheet that encircles the Euclidean time direction and extends in the radial direction has infinite action in the confining geometry, hence the vev of the loop vanishes. On the other hand it becomes finite in the black-hole geometry yielding a finite value for the associated vev [4].

- The latent heat per unit volume is of order $N_c^2 T_c^4$;

- At very high temperature the thermodynamic quantities behave like in a conformal theory, although the approach to conformality is logarithmically slow. With a suitable choice of the relation between the 5D Planck scale and the AdS length, in the limit $T \to \infty$ we find a free gas, as appropriate for a gravity dual of pure Yang-Mills and unlike strongly coupled theories like $\mathcal{N} = 4$ sYM .

JHEP05(2009)033

- The speed of sound is small near the phase transition, and it approaches the conformal value $c_s^2 \to 1/3$ at high temperature.[1]

The topological vacuum density. The vacuum expectation value of the topological density, $\langle \mathrm{Tr} F \wedge F \rangle$ can be computed by including, on the gravity side, a 5D axion, dual to the YM theta parameter [28]. We show that in the black-hole phase (deconfinement) the profile of the axion is necessarily trivial, unlike the low temperature phase (confinement). This causes the vev of the topological density to vanish. It is in agreement with the large N_c expectations and with the lattice calculations in finite temperature Yang-Mills [41].

Explicit calculation of the free energy and the role of the gluon condensate. We compute explicitly the free energy of the black-hole solutions, relative to the vacuum, as the difference between the on-shell actions. A crucial role in this computation and in the dynamics of the phase transition is played by (the holographic dual of) the thermal vev of $\mathrm{Tr} F^2$. This quantity appears in the near-boundary expansion of the difference between the black-hole metric scale factor $b(r)$ and its zero-temperature analogue, $b_o(r)$. If r denotes the conformal coordinate of both metrics, the AdS boundary is at $r = 0$. We show that, once the UV asymptotics are fixed to be the same for all the solutions, then as $r \to 0$:

$$b(r) - b_o(r) = b_o(r) \left(\mathcal{G} \frac{r^4}{\ell^3} + \text{subleading} \right). \tag{1.2}$$

The quantity $\mathcal{G}$ is proportional to $\langle \mathrm{Tr} F^2 \rangle_T - \langle \mathrm{Tr} F^2 \rangle_o$. It is a function of temperature, and it provides a measure of the deviation from conformality. It plays a crucial role for the existence of the phase transition.

Indeed, an explicit calculation shows that the free energy difference between a black-hole and the vacuum solution is given schematically (omitting 3-space volume and other numerical factors) by:

$$\mathcal{F} \sim \mathcal{G} - \frac{TS}{4}. \tag{1.3}$$

The second term is negative definite, and it is the only one present in a conformal field theory. The gluon condensate is therefore crucial for the existence of a phase transition.

One important point is that the free energy written above receives contributions from the UV boundary alone: to compute $\mathcal{F}$ it is sufficient to know the metric close to the AdS boundary. This is important for at least two reasons:

1. In the context of AdS/CFT all the information about observable quantities must be encoded in near-boundary data. No explicit contributions are obtained from the IR regime. The IR influences only indirectly by fixing normalizable modes near the boundary via regularity conditions.

2. The specific dynamics of the IR singularity is irrelevant for the computation of the thermodynamics. By contrast, in other studies claiming the existence of deconfining phase transitions in simple 5D models [8, 9], it is the IR boundary or singularity that gives the required positive contribution to the free energy.

[1] Reproducing this behavior was the main motivation of [31], and it emerges quite naturally in our setup

JHEP05(2009)033

Matching the β-function to the trace anomaly. We provide a non-trivial check of the gauge/gravity correspondence applied to the 5D theories of [28]: the matching of the (flat space) conformal anomaly, encoded in the YM β-function, to lowest order in a small λ expansion.[2]

From the free energy, we can compute the trace of the thermal stress tensor in the deconfined phase, which turns out to be proportional to the gluon condensate:

$$\langle T^{\mu}_{\mu} \rangle \quad \sim \quad \mathcal{G}. \tag{1.4}$$

On the other hand, in 4D Yang-Mills theory the same quantity $\langle T^{\mu}_{\mu} \rangle$ obeys the dilatation Ward identity:

$$\langle T^{\mu}_{\mu} \rangle = \frac{\beta(\lambda)}{4\lambda^2} \langle \mathrm{Tr} F^2 \rangle. \tag{1.5}$$

By a holographic computation we can find the relation between $\langle \mathrm{Tr} F^2 \rangle$ and $\mathcal{G}$ (the latter being defined by eq. (1.2)), to lowest order in the $\lambda \to 0$ limit, and can show that the two expressions for T^{μ}_{μ} coincide precisely.

Part of the analysis in this paper is performed with the help of some new technical tools that we believe are interesting by themselves:

- The *thermal generalization of the superpotential:* This is widely used in the zero-temperature counterpart (see e.g. [39, 40]). A superpotential W allows to recast Einstein's equations for the dilaton and scale factor in the first order form, and to decouple them from the equations governing the evolution of the thermal function appearing in the metric;

- The *scalar variables:* this is a pair of functions of λ, X and Y, that are invariant under radial diffeomorphisms. They satisfy a coupled system of first-order differential equations. These functions encode all the information about the UV and IR properties of the full solution. From them one can easily derive all the thermodynamic observables and relations.

The paper is organized as follows. In section 2 we review the setup, the vacuum solutions, and the results about confinement found in [28]. We analyze the possible types of singularity and we give a more exhaustive analysis of this issue as compared to [28].

In section 3 we describe the black-hole solutions their existence and uniqueness properties and define the relevant thermodynamic quantities. We then compute the free energy difference between the black-hole and vacuum solutions, as a function of entropy, temperature, and the value of the gluon condensate.

In section 4 we show that, to lowest order in λ as $\lambda \to 0$, the trace anomaly computed from the equation of state matches the holographic computation of the the vev of $\mathrm{Tr} F^2$.

In section 5 we prove that confinement at zero temperature is in one-to-one correspondence with the presence of a phase transition at a finite temperature T_c. We find the explicit form of the black-hole solutions in the two opposite regimes when the black-hole

[2] This is the initial and simplest step in a rigorous program for the renormalization of asymptotically logarithmically AdS theories, that will appear shortly, [49].

JHEP05(2009)033

horizon is very close to or very far from the UV boundary. We then show that in confining theories there is always a finite, minimum black-hole temperature, whereas in non-confining theories black-holes exist with arbitrarily small temperatures. This fact, together with the first law of black-hole thermodynamics, is used to prove the main statement of this section in the particular case when there are only two black-hole solutions for each temperature. The proof in the most general case is left to appendix G.

In section 6 we study the dynamics of the 5D axion, dual to the Yang-Mills vacuum angle, showing that above the critical temperature the axion profile is necessarily constant, and the topological density has zero vev.

In section 7 we define the *scalar variables*, and show that their use helps in computing all the thermodynamic quantities, as well as the UV and IR asymptotic properties of the solutions. In particular, in Subsection 7.2 we compute the near-boundary expansion of the black-hole metric components and dilaton profile, with respect to the vacuum solution. Section 8 contains a brief outlook.

Most technical details are left to the appendices. In appendix A we give details about Einstein's equations in various frames, and the relation between fluctuations in different frames. In appendix B we revisit the case of a constant potential and derive AdS and dilaton flow solutions and the corresponding black-holes. In appendix C we give the details of the computation of the black-hole on-shell action and ADM mass. In appendix D we provide the high-T asymptotics of the gluon condensate. Appendix E is devoted to the discussion of the general solution to the zero-temperature superpotential equation, and the classification of zero-temperature singularities. In appendix F we introduce the finite temperature generalization of the superpotential, and use it to solve explicitly the black-hole equations for large λ_h. In appendix G we give the general proof of the statement in section 5, in the case where more than 2 black-holes exist for certain temperature ranges. In appendix H we provide some details of the computations with scalar variables. In particular in Subsection H.4 we show that a black-hole solution with a regular horizon always connects with the UV boundary, thus providing the proof of the existence of black-hole solutions for arbitrary λ_h. In appendix I we give the high-T asymptotics of various quantities. Finally in appendix J we show some interesting analytical solutions of the system.

2 Review of vacuum solutions

The holographic duals of large N_c Yang Mills theory proposed in [28] are based on five-dimensional Einstein-dilaton gravity with a dilaton potential. The basic fields for the pure gauge sector are the 5D metric $g_{\mu\nu}$ (dual to the 4D stress tensor) and a scalar field Φ (dual to TrF^2). The action for these fields is taken to be:[3]

$$\mathcal{S}_5 = -M_p^3 N_c^2 \int d^5x\sqrt{g}\left[R - \frac{4}{3}(\partial\Phi)^2 + V(\Phi)\right] + 2M_p^3 N_c^2 \int_{\partial M} d^4x\sqrt{h}\; K. \tag{2.1}$$

Here, M_p is the five-dimensional Planck scale and N_c is the number of colors. The last term is the Gibbons-Hawking term, with K being the extrinsic curvature of the boundary.

[3] See appendix A for our sign conventions.

JHEP05(2009)033

The effective five-dimensional Newton constant is $G_5 = 1/(16\pi M_p^3 N_c^2)$, and it is small in the large-N_c limit.

The vacuum solutions are of the form

$$ds^2 = b(r)^2 \left(dr^2 + \eta_{ij} dx^i dx^j\right), \qquad \Phi = \Phi(r), \tag{2.2}$$

where the metric is written in conformally-flat coordinates.

The radial coordinate r corresponds to the 4D RG scale. In the holographic dictionary, we identify the 4D energy scale E with the metric scale factor, $E = E_0 b(r)$, up to an arbitrary energy unit E_0. Also, we identify $\lambda \equiv e^{\Phi}$ with the running 't Hooft coupling $\lambda_t \equiv N_c g_{\rm YM}^2$, up to an *a priori* unknown multiplicative factor, $\lambda = \kappa \lambda_t$. All physical observables are independent of the parameter κ, as explained in appendix A.3.[4]

With the above identifications, one can give a holographic definition of the β-function of the system in terms of the background solution:

$$\beta(\lambda) = \frac{d\lambda}{d\log E} = \lambda \frac{\dot\Phi}{\dot A}, \qquad A(r) \equiv \log b(r). \tag{2.3}$$

Above and throughout this paper a dot stands for a derivative with respect to the radial (conformal) coordinate r.

With the ansatz (2.2), Einstein's equations are

$$6\frac{\dot b^2}{b^2} + 3\frac{\ddot b}{b} = b^2 V, \qquad 6\frac{\dot b^2}{b^2} - 3\frac{\ddot b}{b} = \frac{4}{3}\dot\Phi^2, \tag{2.4}$$

The dilaton field equation is not an independent equation, but it follows from (2.4).

It is sometimes useful to work with the *domain wall coordinates*, in which the metric reads:

$$ds^2 = du^2 + e^{2A(u)} \eta_{ij} dx^i dx^j, \qquad dr = e^{-A(u)} du, \qquad b(u) = e^{A(u)}. \tag{2.5}$$

In this frame Einstein's equations take the form:

$$3A'' + 12A'^2 = V(\Phi), \qquad A'' = -\frac{4}{9}\Phi'^2. \tag{2.6}$$

where a prime denotes a derivative w.r.t. u. In particular, the second equation implies that the scale factor of an asymptotically AdS_5 spacetime (for which $A \sim -u/\ell$ as $u \to -\infty$) is monotonically decreasing, and it therefore provides a consistent definition of the holographic energy scale.

Einstein's equations can be put in first order form by defining a *superpotential* $W(\Phi)$, i.e. one solution to the equation:

$$V(\Phi) = -\frac{4}{3}\left(\frac{dW}{d\Phi}\right)^2 + \frac{64}{27} W^2. \tag{2.7}$$

[4] More precisely, this statement applies to quantities that can be computed within the Einstein frame. Quantities that involve the string frame metric may depend on κ in a nontrivial way. In this paper we will not be concerned with any such quantity, and we leave a more detailed discussion of this issue for an upcoming work [36].

JHEP05(2009)033

With this definition, Einstein's equations (2.6) become:

$$\Phi'(u) = \frac{dW}{d\Phi}, \quad A'(u) = -\frac{4}{9}W(\Phi). \tag{2.8}$$

The system of eqs. (2.7)–(2.8) has three integration constants, one of which is an artifact due to reparametrization invariance.[5] The solution is completely specified by a choice of $W(\Phi)$, up to an integration constant that consists in a simultaneous rescaling of $b(r)$ and r, and only affects the overall scale of the system. In other words, all nontrivial physics is encoded in $W(\Phi)$.

The general solution of eq. (2.7) is discussed in detail in appendix E. As we will discuss at the end of this section, for any $V(\Phi)$, there is a *single choice* of $W(\Phi)$ that satisfies some reasonable physical conditions. We are thus left with a one-parameter family of solutions, distinguished only by a choice of scale. This parallels the situation in the gauge theory.

Another useful reformulation of the Einstein's equations is in terms of the logarithmic derivative of $W(\Phi)$, which is directly related to the β-function:

$$X(\Phi) = -\frac{3}{4}\frac{d\log W}{d\Phi} = \frac{\beta(\lambda)}{3\lambda} \tag{2.9}$$

The complete solution of the system is encoded in this function. It is determined from the potential by solving a first-order equation:

$$\frac{dX}{d\Phi} = -\frac{4}{3}(1-X^2)\left(1+\frac{3}{8X}\frac{d\log V}{d\Phi}\right). \tag{2.10}$$

Once X is known the scale factor and the dilaton are obtained from it by solving the first order equations (H.1) and (H.2). Thus, this formulation reduces the Einstein equations to three first order equations. In section 7, we shall present a natural generalization of this formulation to the black-hole solutions.

The small-λ and large-λ asymptotic of $W(\lambda)$ (or $X(\lambda)$) determine the solution in the UV and the IR of the geometry, corresponding to the large- and small-b regions, respectively.

2.1 UV asymptotics

In the UV, asymptotic freedom with logarithmically running coupling requires the background to be asymptotically Anti-de Sitter. The perturbative β-function, $\beta \sim -b_0\lambda^2 - b_1\lambda^3 + \ldots$, requires an expansion of X in the form:

$$X(\lambda) = -\frac{b_0}{3}\lambda - \frac{b_1}{3}\lambda^2 + \mathcal{O}(\lambda^3) \tag{2.11}$$

where b_0 and b_1 are the β-function coefficients. Using (2.9) one finds the expansion of the superpotential as,

$$W(\lambda) = \frac{9}{4\ell}\left(1 + w_0\lambda + w_1\lambda^2 + \ldots\right), \tag{2.12}$$

[5] This can be seen by choosing Φ as a coordinate: then the first equation in (2.8) becomes vacuous, and only two first order equations remain.

which implies a potential of the form

$$V(\lambda) = \frac{12}{\ell^2}(1 + v_0\lambda + v_1\lambda^2 + \ldots). \tag{2.13}$$

Here ℓ is the AdS length, and the dimensionless parameters w_i, v_i are fixed in terms of the β-function coefficients. In particular the small-λ expansion parameters w_i of the superpotential are *universal*, and do not depend on the particular choice of solution of eq. (2.7): as shown in appendix E, different solutions of eq. (2.7) differ by subleading non-analytic terms. For a general potential (2.13), the β-functions coefficients and the parameters of the potential are related as follows:

$$b_0 = \frac{9}{8}v_0 = \frac{9}{4}w_0, \qquad b_1 = \frac{9}{4}v_1 - \frac{207}{256}v_0^2 = \frac{9}{2}w_1 - \frac{9}{4}w_0^2. \tag{2.14}$$

Let us here also define the ratio,

$$b = \frac{b_1}{b_0^2}, \tag{2.15}$$

which will prove useful in what follows. Note that b is invariant under the rescaling $\lambda \to \kappa\lambda$.

The UV region corresponds to $r \to 0$ in conformal coordinates, and the asymptotic solution is given by:

$$b(r) = \frac{\ell}{r}\left[1 + \frac{4}{9}\frac{1}{\log r\Lambda} - \frac{4}{9}\, b\, \frac{\log(-\log r\Lambda)}{\log^2 r\Lambda} + \ldots\right], \tag{2.16}$$

$$b_0\lambda(r) = -\frac{1}{\log r\Lambda} + b\, \frac{\log(-\log r\Lambda)}{\log^2 r\Lambda} + \ldots \tag{2.17}$$

The scale Λ appearing in the expansion is the only physical integration constant, and it is the holographic manifestation of the strong coupling scale in QCD perturbation theory. The UV boundary conditions for the metric and dilaton are completely specified by the choice of this scale. In practice Λ is determined by a combination of the initial conditions of λ and A, given at a point r_0 close to the boundary, as,

$$\Lambda\, \ell = \exp\left[A(\lambda_0) - \frac{1}{b_0\lambda_0}\right](b_0\lambda_0)^{-b} + \cdots . \tag{2.18}$$

The ellipsis refer to contributions that vanish as one takes the cut-off away, $\lambda_0 \to 0$. The coefficients b_0 and b are defined in (2.14) and (2.15). The derivation of (2.18) follows from appendix H.1 and the eqs. (2.16)–(2.17) above.

2.2 IR asymptotics

The IR properties such as confinement of the electric color charges (signaled by an area law for the Wilson loop) and the features of the glueball spectrum are determined by the behavior of $W(\lambda)$ (or $X(\lambda)$) for large λ. In particular, the Wilson loop follows an area law if and only if $W(\lambda)$ grows as $\lambda^{2/3}$ or faster. The same condition ensures a mass gap in the spectrum. In other words one has the criterion:

$$\textit{Confinement} \Leftrightarrow W(\lambda) \geq O(\lambda^{2/3}) \textit{ as } \lambda \to \infty.$$

JHEP05(2009)033

The form of the IR geometry depends on the details of the asymptotics. The Einstein-frame scale factor is guaranteed to decrease monotonically from the UV to the IR, and eventually the spacetime terminates in a singularity at some $r = r_0$. We classify the singularity into *good* and *bad* according to the following criterion [28]:

A good singularity is screened, i.e. it is repulsive to physical modes.

On the other hand, *bad* singularities are such that finite energy modes can probe arbitrarily deep into the region close to the singularity. Typically this means that one needs to specify extra boundary conditions at the singularity, i.e. the information provided with the classical action is not enough to compute physical quantities. For good singularities, all (physical) boundary conditions must be imposed in the UV region. Therefore we believe that only "good" singularities have a meaningful holographic interpretation.

The most interesting geometries are those with the singularity at $r_0 = \infty$, and with the asymptotics:

$$b(r) \sim e^{-\left(\frac{r}{L}\right)^{\alpha}}, \qquad \lambda(r) \sim e^{3/2\left(\frac{r}{L}\right)^{\alpha}} \left(\frac{r}{L}\right)^{\frac{3}{4}(\alpha-1)}, \qquad r \to \infty \tag{2.19}$$

Here, the length scale L is set by the same integration constant that fixes Λ in eq. (2.16).

In such solutions the curvature of the string-frame metric vanishes in the extreme IR. These solutions occur when $W(\lambda)$ and $X(\lambda)$ behave for large λ as:

$$W(\lambda) \sim \lambda^{2/3} (\log \lambda)^{\frac{\alpha-1}{2\alpha}}, \qquad X(\lambda) \sim -\frac{1}{2} - \frac{3}{8}\frac{\alpha-1}{\alpha}\frac{1}{\log\lambda} + \ldots, \quad \lambda \to \infty, \tag{2.20}$$

which in turn requires the potential to grow as

$$V(\lambda) \sim \lambda^{4/3} (\log \lambda)^{\frac{\alpha-1}{\alpha}}, \qquad \lambda \to \infty, \tag{2.21}$$

These solutions are confining iff $\alpha \geq 1$.[6]

The parameter α determines the asymptotic spectrum of normalizable fluctuations around the solution, which corresponds to the spectrum of composite states (*glueballs*) of the gauge theory, with masses that scale as:

$$m_n \sim n^{(\alpha-1)/\alpha}. \tag{2.22}$$

For a linear glueball spectrum, $m_n^2 \sim n$, one should choose $\alpha = 2$.

The borderline confining case, $\alpha = 1$ has interesting properties: the asymptotic geometry in the string frame reduces to flat space with a linear dilaton. The spectrum has a mass gap and it is discrete up to a certain energy level, above which it becomes continuous. We will see that this case also has special thermodynamic properties.

Solutions with a singularity at a *finite value* r_0 of the conformal coordinate are also confining, and correspond to $W(\lambda)$ growing as λ^Q with $Q > 2/3$. Close to the singularity $r = r_0$ the scale factor vanishes as

$$b(r) \sim (r_0 - r)^{\delta}, \qquad Q = \frac{2}{3}\sqrt{1+\delta^{-1}}. \tag{2.23}$$

[6] Solutions such that $b(r)$ decays as a power-law as $r \to \infty$ are not confining.

JHEP05(2009)033

The glueball spectrum has quadratic growth, $m_n^2 \sim n^2$, as in the hard wall models.

The case $\delta < 1$ ($Q > 2\sqrt{2}/3$) should be discarded, since in this case the singularity is a *bad* one according to the our classification, i.e. it is not screened from the physical fluctuations [28].

An example of this type (with $\delta = 1/3$) is the "dilaton flow" solution of 5D Einstein-dilaton gravity with a negative cosmological constant, discussed in [42, 43], which was argued to be dual to an SO(6) invariant mass deformation $\mathcal{N} = 4$ SYM. Although this description can be adequate in the UV, calculation of any physical quantity requires extra knowledge about the details of the singularity, which is not available in the classical gravity approximation.

2.3 The superpotential vs. the potential

The action (2.1) is defined in terms of $V(\lambda)$, not $W(\lambda)$ or $X(\lambda)$. Therefore it is important to know what other large-λ asymptotics for W and $X(\lambda)$ can occur for a given $V(\lambda)$. This problem is analyzed in appendix E (for W) and in appendix H.3 (for X), where the form of the general solution of eqs. (2.7) and (2.10) is discussed in detail. Essentially, for any given monotonic $V(\lambda)$, a solution with a good infrared singularity, if it exists, is unique.

In the UV region, $\lambda \to 0$, all solutions to eq. (2.7) have the same expansion, given by eq. (2.12) with the same coefficients w_i. In other words, in the UV all solutions to Einstein's equations flow to the same log-corrected AdS (eqs. (2.16)–(2.17)).

In the IR, the situation is more complicated. We consider a potential $V(\lambda)$ defined over the whole range $0 < \lambda < \infty$, and such that for large enough λ it is well approximated by the form:

$$V(\lambda) \simeq V_\infty \lambda^{2Q} (\log \lambda)^P \tag{2.24}$$

for some real P and Q.[7] We will assume $V(\lambda)$ is a positive, monotonic function, to avoid the presence of conformal fixed points at finite λ. Thus, we take $V_\infty > 0$ and $Q \geq 0$.

All the interesting physics is found for $Q \leq 4/3$. As shown in appendix E, if $Q \leq 4/3$, there exist three classes of solutions to the superpotential equation:

1. **Special:** A *single* solution such that $W(\lambda) \sim \sqrt{V(\lambda)}$ for $\lambda \to \infty$.
2. **Generic:** A continuous family with leading asymptotics

$$W(\lambda) \simeq C\lambda^{4/3} \qquad \lambda \to \infty \tag{2.25}$$

   where C is an arbitrary constant.
3. **Bouncing:** A continuous family which never reaches the asymptotic large-λ region: the variable λ attains a maximum value λ_*, then decreases again to zero towards a region where

$$W \simeq \tilde{C}\lambda^{-4/3}, \qquad \lambda \to 0, \tag{2.26}$$

[7] Although we parametrize the IR asymptotic in this particular form, all our discussion also applies to any potential that has intermediate IR growth between two values of Q or P that share the same behavior, for example $V(\lambda) \sim \lambda^Q (\log \lambda)^P (\log\log \lambda)^R \ldots$. However if Q or P take values that mark the boundary between two different qualitative behaviors of the solution (e.g. $Q = 4/3$, see below), extra work is needed to understand the intermediate asymptotics.

JHEP05(2009)033

On the other hand, if $Q > 4/3$ only the bouncing solution exists,[8] and the dilaton never reaches infinity.

The special solution has asymptotic behavior:

$$W_o(\lambda) \simeq W_\infty \lambda^Q (\log \lambda)^{P/2} \qquad \lambda \to \infty, \qquad W_\infty = \sqrt{\frac{27 V_\infty}{4(16 - 9Q^2)}}. \tag{2.27}$$

It presents a good IR singularity for $Q < 2\sqrt{2}/3$, and it is confining for $Q > 2/3$, or $Q = 2/3$ and $P > 0$. The generic and bouncing solutions, on the other hand, always have bad singularities.

As we shall discuss in section 5, the special solution is also the only one that can be obtained in the zero-mass limit of black-hole solutions of the same bulk theory. This gives another characterization of the special solution, and singles it out as the only physically sensible choice [29].

Thus, given a potential $V(\lambda)$ with asymptotics (2.21), there is a *single* solution with the large-λ behavior (2.20) corresponding to a "good" singularity. All other solutions have *bad* singularities in the IR, and cannot be lifted to black-holes. Requiring the absence of bad singularities is what ultimately fixes the integration constant of the W equation in the zero-temperature system, or equivalently, the integration constant of (2.10).

As shown in appendix E.2, changing this integration constant adds a perturbation in the metric and dilaton that goes as r^4 close to the boundary. Thus, this corresponds to changing the expectation value of the corresponding dimension 4 operator, i.e. $\mathrm{Tr}F^2$. In other words, the integration constant in the superpotential controls the value of $\langle \mathrm{Tr}F^2 \rangle$ in the gauge theory and there is a unique value such that no bad singularities appear.[9].

To summarize: the physically interesting situation when a good solution exists *and* corresponds to confined color, is the case $2/3 \leq Q \leq 2\sqrt{2}/3$.

3 Finite-temperature solutions and thermodynamics

We now consider the dilaton-gravity system described in the previous section with a good potential according to the aforementioned criteria and study it at finite temperature T. As usual, this can be implemented by going to Euclidean signature and compactifying the Euclidean time (that for simplicity of notation will be still called t) on a circle with period $\beta = 1/T$. This breaks the Poincaré invariance of the vacuum to spatial rotations, and allows for a larger class of solutions. According to the AdS/CFT prescription, the partition sum is constructed by considering all solutions with fixed UV boundary conditions.[10] From now on we will introduce a subscript "o" for the quantities related to the zero-temperature solution.

The thermal solutions are of two types:

[8] This includes the case when the potential grows faster than (2.24) for any Q, e.g. if $V(\lambda) \sim e^{c\lambda}$.

[9] This situation has an analogue in the case of constant potential, $V(\lambda) = 12/\ell^2$: also in this case there is a single "good" solution, AdS_5 spacetime with constant dilaton. Even in this theory it is well known [42, 43] that there is a continuous family of solutions with a running dilaton, all of which have bad singularities in the interior. This is presented in detail both at zero and finite temperature in appendix B.

[10] Later in this section we will be more specific about what we mean by "fixed UV boundary conditions."

JHEP05(2009)033

1. **Thermal gas solution:** this is the same as (2.2),

$$ds^2 = b_o^2(r)\left(dr^2 - dt^2 + dx_m dx^m\right), \qquad \Phi = \Phi_o(r), \tag{3.1}$$

except for the identification $t \sim t + i\beta$. It corresponds to a gas of thermal excitations above the same vacuum described by the original solution, from which it inherits all the non-perturbative features (confinement, spectrum, values of condensates, etc.)

2. **Black hole solutions:** they are of the form

$$ds^2 = b(r)^2\left[\frac{dr^2}{f(r)} - f(r)dt^2 + dx_m dx^m\right], \qquad \Phi = \Phi(r) \tag{3.2}$$

and are characterized by the presence of a horizon r_h where $f(r_h) = 0$. This implies that such a solution, if it exists, corresponds to a non-confined phase, since the confining string tension is proportional to $\mathrm{Min}_r(\sqrt{g_{xx}(r)g_{tt}(r)}) = 0$ [44]. In the Euclidean version, deconfinement is signaled by a non-zero value of the Polyakov loop, as discussed in [4]. Since we want to study the theory on $S^1 \times R^3$ we consider black-holes with flat horizon topology.

Notice that in general the functions $b(r)$ and $\Phi(r)$ appearing in eq. (3.2) are different from their zero-temperature counterparts, and have also a nontrivial temperature dependence.

In the rest of this section we will discuss the features of the black-hole solutions to the general system (2.1), and the thermodynamics in the canonical ensemble.

3.1 5D Einstein-dilaton black holes

We require that the solution has the same UV asymptotics as the one at zero temperature: an AdS boundary at $r = 0$ where $b(r) \sim \ell/r$ and e^{Φ} vanishes logarithmically; we have to impose $f(0) = 1$, so that the black-hole solution (3.2) coincides with the zero-temperature and thermal gas solutions, (3.1) in the UV limit $r \to 0$.

A black-hole solution with a regular horizon is characterized by the existence of a surface $r = r_h$, where the dilaton and scale factor are regular, and

$$f(r_h) = 0, \quad \dot{f}(r_h) < 0. \tag{3.3}$$

The Euclidean version of the solution is defined only for $0 < r < r_h$. The horizon $r = r_h$ is a regular surface if Euclidean time is identified as $\tau \to \tau + 4\pi/|\dot{f}(r_h)|$. This determines the temperature of the solution as:

$$T = \frac{|\dot{f}(r_h)|}{4\pi}. \tag{3.4}$$

The independent field equations are:

$$6\frac{\dot{b}^2}{b^2} - 3\frac{\ddot{b}}{b} = \frac{4}{3}\dot{\Phi}^2 \quad , \quad \frac{\ddot{f}}{\dot{f}} + 3\frac{\dot{b}}{b} = 0, \tag{3.5}$$

$$6\frac{\dot{b}^2}{b^2} + 3\frac{\ddot{b}}{b} + 3\frac{\dot{b}}{b}\frac{\dot{f}}{f} = \frac{b^2}{f}V. \tag{3.6}$$

Integrating once the second equation of (3.5), we obtain:

$$\dot{f} = -\frac{C}{b^3}, \tag{3.7}$$

for some integration constant C. This shows that $\dot{f}$ cannot change sign. For a black-hole, $f(r)$ has to decrease from $f = 1$ at the boundary to $f = 0$ at the horizon, therefore $C > 0$.

The general solution for f is

$$f(r) = 1 - C\int_0^r \frac{dr'}{b(r')^3}, \tag{3.8}$$

where we have chosen the second integration constant so that $f(0) = 1$.[11] Setting $C = 0$ and $f(r) = 1$ we recover the zero-temperature Einstein's equations.

The quantity C is related to the horizon location as:

$$C = \frac{1}{\int_0^{r_h} \frac{dr'}{b(r')^3}} \tag{3.9}$$

Note that $b(r)$ is regular in the whole region of integration. We can compute the temperature by eq. (3.4):

$$\beta = \frac{1}{T} = \frac{4\pi}{|\dot{f}(r_h)|} = 4\pi b^3(r_h)\int_0^{r_h}\frac{du}{b(u)^3} = \frac{4\pi b^3(r_h)}{C}. \tag{3.10}$$

The horizon area is given by

$$\mathcal{A}(r_h) = b^3(r_h)V_3, \tag{3.11}$$

where V_3 is the volume of 3-space, and it is related to the entropy as usual by $S = \mathcal{A}/4G_5$.

In the particular case $V(\Phi) = 12/\ell^2$, $\dot{\Phi} = 0$, we have the AdS-Schwarzschild solution in Poincaré coordinates,

$$b(r) = \frac{\ell}{r}, \qquad f(r) = 1 - \left(\frac{r}{r_h}\right)^4, \qquad T = \frac{1}{\pi r_h}, \qquad \mathcal{A} = \left(\frac{\ell}{r_h}\right)^3 V_3. \tag{3.12}$$

Notice that in this case the scale factor is temperature-independent. This is not true in general: for V depending non-trivially on Φ, different $f(r)$ will result in different $b(r)$.

Near the AdS boundary (UV), this difference can be made more precise:

- As shown in appendix F.3.1, near the AdS boundary $b(r)$ and $\lambda(r)$ have AdS asymptotics, an expansion in inverse logs of the same form as $b_o(r)$ and $\lambda_o(r)$, eqs. (2.16)–(2.17), specified by an integration constant Λ. In particular, $\lambda(r) \to 0$ in the UV for all the solutions. Fixing the UV boundary conditions therefore, means specifying the scale Λ appearing in this expansion.

  Here, and from now on, by stating that two solutions obey the "same UV boundary conditions"*, we require that* "the scale Λ appearing in the expansion in the perturbative UV log must be the same".[12]

[11] Recall that $b(r) \sim r^{-1}$ as $r \to 0$, so the second term in eq. (3.8) vanishes at the boundary.

[12] As it should be clear, it is not enough to specify that the metric be asymptotically AdS and that $\lambda(r)$ asymptotes some fixed value as $r \to 0$, since for all solutions $\lambda(0) = 0$.

JHEP05(2009)033

- Assuming for $b(r)$ and $\lambda(r)$ the *same* value of the integration constant Λ, as for $b_o(r)$ and $\lambda_o(r)$, then:

$$b(r) = b_o(r)\left[1 + \mathcal{G}\,\frac{r^4}{\ell^3} + \dots\right], \qquad r \to 0, \tag{3.13}$$

$$\lambda(r) = \lambda_o(r)\left[1 + \frac{45}{8}\mathcal{G}\,\frac{r^4 \log \Lambda r}{\ell^3} + \dots\right], \qquad r \to 0 \tag{3.14}$$

$$f(r) = 1 - \frac{C}{4}\frac{r^4}{\ell^3} + \dots \qquad r \to 0, \tag{3.15}$$

  where C is defined in (3.7), and $\mathcal{G}$ is a temperature-dependent constant with the dimensions of energy. Eq. (3.15) is obtained from the expression (3.8) and the fact that $b(r) \to \ell r^{-1}$ as $r \to 0$; eqs. (3.13)–(3.14) will be derived explicitly in section 7.2.

According to the standard rules of the correspondence, the quantity $\mathcal{G}(T)$ is interpreted (up to a multiplicative constant, to be determined later) as the difference between the vev's of the corresponding dimension-four operator in the black-hole and in the vacuum solution. Since we have assumed that Φ couples to TrF^2 as $\int e^{-\Phi} TrF^2$, the appropriate operator is the gluon condensate $\lambda^{-1} TrF^2$. The precise relation between $\mathcal{G}$ and $\langle TrF^2 \rangle$ will be obtained in section 4.

Integration constants. The quantities C and $\mathcal{G}$ are related to two of the five independent integration constant of the system of Einstein's equations. For C, this is clear from its definition, eq. (3.7): it determines the temperature of the black-hole. $\mathcal{G}$ can be regarded as the integration constant for the thermal generalization of the superpotential equation, given in appendix F. In the zero-temperature case it was fixed to single out the special solution, with the "good" IR behavior; in the black-hole it is fixed by the requirement of regularity of the horizon.[13] Two more integration constants are fixed by setting $f(0) = 1$, and by choosing the scale Λ in the UV perturbative expansion, i.e. by requiring that the solution has the same boundary behavior as at $T = 0$. The last integration constant, as in the $T = 0$, is unphysical and is due to reparametrization invariance. It can be eliminated by rewriting the solution using λ as a coordinate. As we show in appendix F.2, a better way of counting integration constants is by giving "initial values" directly at the horizon. This results in the following statement:

For any positive and monotonic potential $V(\lambda)$ that grows no faster[14] *than $\lambda^{4/3}$ as $\lambda \to \infty$, and for any value λ_h, there exists one and only one black-hole such that:*

1. *$\lambda \to \lambda_h$ at the horizon*

2. *it has the same UV asymptotics as the zero-temperature solution (2.16)–(2.17)*

[13] In our analysis we cannot determine uniquely what is the value of the gluon condensate in a given background, but only the differences between $\mathrm{Tr}F^2$ in two backgrounds with the same asymptotics. In order to compute the v.e.v. of the gluon condensate unambiguously in a given background one would need to perform the full procedure of holographic renormalization, which for the asymptotics we are considering is not yet fully developed but will be available soon, [49].

[14] This restriction is necessary to ensure that (vacuum and black-hole) solutions that extend to arbitrarily large values of λ exist.

JHEP05(2009)033

The existence, for each λ_h, of a black-hole solution with regular horizon that extends all the way to the UV AdS boundary, is shown in appendix H.4 using the method of scalar variables. Uniqueness, on the other hand, follows from the discussion in appendix F.2.

Thus, the value of the dilaton at the horizon, λ_h, is the most natural candidate to classify the black-holes, and all the thermodynamic quantities like e.g. temperature and entropy which are single valued functions of λ_h (the same does not necessarily hold if one writes them as a function of the horizon position, i.e. $T(r_h)$ is not necessarily single valued. We have found numerically examples of this behavior).

3.2 Thermodynamics

In this section we compute the free energy differences of various solutions at a given temperature. This will allow us to compute all other thermodynamic quantities. The details of the relevant calculations can be found in appendices C.1 and C.2.

The free energy at fixed temperature β^{-1} of a given solution is given by:

$$\beta\mathcal{F} = \mathcal{S}^{\epsilon}, \tag{3.16}$$

where $\mathcal{S}^{\epsilon}$ is the regularized Euclidean action evaluated on the solution. The action needs to be regularized, due to the divergences near the AdS boundary. To achieve this, we take 3-d space to be a torus with finite volume V_3, and cut-off the radial direction in the UV up to a minimum radius $r = \epsilon > 0$, so all the integrals are limited below by ϵ. Free-energy differences will be finite (and proportional to V_3) as $\epsilon \to 0$ since the large-volume divergences do not depend on the detailed solutions but only on the asymptotics.

As shown in appendix C.1, the regularized Einstein action (2.1) evaluated on a black-hole solution is:

$$\mathcal{S}^{\epsilon} = \mathcal{S}^{\epsilon}_{E} + \mathcal{S}^{\epsilon}_{GH} + \mathcal{S}^{\epsilon}_{\text{count}} = 2\beta\,\sigma\,\left[3b^2(\epsilon)f(\epsilon)\dot{b}(\epsilon) + \frac{1}{2}\dot{f}(\epsilon)b^3(\epsilon)\right] + \mathcal{S}^{\epsilon}_{\text{count}}, \tag{3.17}$$

where we have defined:

$$\sigma \equiv M_p^3 N_c^2 V_3. \tag{3.18}$$

The counterterm action $\mathcal{S}^{\epsilon}_{\text{count}}$ is required to make the above expression finite in the limit $\epsilon \to 0$ [45]. As we can see, eq. (3.17) depends solely on the metric evaluated at the UV cutoff: the contribution to the bulk Einstein action coming from the horizon region vanishes.

Instead of explicitly calculating $\mathcal{S}^{\epsilon}_{\text{count}}$, we can define the free energy by subtracting a given reference background, following the prescription of [46]. We should take as reference the thermal gas background with the same temperature and the same Λ as the black-hole, obtained by setting $f(r) = 1$, and replacing $b(r)$ with $b_o(r)$. However, this is correct for the unregularized action that extends all the way to $r = 0$. When we deal with regularized geometries, we must make sure that [46]

(i) the intrinsic geometry of the 4-dimensional boundary be the same for the two solutions,

JHEP05(2009)033

(ii) the boundary values of scalar field, λ and λ_o are the same.

To satisfy (i), we must demand that the proper lengths of the time circles of the solutions (3.1) and (3.2) and the proper volume of 3-space be the same at $r = \epsilon$. Denoting by $\tilde{\beta}$ and $\tilde{V}_3$ the period of the time coordinate and the volume of 3-space in the thermal gas case, this requirements imply:

$$\tilde{\beta}\, b_o(r)\Big|_{cut-off} = \beta\ b(r)\sqrt{f(r)}\Big|_{cut-off}, \qquad \tilde{V}_3\, b_o^3(r)\Big|_{cut-off} = V_3\ b^3(r)\Big|_{cut-off}. \tag{3.19}$$

The condition (ii) means that we must require $\lambda(\epsilon) = \lambda_o(\epsilon)$. This actually implies that the two backgrounds are characterized by *different* values Λ and $\tilde{\Lambda}$ of the scale that defines the UV boundary conditions. This makes the calculation of differences such as $b(\epsilon) - b_o(\epsilon)$ quite complicated, since one cannot use directly the UV expansion (3.13), which relies on the two scales being equal. However, since we are dealing with only one scalar field, we can equivalently keep $\tilde{\Lambda} = \Lambda$ and set the cut-off of the background at a *different* location $r = \tilde{\epsilon}$, such that[15]

$$\lambda(\epsilon) = \lambda_o(\tilde{\epsilon}). \tag{3.20}$$

Since the cut-off coordinates do not coincide in the two solutions, in the conditions (3.19) one now has to evaluate each side of the equality at the appropriate value of the coordinate r. Now we can use eq. (3.14) to determine the needed shift in the boundary positions:

$$\tilde{\epsilon} - \epsilon = -\frac{45}{8}\frac{\mathcal{G}}{\ell^3}\frac{\epsilon^4}{\dot{\lambda}_o(\epsilon)} = -\frac{45}{8}\frac{\mathcal{G}}{\ell^3}\epsilon^5(\log\epsilon\Lambda)^2. \tag{3.21}$$

The regularized action for the thermal gas background, in the case that the IR singularity is of the good type, is given by:

$$\tilde{\mathcal{S}}^{\tilde{\epsilon}} = 2\tilde{\beta}\,\tilde{\sigma}\,\left[3b_o^2(\tilde{\epsilon})\dot{b}_o(\tilde{\epsilon})\right] + \mathcal{S}^{\tilde{\epsilon}}_{\rm count}, \qquad \tilde{\sigma} = M_p^3 N_c^2 \tilde{V}_3. \tag{3.22}$$

As for the black-hole, eq. (3.22) only receives contributions from the metric evaluated at the UV cut-off. Indeed, evaluating the Einstein term on shell in general gives an extra negative term localized in the IR, of the form $\mathcal{S}_{\rm IR} = 2\tilde{\beta}\tilde{\sigma}b_o^2(r_0)\dot{b_o}(r_0) \leq 0$, where r_0 is the position of the singularity in the vacuum background. *This contribution vanishes exactly, if r_0 is a good singularity.* This is good news, since this means that the details of the physics of the singular region are irrelevant for the calculation of the free energy (as for other physical quantities [28]), and only the UV data matter. Similarly a Gibbons-Hawking term at the singularity (which in principle could be there) also does not give any new contribution, since on shell it is also proportional to $b_o^2(r_0)\dot{b_o}(r_0)$ and it vanishes for good singularities.[16]

Therefore the free energy (difference) $\mathcal{F}$ is:

$$\beta\mathcal{F} = \lim_{\epsilon\to 0}(\mathcal{S}_\epsilon - \tilde{\mathcal{S}}_{\tilde{\epsilon}}). \tag{3.23}$$

[15] This strategy will not work in the case of multiple bulk scalar fields.

[16] For a recent example of a similar study, where the free energy does receive contributions from the deep IR, see [9].

JHEP05(2009)033

In the difference above, it is *guaranteed* that the contribution coming from the counterterms exactly cancel even at finite ϵ, since these terms are build out of invariants of the induced boundary geometry and the boundary values of the scalar field.[17] Therefore this subtraction prescription makes it unnecessary to know the explicit form of $S_{\rm count}$.

Using the results (3.17) and (3.22) in (3.23), together with the relations (3.19), we have:

$$\mathcal{F} = \sigma \lim_{\epsilon\to 0} \left\{ 6b^2(\epsilon)\sqrt{f(\epsilon)} \left[\dot{b}(\epsilon)\sqrt{f(\epsilon)} - \frac{b^2(\epsilon)}{b_o^2(\tilde{\epsilon})}\dot{b}_o(\tilde{\epsilon}) \right] + \dot{f}(\epsilon) b^3(\epsilon) \right\} \tag{3.24}$$

Using the UV expansions (3.15)–(3.13) and the relation (3.21) n eq (3.24), and taking the limit $\epsilon \to 0$, we obtain the final result for the free energy,

$$\mathcal{F} = \sigma \left(15\,\mathcal{G}(T) - \frac{C}{4} \right) = 15\,\sigma\,\mathcal{G}(T) - \frac{1}{4} TS, \tag{3.25}$$

where the entropy S is given by the area of the horizon:

$$S = \frac{\mathcal{A}}{4G_5} = 4\pi\sigma b^3(r_h) = \sigma \frac{C}{T}. \tag{3.26}$$

In the second equality we have used eq. (3.18) and $G_5 = 1/(16\pi M_p^3 N_c^2)$, and in the third one eq. (3.10).

The black-hole energy E can be obtained either by the thermodynamic formula $E = \mathcal{F} + TS = -\partial_\beta(\beta\mathcal{F})$, or by computing the ADM mass, and consistency requires that the two computations give the same result. This is indeed the case: as shown in appendix C.3, the black-hole mass is given by

$$E = \sigma \left(15\,\mathcal{G} + \frac{3}{4} C \right) = \mathcal{F} + TS. \tag{3.27}$$

The presence of the gluon condensate term in eq. (3.25) is the source of the breaking of conformal invariance, since in a conformal theory the relation $\mathcal{F} = -TS/4$ is exactly satisfied. As we will see in section 4, the holographic computation of the conformal anomaly in flat space matches the field theory result.

Notice that second term in eq. (3.25) is negative for any T. It is the presence of a non-trivial gluon condensate that may allow a change in sign of the free energy, corresponding to a first order phase transition. While the calculation of $\mathcal{G}(T)$, in general, is only possible numerically, in section 5 we will give a general argument to determine whether or not a given Einstein-dilaton theory exhibits a phase transition at some critical temperature.

Finally, we note that the Gibbons-Hawking term contributes importantly to this expression. A simple calculation shows that the Einstein term in the action contributes as $\mathcal{F}_E = -5\sigma\mathcal{G} - T\ S/4$ whereas the Gibbons-Hawking contribution is $\mathcal{F}_{GH} = +20\sigma\mathcal{G}$. Note that the Einstein term itself is negative-definite, therefore the GH term is crucial for the existence of a phase transition. This is *unlike* the usual Hawking-Page phase transition in global AdS, where the change in sign of the free energy is due solely to the Einstein term.

[17] This cancelation may not hold in the case of the counterterms that diverge as $\log\epsilon$, i.e. those that give rise to the conformal anomaly. However, the free energy difference due to these counterterms, if any, is of the order $\epsilon^4 \log\epsilon$. Therefore these terms do not result in any finite contribution to $\Delta\mathcal{F}$

JHEP05(2009)033

4 The holographic conformal anomaly (in flat 4-space)

The expectation value of the gluon condensate plays an important role in the thermodynamics of the system we are investigating. As we will see, it can be related to the thermal version of the anomalous trace of the stress tensor. In this section we will show that a holographic calculation of the trace anomaly in flat space to lowest order in λ matches the four-dimensional result as advocated in [28]. This is a non-trivial check of the validity of the gauge/gravity duality in our setup, in particular of our identification of the holographic β-function.

In four-dimensional Yang-Mills theory, breaking of scale invariance is expressed by the operator equation:

$$T^{\mu}_{\mu} = \frac{\beta(\lambda_t)}{4\lambda_t^2}\mathrm{Tr}F^2, \tag{4.1}$$

where λ_t is the 4D 't Hooft coupling.

Defining the pressure p and energy density ρ,

$$p = -\frac{\mathcal{F}}{V_3}, \qquad \rho = \frac{\mathcal{F}+TS}{V_3}, \tag{4.2}$$

the trace of the thermodynamic stress tensor can be obtained immediately from eq. (3.25):

$$\langle T^{\mu}_{\mu}\rangle_R = \rho - 3p = 60M_p^3N_c^2\mathcal{G}(T), \tag{4.3}$$

where we have used the definition of σ, eq. (3.18). The left hand side of (4.3) is the trace of the renormalized thermal stress tensor, $\langle T^{\mu}_{\mu}\rangle_R = \langle T^{\mu}_{\mu}\rangle - \langle T^{\mu}_{\mu}\rangle_o$, and it is proportional to $\mathcal{G} \sim \langle \mathrm{Tr}F^2\rangle$, in qualitative agreement with (4.1).

To check the detailed agreement between eqs. (4.1) and (4.3), we need to derive the precise relation between $\mathcal{G}$ and $\langle \mathrm{Tr}F^2\rangle$. In what follows we work to lowest order in λ. To compute $\langle \mathrm{Tr}F^2\rangle$ holographically, we use the prescription established in [47]: we recall that for any fluctuation of a bulk scalar with a canonically normalized kinetic term,

$$S_{\mathrm{fluc}} = \frac{1}{2}\ell^{-3}\int \sqrt{g}d^5x(\partial\chi)^2, \tag{4.4}$$

and coupling to a boundary operator $\mathcal{O}(x)$ as

$$S_{\mathrm{coup}} = \int d^4x\chi\mathcal{O}, \tag{4.5}$$

one can read off the vev of the operator $O(x)$ from the UV asymptotics of $\chi(x,r)$: if the UV expansion is of the form

$$\chi \approx r^{\Delta_-}\chi_0(x) + r^{\Delta_+}\chi_1(x), \tag{4.6}$$

with Δ_+ being the canonical dimension of the dual operator, and $\Delta_- = d - \Delta_+$ for a d-dimensional gauge theory, then the vev of the operator is given by the formula:

$$\langle\mathcal{O}(x)\rangle = (2\Delta_+ - d)\,\chi_1(x). \tag{4.7}$$

JHEP05(2009)033

Now, we apply this prescription to the dilaton fluctuation. In our setup the dilaton Φ is related to the 't Hooft coupling λ_t by $e^{\Phi} \equiv \lambda = \kappa\lambda_t$.[18] The coupling of the dilaton to the YM field strength is given by

$$S_{\rm coup} = -\int d^4x \, \frac{1}{4\lambda_t} \mathrm{Tr}\ F^2 = -\frac{\kappa}{4}\int d^4x \, e^{-\Phi}\ \mathrm{Tr}\ F^2. \tag{4.8}$$

Thus, the dilaton fluctuation couples as,

$$\delta S_{\rm coup} = \frac{\kappa}{4}\int d^4x \, \delta\Phi \, e^{-\Phi}\ \mathrm{Tr}\ F^2. \tag{4.9}$$

From the bulk action (2.1) we learn that $\delta\Phi$ and the canonically normalized fluctuation (4.4) are related by[19]

$$\chi = \left(\frac{8}{3}(M_p\ \ell)^3\ N_c^2\right)^{\frac{1}{2}} \delta\Phi. \tag{4.10}$$

Using the relation $e^{\Phi} = \kappa\lambda_t$ we find the coupling

$$\int d^4x \, \chi\, \mathcal{O} = \int d^4x \, \chi \left[\frac{\kappa}{4\lambda}\left(\frac{8}{3}(M_p\ell)^3 N_c^2\right)^{-\frac{1}{2}} \mathrm{Tr}\ F^2\right]. \tag{4.11}$$

The particular dilaton fluctuation we are interested is the difference $\delta\Phi = \Phi - \Phi_o$: this allows to compute the difference between the thermal and vacuum values of $\langle \mathrm{Tr}\ F^2(0)\rangle$. Notice that this difference is well defined, contrary to e.g. $\langle \mathrm{Tr}\ F^2(0)\rangle_o$, which suffers from UV ambiguities. Moreover, it is a purely *normalizable* fluctuation close to the boundary (i.e. it only contains terms like the second one in (4.6), since we assumed that the black-hole and vacuum backgrounds obey the same UV boundary conditions.

The fluctuation $\delta\Phi$ is obtained from eq. (3.14). To leading order in powers of λ (or equivalently in inverse powers of $\log(r\Lambda)$):

$$\delta\Phi \simeq \frac{45}{8}\,\mathcal{G}\,\frac{r^4}{\ell^3}\log(r\Lambda), \tag{4.12}$$

Recalling the leading dilaton asymptotics $(b_0\lambda)^{-1} = -\log(r\ \Lambda)$, and using (4.10) and (4.12) together with (4.7) and (4.11) yields the relation between $\mathcal{G}$ and $\mathrm{Tr}\ F^2$:

$$\langle \mathrm{Tr}\ F^2\rangle_T - \langle \mathrm{Tr}\ F^2\rangle_o = -\frac{240}{\kappa b_0} M_p^3 N_c^2\ \mathcal{G}. \tag{4.13}$$

Eq. (4.13) is the holographic computation of the vev of the r.h.s. of the trace identity (4.1), to leading order in the expansion in λ. Using the expansion $\beta(\lambda) = -b_0\lambda^2 + \ldots$ together with the relation $\lambda = \kappa\lambda_t$, we obtain from (4.13):

$$\frac{\beta(\lambda_t)}{4\lambda_t^2}\langle \mathrm{Tr}F^2\rangle_R = 60 M_p^3 N_c^2\ \mathcal{G}. \tag{4.14}$$

[18] We will keep the multiplicative constant κ unspecified, as it will drop out of the calculation, i.e. matching of the anomalies does not depend on the value of κ.

[19] In doing this computation one should actually use a gauge-invariant fluctuation. This can be defined as $\delta\Phi_{G.I.} = \delta\Phi - \dot{\Phi}/\dot{A}\delta\psi$, where ψ is the part of the metric fluctuation that couples to T^μ_μ, and is proportional to δA. However, close to the UV boundary, $\delta\psi \sim r^4$, $\delta\Phi \sim r^4 \log r$ and $\dot{\Phi}/\dot{A} \sim (\log r)^{-1}$, therefore $\delta\Phi_{G.I.} \to \delta\Phi$ as $r \to 0$.

JHEP05(2009)033

which exactly matches the l.h.s, eq. (4.3). This is a nontrivial consistency check of our setup.

Notice that the matching of the conformal anomaly is independent of both κ and b_0, i.e. it is insensitive to the relative normalization of the dilaton field λ with respect to the true 4D Yang-Mills coupling, λ_t.

5 Thermal phase transitions

In this section we will derive the building blocks necessary to obtain the main theoretical result of this paper: *confining backgrounds exhibit a first order phase transition*, whose features precisely mimic those of the large-N_c Yang-Mill deconfinement transition. We also show the converse: non-confining theories do not have a phase transition at finite T.

The primary information we will need to extract is the dependence of the temperature on the horizon position r_h, or better on the value of the dilaton at the horizon, λ_h. Although this is difficult to obtain for generic λ_h, it is nevertheless possible to determine the asymptotic form of $T(\lambda_h)$ for λ_h very small and very large (in a sense that will be defined below), corresponding to very large and very small horizon area, respectively.

5.1 Horizon in the UV region

As we have discussed in section 3, the black-hole metric approaches asymptotically the AdS-Schwarzschild solution for small r, with $b(r) \simeq \ell/r$ and $f(r) \simeq 1 - (C/4)r^4/\ell^3$, and with a logarighmically running dilaton, $\lambda(r) \simeq (-b_0 \log r\Lambda)^{-1}$.

For a large enough value of the constant C, f vanishes at a small enough r such that this approximation is valid all the way to the horizon. In this case, $f(r)$ vanishes at $r_h^4 \simeq 4\ell^3 C^{-1}$. This approximation gets better for smaller values of r_h (i.e. horizon closer to the AdS boundary). Then, the temperature and entropy are given approximately by the AdS formulas (see eqs. (3.12) and (3.26)) :

$$T \simeq \frac{1}{\pi r_h}, \qquad S = 4\pi\sigma \left(\frac{\ell}{r_h}\right)^3, \tag{5.1}$$

with σ defined by eq. (3.18). These expressions can be converted into functions of λ_h, by using the UV asymptotics of $\lambda(r)$, (2.17) evaluated at the horizon:[20]

$$r_h \simeq \frac{1}{\Lambda}\lambda_h^{-b} e^{-\frac{1}{b_0\lambda_h}} \tag{5.2}$$

In particular, $T(\lambda_h)$ is a decreasing function near the boundary.

The relation (5.1) is corrected by the logarithmic running in the UV. Neglecting non-perturbative contributions, the scale factor is given by eq. (2.16), from which we can obtain the logarithmic corrections to the thermal function $f(r)$ through eq. (3.8) and (3.9). Through (3.10) we obtain the corrected relation between T and r_h (see appendix D for the details):

$$T = \frac{1}{\pi r_h}\left[1 - \frac{4}{9}\frac{1}{(\log r_h\Lambda)^2} + \dots\right]. \tag{5.3}$$

[20] This is justified in the limit of small r_h (small λ_h), since as we have discussed in section 3, the deviations from the zero-temperature solution are $O(r^4)$ for small r, so eq. (2.17) is a good approximation all the way to the horizon.

The results above allow us to compute the temperature dependence of the term $\mathcal{G}(T)$ in the free energy coming from the gluon condensate. From eq. (3.25) we can write:[21]

$$15\sigma\,\mathcal{G} = \mathcal{F} + \frac{1}{4}TS = -\int SdT + \frac{1}{4}TS, \tag{5.4}$$

where $S = 4\pi\sigma b^3(r_h)$. For small r_h, we can use the UV asymptotic form for the scale factor, eq. (2.16), and the relation (5.3), to obtain the asymptotic form of $\mathcal{G}$. The calculation is carried out explicitly in appendix D, and the result is:

$$\mathcal{G} \to \frac{\pi^4}{45}\frac{\ell^3\,T^4}{(\log\frac{\pi T}{\Lambda})^2}, \qquad T\to\infty. \tag{5.5}$$

This equation has important consequences. It implies that the gluon condensate contribution to the free energy is subleading at large T, by a factor $(\log T)^{-2}$, with respect to the term $TS/4 \sim T^4$. Therefore, for very large BH's we can write:

$$\mathcal{F} \to -\frac{TS}{4} \simeq -(\pi^4\sigma\ell^3)\,T^4, \qquad T\to\infty. \tag{5.6}$$

On the other hand, at very high temperatures, pure SU(N_c) Yang-Mills theory behaves as a free gas with $\sim N_c^2$ degrees of freedom, and its free energy is approximated by the Stefan-Boltzmann formula[22]

$$\frac{\mathcal{F}_{\rm YM}}{V_3} \simeq -\frac{\pi^2}{45}N_c^2\,T^4, \qquad T\to\infty. \tag{5.7}$$

Comparing the last two equations allows us to fix $\sigma = V_3N_c^2/(45\pi^2)$. From the definition of σ, eq. (3.18), this is equivalent to fixing the 5D Planck scale in AdS units, in a model independent way:

$$(M_p\ell)^3 = \frac{1}{45\pi^2}. \tag{5.8}$$

5.2 Horizon in the IR region

Now, we are going to answer the question: what is the behavior of the function $T(r_h)$, for large r_h? We will find that the answer depends exclusively on whether or not the corresponding zero-temperature solution (more specifically, the *special* solution in the classification of section 2) is confining. In the non-confining case, the black-hole temperature decreases to zero for large r_h; on the contrary, for confining theories, $T(r_h)$ asymptotically grows with r_h. This distinction has dramatic consequences for the thermodynamics of the model: as we will show in the next section, it implies that confinement is in one-to-one correspondence with the existence of a phase transition at a finite T_c.

As a byproduct of our analysis, we will find that when the horizon is deep in the IR (i.e. the black-hole mass is very small), the black-hole geometry is well approximated by the

[21] It is enough to write the relation below as an indefinite integral, since adding a constant does not affect the result for the high temperature asymptotics (5.5). A more precise relation, with integration limits, will be given in section 5.2.3

[22] This is *unlike* the case of $\mathcal{N}=4$ super YM. There the theory in the UV is strongly coupled and a non-trivial strong coupling calculation is needed to establish the correct coefficient, [48].

JHEP05(2009)033

geometry of the zero-temperature special solution (provided it exists). More precisely: the special solution is the only zero-T geometry that can be lifted to a black-hole of arbitrarily small mass.

To find the large r_h behavior of the black-hole temperature, we must solve eqs. (3.5)–(3.6) for r and r_h "close to the singularity" of the zero-temperature solution. This question is somewhat ambiguous, since in different zero-T backgrounds the singularity can be at a finite or infinite value of the conformal coordinates, and it is unclear how exactly to identify the "asymptoti" region.

A coordinate-independent resolution of this ambiguity consists in solving the equations using Φ as a radial coordinate, and identifying the asymptotic regions according to the value of 't Hooft coupling $\lambda \equiv e^{\Phi}$. Indeed, in the zero-temperature background this quantity covers the whole range from 0 in the UV to $+\infty$ in the deep IR, no matter what is the position of the IR singularity in conformal coordinates. So it makes sense to define the black-holes whose horizon is in the deep IR (with respect to the zero-temperature background) as those where λ attains a large value at the horizon. In any given black-hole solution $\lambda(r)$ is a monotonically increasing function, and $\lambda_h \equiv \lambda(r_h)$ is the maximum value it can attain. More precisely, we consider "large" λ as the region $\lambda \gg \lambda_0$ such that the potential $V(\lambda)$ is well approximated by its asymptotic form:

$$V(\lambda) \simeq V_\infty \lambda^{2Q} (\log \lambda)^P, \qquad \lambda \gg \lambda_0, \tag{5.9}$$

for some real P, and $Q \geq 0$. The actual value λ_0 of course depends on the specific form of $V(\lambda)$. Recall that confining theories correspond to $Q > 2/3$ or $Q = 2/3$, $P > 0$, and to make sure that there exists a special solution with a good (i.e. repulsive) singularity we must further restrict $Q < 2\sqrt{2}/3$. The zero-temperature superpotential for such solution obeys the asymptotics:

$$W_o(\lambda) \simeq W_\infty \lambda^{Q} (\log \lambda)^{P/2}, \qquad \lambda \gg \lambda_0 \tag{5.10}$$

As shown in appendix F.2, the horizon value λ_h uniquely determines the temperature, once the UV asymptotics are kept fixed. In the next two subsections we will determine the behavior of $T(\lambda_h)$ for λ_h in the asymptotic region, $\lambda_h \gg \lambda_0$. An efficient way to attack this problem is to generalize the superpotential technique described in section 2 to the finite-temperature case. This will allow us to give a solution of the system, for large λ_h, in the entire large-λ region. Another method that uses diffeomorphism invariant variables is described in section 7.

5.2.1 Solution in the large-λ region

We will now investigate the features of the black-hole solutions, in the case when the horizon is deep in the IR. Consider the situation where the horizon value of the 't Hooft coupling λ_h, is large enough to be deep in the IR asymptotic region, $\lambda_h \gg \lambda_0$, defined in the previous section.

In this case it is possible to find analytically a good approximation to the solution in the region $\lambda_0 \ll \lambda \leq \lambda_h$, and to match it to the zero-temperature solution in the part of

JHEP05(2009)033

the asymptotic region far from the horizon, $\lambda_0 \ll \lambda \ll \lambda_h$. This will fix all the integration constants, and give the temperature unambiguously as a function of λ_h for $\lambda_h \gg \lambda_0$.

An explicit (approximate) solution for large λ_h is found by defining a *thermal superpotential*, i.e. a function $W(\Phi)$, that generalizes the zero-temperature superpotential $W_o(\Phi)$ to the black-hole background, such that the scale factor and dilaton equations (in domain wall coordinates) reduce to the form:

$$A'(u) = -\frac{4}{9}W, \qquad \Phi'(u) = \frac{dW}{d\Phi} \tag{5.11}$$

The details of this formalism are developed in appendix F. As shown there, the superpotential $W(\Phi)$ and the logarithm g of the thermal function f appearing in the metric satisfy a pair of coupled differential equations in the variable Φ, which take the form:

$$\left(\partial_\Phi g + \frac{\partial_\Phi^2 g}{\partial_\Phi g}\right)\partial_\Phi W + \partial_\Phi^2 W = \frac{16}{9}W, \qquad g \equiv \log f \tag{5.12}$$

$$-\frac{4}{3}W(\partial_\Phi W)(\partial_\Phi g) - \frac{4}{3}(\partial_\Phi W)^2 + \frac{64}{27}W^2 = e^{-g}V(\Phi). \tag{5.13}$$

In these variables the system of Einstein's equations splits into two separate decoupled systems, and solving eq. (5.12)–(5.13) determines the metric and dilaton through eqs. (5.11) solely from the knowledge of $W(\Phi)$, as in the zero-temperature case. Here, though, the superpotential cannot be taken as an independent function, but it depends on temperature through the coupling to $g(\Phi)$ in eq. (5.13)

As shown in appendix F.3.2, the solution of the system (5.12)–(5.13) in the whole region where (5.9) is valid has the form:

$$f(\Phi) \simeq 1 - \left(\frac{\Phi}{\Phi_h}\right)^R e^{-K(\Phi_h - \Phi)}, \qquad W(\Phi) \simeq W_\infty \lambda^Q (\log\lambda)^{P/2}, \qquad \Phi_0 \ll \Phi < \Phi_h, \tag{5.14}$$

where the constants K and R are given by:

$$K \equiv \left(\frac{16}{9Q} - Q\right); \qquad R \equiv -\frac{P}{2}\left(1 + \frac{16}{9Q^2}\right). \tag{5.15}$$

More precisely, the approximate equality signs in eq. (5.14) stand for dropping terms of $O(1/\Phi)$ in W and $\log[1-f]$.

Notice that the asymptotic solution for the superpotential has automatically the same asymptotics of the *special* solution $W_o(\lambda)$, eq. (5.10): the presence of a regular horizon at large λ_h has lifted the degeneracy present in the zero-temperature superpotential equation, selecting a single solution, which happens to be the unique one with the good singularity! We will come back to this point later in this section, and in section 7.

The approximation $W \simeq W_o$ is valid in the whole asymptotic region. Thus, the metric and dilaton have the same asymptotics as in the $T = 0$ case, all the way to the horizon. Moreover, $f(\Phi)$ is very close to unity already in the asymptotic region, specifically where $\Phi_0 \ll \Phi \ll \Phi_h$. Thus, for all smaller values of Φ, including those outside the asymptotic region, $f(\Phi) \simeq 1$ and the superpotential equation reduces to the zero-temperature one,

with special solution $W_o(\Phi)$. This implies that $W \simeq W_o$ is a good approximation in the *whole range* of Φ, not only asymptotically. The equations (5.11) for the metric and dilaton therefore reduce to the zero-temperature equations, whose solutions are classified by the value of the integration constant Λ. This implies that we can fix the remaining integration constant of the system (the scale Λ) to the same value as in the $T = 0$ background when we integrate (5.11). With this choice, all the integration constants in the asymptotic solution are fixed. Thus, for large λ_h the complete thermal solution for the scale factor and dilaton is *everywhere* well approximated by the zero-temperature form:

$$A(r) \simeq A_o(r), \qquad \Phi(r) \simeq \Phi_o(r). \tag{5.16}$$

From eq. (5.14), expressed in r-coordinates (by setting $f(r) \equiv f(\Phi(r))$), we observe that, at any fixed r, taking the limit $\Phi_h \to +\infty$ brings the metric to match the vacuum form with $f(r) = 1$. Therefore the limit $\lambda_h \to \infty$ corresponds to the (point-wise) limit of the black-hole going to the zero-temperature metric.

In the particular case of power-law asymptotic and singularity at $r = \infty$, corresponding to $Q = 2/3$, $P = (\alpha - 1)/\alpha$ (see [28]), the solution for large r is:

$$A(r) \sim -\left(\frac{r}{L}\right)^{\alpha}, \tag{5.17}$$

$$\Phi(r) \simeq \frac{3}{2}\left(\frac{r}{L}\right)^{\alpha} + \frac{3}{4}(\alpha - 1)\log\left(\frac{r}{L}\right), \tag{5.18}$$

$$f(r) \simeq 1 - \left(\frac{r}{r_h}\right)^{1-\alpha} \exp\left[-\left(\frac{r_h}{L}\right)^{\alpha} + \left(\frac{r}{L}\right)^{\alpha}\right]. \tag{5.19}$$

where L is the same length scale appearing in the zero-temperature solutions (2.19). The relation between temperature and horizon position for these black-holes is:

$$T = \frac{|\dot{f}(r_h)|}{4\pi} = \frac{1}{4\pi}\frac{r_h^{\alpha-1}}{L^{\alpha}}\left[1 + O\left(\left(\frac{L}{r_h}\right)^{\alpha}\right)\right], \tag{5.20}$$

Notice that, for $\alpha > 1$, i.e. when the theory is confining, the temperature *increases* as a function of r_h. In the next section we will see that this behavior is characteristic of general confining asymptotics.

A no-go theorem. As discussed in detail in appendix E, the asymptotic behavior (5.9) does not fix uniquely the asymptotics of the zero-temperature solution, but rather allows various possibilities summarized in appendix E.4. An important conclusion that can be derived from the discussion above is that black-holes which probe the asymptotic large-λ region *necessarily match the "special" zero-temperature solution* with asymptotic (2.27), as $\lambda_h \to \infty$. All other solutions cannot be lifted to black-holes with arbitrarily small mass (i.e. whose metric is arbitrarily close to the zero-temperature metric) . For an alternative derivation of the same results, see section 7.5. We thus have the following:

> **No-go theorem:** *The only vacuum solutions of Einstein-dilaton gravity, with a potential satisfying (5.9), that can be continuously lifted to a regular black-hole with arbitrarily small mass, are the ones stemming from a superpotential with the "special" asymptotics (2.27).*

JHEP05(2009)033

In particular, this implies that the two continuous families of zero-T solutions with "generic" and "bouncing" superpotentials (all of which have bad singularities) cannot be promoted to black-holes with an arbitrarily small mass (i.e. such that the metric looks like that of those zero-T solutions almost everywhere).

The zero-T superpotentials with bad singularities were already discarded as pathological in [28], since they exhibit singularities which are not screened from physical fluctuations, and do not have a well defined eigenvalue problem. If we subscribe to the criteria laid out in [29], the no-go theorem above gives another reason to discard these kinds of solutions: in [29] a singular background was considered acceptable if the singularity can be "hidden" behind a regular black-hole horizon by an infinitesimally small deformation of the metric.[23]

5.2.2 Big black-holes and small black-holes

Now, let us determine the temperature of the asymptotic solution obtained, for general P and Q in (5.9). It is easiest to do so as a function of Φ_h. We have (see eq. (3.4))

$$4\pi T = \left|\frac{df(r)}{dr}\right|_{r_h} = \left|\frac{df(\Phi)}{d\Phi}\right| \frac{d\Phi}{du}\frac{du}{dr} = \left[\left|\frac{df(\Phi)}{d\Phi}\right| \frac{dW}{d\Phi} e^{A(\Phi)}\right]_{\Phi_h}. \tag{5.21}$$

The quantities $df/d\Phi$ and $dW/d\Phi$ are obtained from eq. (5.14). On the other hand, $A(\Phi)$ can be obtained by combining the two eqs. (5.11),

$$\frac{d\Phi}{dA} = -\frac{9}{4}\frac{d\log W}{d\Phi} \simeq -\frac{9}{4}\left[Q + \frac{P}{2}\frac{1}{\Phi} + \dots\right], \tag{5.22}$$

which upon integration which gives:

$$A(\Phi) \simeq -\frac{4}{9Q}\Phi + \frac{2P}{9Q}\log\Phi. \tag{5.23}$$

Inserting these expressions in eq. (5.21) we obtain:

$$T(\Phi_h) \simeq \frac{KQ}{4\pi} e^{\frac{(Q^2-4/9)}{Q}\Phi_h} \Phi_h^{P/2+(2P/9Q)} \qquad \Phi_h \gg \Phi_0 \tag{5.24}$$

From equation (5.24) we deduce that the thermodynamic behavior of black-hole solutions is very different according to the IR confining properties of the zero-T solution:

1. if $\boldsymbol{Q > 2/3}$, **or** $\boldsymbol{Q = 2/3}$ **and** $\boldsymbol{P > 0}$ **(i.e. the** $\boldsymbol{T = 0}$ **theory confines):** the temperature *increases* with Φ_h, so very small black-holes (large λ_h) corresponds to high temperature solutions.

[23] The physical reason behind this criterion was that, if the singular background has a holographic interpretation as the zero-temperature vacuum of a 4D theory, then it should be possible to obtain it continuously as the $T \to 0$ limit of a thermal state, described holographically by a black-hole. This reasoning assumes that a small black-hole, which is infinitesimally close to the vacuum background, has also an infinitesimally small temperature. In the following section we will see that this is not necessarily true: there are cases (e.g. in the presence of a deconfining phase transition at finite T) when the $M \to 0$ limit of the black-hole corresponds to a *high temperature* limit. Thus, in the most interesting cases of confining backgrounds, the criterion of [29] loses part of its physical motivation.

JHEP05(2009)033

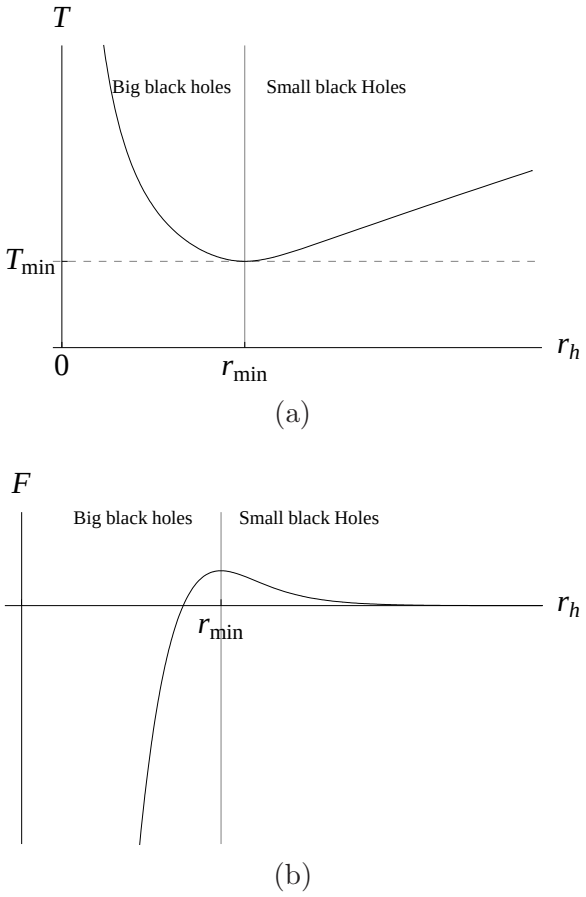

Figure 1. Typical plots of the black-hole temperature (a) and free energy (b) as a function of the horizon position r_h, in a confining background. The temperature features a minimum at $r_{\min}$, that separates the large black-hole from the small black-hole branches.

2. if $Q < 2/3$, or $Q = 2/3$ and $P < 0$ (the $T = 0$ theory does not confine):
   The temperature decreases with Φ_h, and the limit $\Phi_h \to \infty$ corresponds to $T \to 0$.

Since, in all cases, T *decreases* with Φ_h in the UV regime, it follows that:

In confining theories, $T(\Phi_h)$ must have a minimum value $T_{\min}$ below which there is no black-hole solution. In this region the only remaining solution is the thermal gas. In particular, $T_{\min}$ cannot be zero: this would imply the existence of a point where $\dot{f} = 0$, but from eq. (3.7) we observe that if $\dot{f}$ vanishes at some point where b is regular, it must vanish everywhere.

What we have shown implies that confining theories admit (at least) two branches of black-holes with the same temperature, starting at $T = T_{\min}$. For $T < T_{\min}$ there are no black-hole solutions, whereas for high enough temperature there are exactly two black-holes:

1. the *big black-hole* has its horizon closer to the AdS boundary, satisfying the relation (5.1),

$$r_h^{\text{big}} \simeq \frac{1}{\pi T}. \tag{5.25}$$

JHEP05(2009)033

2. the *small black-hole* has its horizon deep in the interior. With the asymptotics (5.19), the horizon position is related to the temperature by (inverting (5.20):

$$r_h^{\text{small}} \simeq L\left(\frac{4\pi}{\alpha}TL\right)^{1/(\alpha-1)}, \qquad \alpha > 1 \tag{5.26}$$

The typical situation (with two branches of solutions) is depicted in figure 1.

Generically, the big black-holes are thermodynamically stable whereas the small black-holes are unstable. Using $c_v = TdS/dT$ and (3.26), we obtain,

$$\frac{dT}{d\lambda_h} = \frac{3ST}{c_V}\frac{dA}{d\lambda_h}. \tag{5.27}$$

If $dA(\lambda_h)/d\lambda_h < 0$, the condition for thermodynamic stability i.e. $c_V > 0$ coincides with $dT/d\lambda_h < 0$, which is true for big black holes; on the other hand for the small black-holes $dT/d\lambda_h > 0$, hence if $A(\lambda_h)$ is monotonic, they have negative specific heat and are unstable. Although typically $dA(\lambda_h)/d\lambda_h < 0$ is satisfied, since generally increasing λ_h means going deeper in the IR, it is hard to tell whether this is true for all values of λ_h: recall that there is a "hidden" dependence on λ_h in $A(\lambda)$, due to the fact that the form of the scale factor is temperature-dependent. The condition $dA(\lambda_h)/d\lambda_h < 0$ is certainly obeyed asymptotically both for small λ_h and for large λ_h, where all black-hole metrics reduce to the zero temperature solution: for small λ_h, $A(\lambda_h) \sim (b_0\lambda_h)^{-1}$, and for large λ_h, $A(\lambda_h) \sim -2/3\log\lambda_h$. However one might have some range of λ_h where $dA(\lambda_h)/d\lambda_h > 0$, thus the small black-holes are stable, or the big ones unstable. We have found some numerical evidence of this behavior, where the violation of monotonicity of $A(\lambda_h)$ is always in a very limited range of λ_h, and only in the small black-hole branch. Since the big black-holes are the thermodynamically dominant solutions above T_c, we don't expect them to become unstable for $T > T_c$, since the dilaton potentials we use can always be written in terms of a superpotential: this guarantees the validity of the Positive Energy Theorem [39], which in turn guarantees stability of the vacuum.

We now illustrate the general behavior just described with a few simple concrete examples, for which we solved numerically Einstein's equations, starting from an explicit form of the dilaton potential. In the case of the explicit potential that was considered in [28], the numerical results for the thermodynamics were discussed in [30], and they indeed agree with the general results discussed above. Here we present the result for a simple class of potentials, which have the IR asymptotics of the form (5.9) for general P and Q:

$$\frac{V(\lambda)}{12} = 1 + \lambda + V_1\lambda^{2Q}\left[\log\left(1+V_2\lambda^2\right)\right]^P \tag{5.28}$$

where we have set the AdS scale to unity. Also, we have set the coefficient of the linear term to one. This can be done by rescaling λ and redefining the coefficients V_1, V_2.

The numerical results for the function $T(\lambda_h)$ for $Q = 2/3$, fixed V_i, and various values of P are shown in figure 2. They confirm our general analysis: confining potentials ($P \geq 0$) feature a minimum black-hole temperature, whereas in non-confining ones ($P < 0$) the temperature can be arbitrarily low.

JHEP05(2009)033

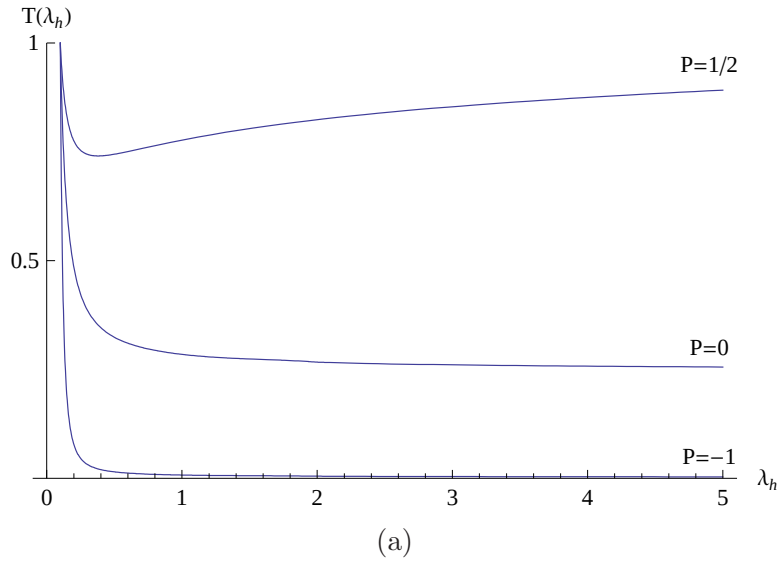

(a)

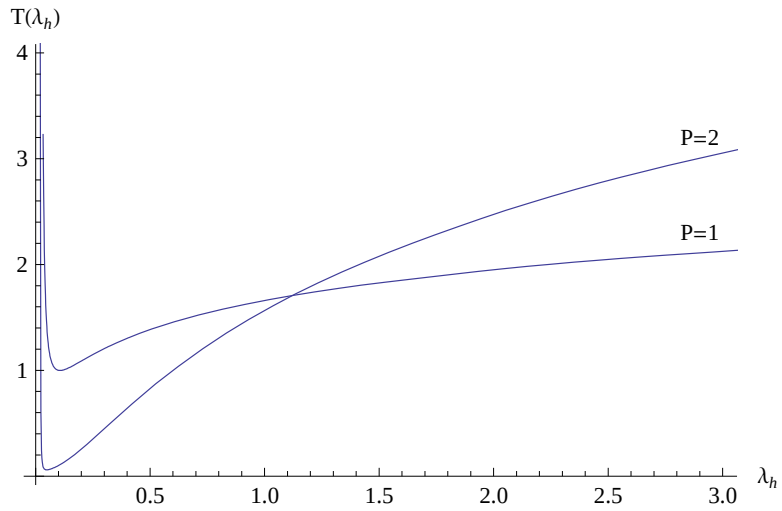

(b)

Figure 2. The temperature as a function of the horizon value of λ in the model specified by the potential (5.28), for $Q = 2/3$ and various values of P. The other coefficients are fixed to $V_1 = 10$, $V_2 = 100$. The confining models ($P > 0$) feature a minimum temperature at finite λ_h; in the non-confining model ($P = -1$) the $T(\lambda_h)$ monotonically decreases to zero; In the borderline case ($P = 0$) $T(\lambda_h)$ decreases monotonically to a finite value as $\lambda \to \infty$.

As discussed earlier, the temperature is guaranteed to be a single-valued function of λ_h, but the same is not necessarily true if we consider T as a function of the horizon position r_h. A rather striking example of this fact is shown in figure 3: it displays the plot of the curve $T(r_h)$ in a case ($Q = 2/3$, $P = 2$) where the singularity of the vacuum solution is at a finite value r_0 of the conformal coordinate. For comparison, the curve $T(\lambda_h)$ in the same model, shown in figure 2 (b), is single-valued. One unexpected feature is that in this case there are

JHEP05(2009)033

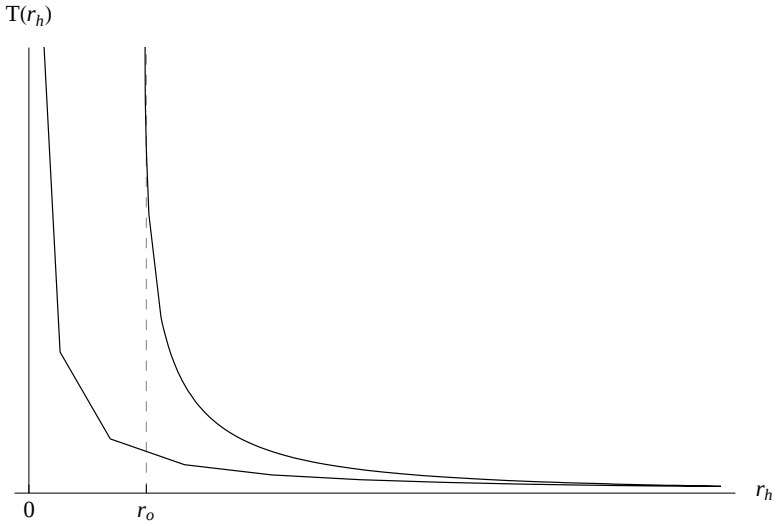

Figure 3. Temperature as a function of (a) r_h in the model (5.28) for $Q = 2/3$ and $P = 2$. The temperature diverges for $\lambda_h \to \infty$, for which $r_h \to r_0$. It is a single-valued function of λ_h, but not of r_h.

black-holes whose horizon is well beyond the position of the zero-temperature singularity at $r = r_0$. Nevertheless, as the temperature increases along the small black-hole branch, we have $r_h \to r_0$ as expected.

5.2.3 An integral representation for the free energy

As described above, in many cases there are more than one black-hole solutions, some of them having negative specific heat. This is reflected in the fact that λ_h (or r_h) as a function of T is generically multi-valued. The formula for the free energy that we derive here will encompass all of the different branches under one integral representation. This form will be used to prove the proposition in the next subsection. It is also a very convenient form for numerical evaluation of the free energy, in the process of determining the thermodynamics of the system numerically. Here we present the discussion for the case of two branches of solutions, one small and one big black-hole for simplicity of the presentation. However the final result is easily generalized to multi-black-hole cases.

Let us denote the free energies of the small and the big black-hole by $\mathcal{F}_S$ and $\mathcal{F}_B$ respectively.

Integrating the first law, $S = -d\mathcal{F}/dT$ for the big BH, one obtains,

$$\mathcal{F}_B(T) = \mathcal{F}_{\rm min} - \int_{T_{\rm min}}^{T} S_B dT, \qquad T > T_{\rm min} \tag{5.29}$$

where $\mathcal{F}_{\rm min} = \mathcal{F}(T_{\rm min})$.

In order to determine the integration constant in (5.29) one can make use of the same formula but *on the small BH branch*. This is clearly suggested from figure 4 where we depict a generic form for the function $\mathcal{F}(T)$ in case of two-branches. First, note that $\mathcal{F}_{\rm min}$

JHEP05(2009)033

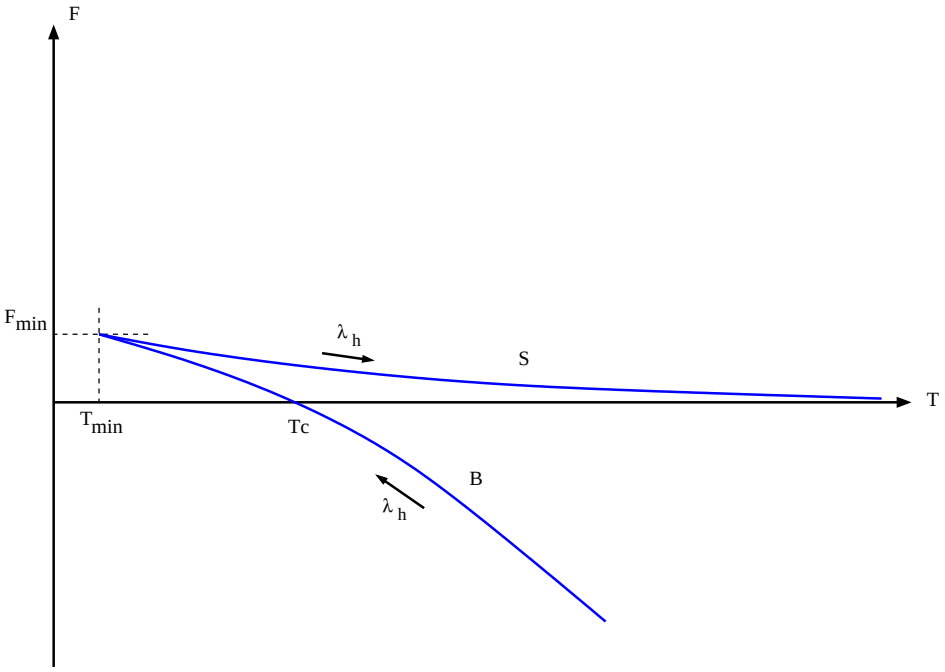

Figure 4. Black hole free energy

is the same on both branches (see figure 4):

$$\mathcal{F}_B(T_{\rm min}) = \mathcal{F}_S(T_{\rm min}) = \mathcal{F}_{\rm min}. \tag{5.30}$$

Thus one has:

$$\mathcal{F}_S(T) = \mathcal{F}_{\rm min} - \int_{T_{\rm min}}^{T} S_S dT, \qquad T > T_{\rm min} \tag{5.31}$$

The small black-hole free energy vanishes in the limit of zero black-hole size (where the metric coincides with the zero-temperature background), which for confining backgrounds is the $T \to \infty$ limit. This allows to write $\mathcal{F}_{\rm min}$ as:

$$\mathcal{F}_{\rm min} = -\int_{+\infty}^{T_{\rm min}} S_S \; dT, \tag{5.32}$$

Combining (5.29) with (5.32) one obtains an integral representation for the free energy that only depends on the area of the horizon, and is valid on both branches. It can be put in a simpler form in the λ_h variable. Using (3.26) one obtains,

$$\mathcal{F}_B(\lambda_h) = -4\pi\sigma \int_{\infty}^{\lambda_h} b^3(\tilde{\lambda}_h) \frac{dT}{d\tilde{\lambda}_h} d\tilde{\lambda}_h, \qquad \lambda_h < \lambda_{\rm min}, \tag{5.33}$$

where $\lambda_{\rm min}$ is the horizon position of the minimum temperature black-hole. Note that the two branches are combined in the integral as both b and T are single-valued as functions of λ_h, but are not as functions of T. In appendix H.10 we present further useful formulas regarding this integral representation. We remark that r.h.s. of (5.33) is finite everywhere

JHEP05(2009)033

except at $\lambda_h = 0$ where $\mathcal{F}_B \to -\infty$. Finiteness near the singularity $\lambda_h = \infty$ follows from the fact that, for all of the confining cases, b^3 vanishes exponentially faster than $dT(\lambda_h)/d\lambda_h$.

We note the remarkable fact that the free energy is completely determined by the knowledge of area of (the small and the big) black-hole horizons. This means that the entire thermodynamic properties of the dual field theory is encoded in the horizon areas, as a function of T. We stress that the area of the big BH horizon only is not sufficient; this misses the integration constant (5.30). It is therefore not sufficient to determine T_c for instance. An alternative way to say this is as follows: as we showed in eq. (3.25) there are two contributions to the free energy: the entropy and the condensate. Here we learn that, *we need both branches to disentangle the two contributions.*

5.3 Confinement and phase transitions

In this section we show the one-to-one connection between color confinement (in the vacuum background) and the presence of a deconfining transition:

Proposition:

i. *There exists a confinement-deconfinement phase transition at finite T, if and only if the zero-T theory confines.*

ii. *This transition is of the* **first order** *for* **all** *of the confining geometries, with a single exception:*

iii. *In the limit confining geometry $A_o(r) \to -r/L$ (as $r \to \infty$), the phase transition is of the* **second order** *and happens at $T = 3/(4\pi L)$.*

iv. *All of the non-confining geometries at zero-T are always in the black-hole phase at finite T. They exhibit a second order phase transition at $T = 0^+$.*

We outline our demonstration in the coordinate system where λ is chosen as the radial variable. Being diffeomorphism invariant, our arguments apply to all of the confining zero-T geometries that are described in section 2.[24]

We first consider the geometries that confine the color charge at zero T. In section (5.2) we have shown that there exists an extremum of $T(\lambda_h)$ if and only if the zero T theory confines. Thus, for confining potentials there exists such points $\lambda_{\rm min}$ that satisfy,

$$\left.\frac{dT}{d\lambda_h}\right|_{\lambda_{\rm min}} = 0 \qquad where \qquad T(\lambda_{\rm min}) \equiv T_{\rm min} > 0. \tag{5.34}$$

In figure 5 a schematic plot of $T(\lambda_h)$ for the typical examples of confining, non-confining and the borderline cases is shown.

Now, it follows from the positivity of the entropy and the first law of thermodynamics $S = -d\mathcal{F}/dT$, that the extrema of $T(\lambda_h)$ coincide with the extrema of $\mathcal{F}(\lambda_h)$. To see this we write $-S = d\mathcal{F}/dT = (d\mathcal{F}/d\lambda_h)/(dT/d\lambda_h)$ and observe that in order for $S > 0$ at all λ_h,

[24] One can state the part iii of the theorem in a diffeomorphism-invariant way by stating that the borderline geometry is defined as $\lim_{\lambda\to\infty}(X + \frac{1}{2})\log\lambda = 0$ [28].

JHEP05(2009)033

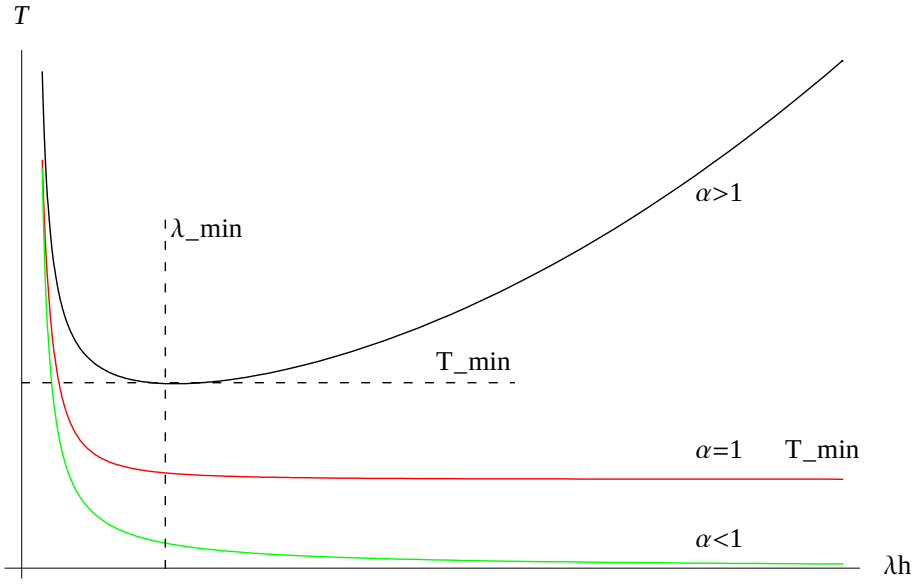

Figure 5. Temperature as a function of λ_h for the infinite r geometries of the type $A \to r^\alpha$. Black holes exist only above $T_{\rm min}$ whose precise value depend on the particular zero-T geometry.

the extrema of $T(\lambda_h)$ should coincide with the extrema of $\mathcal{F}(\lambda_h)$. Hence, for the confining potentials there exist at least one extremum of $\mathcal{F}(\lambda_h)$. See figure 6 for a schematic plot of $\mathcal{F}(\lambda_h)$.

For simplicity, here we shall assume that there exists a single $\lambda_{\rm min}$ in the confining geometries, and no extremum in the non-confining ones. We shall comment on the multi-extrema cases in the next subsection and carry out a detailed analysis in appendix G.

Let us first reproduce here the integral representation derived in the previous subsection:

$$\mathcal{F}(\lambda_h) = -4\pi M^3 V_3 \int_\infty^{\lambda_h} b^3(\tilde{\lambda}_h) \frac{dT}{d\tilde{\lambda}_h} d\tilde{\lambda}_h. \tag{5.35}$$

The integrand is positive definite for $\lambda_h > \lambda_{\rm min}$ and negative definite for $\lambda_h < \lambda_{\rm min}$. Therefore, evaluating it at $\lambda_{\rm min}$, one has,

$$\mathcal{F}(\lambda_{\rm min}) > 0. \tag{5.36}$$

On the other hand, when one evaluates (5.35) on the boundary, one finds

$$\lim_{\lambda_h \to 0} \mathcal{F}(\lambda_h) = -\infty. \tag{5.37}$$

This follows from the UV asymptotics described in section 5.1. Therefore there must exist a point λ_c where it vanishes:

$$\mathcal{F}(\lambda_c) = 0, \tag{5.38}$$

see figure fig, 6. This proves that *there exists a phase transition if the zero-T theory confines.* The transition temperature T_c is greater than $T_{\rm min}$ because $\lambda_c < \lambda_{\rm min}$ and $dT/d\lambda_h < 0$ at λ_c. This result confirms our intuitive picture that, as the temperature is increased, first the

JHEP05(2009)033

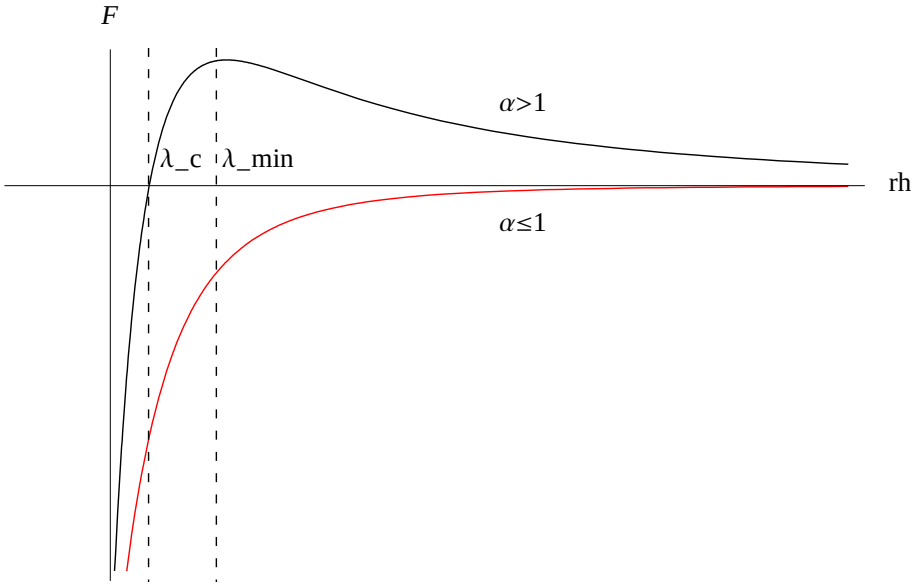

Figure 6. Free energy density as a function of λ_h for the infinite r geometries of the type $A \to r^\alpha$.

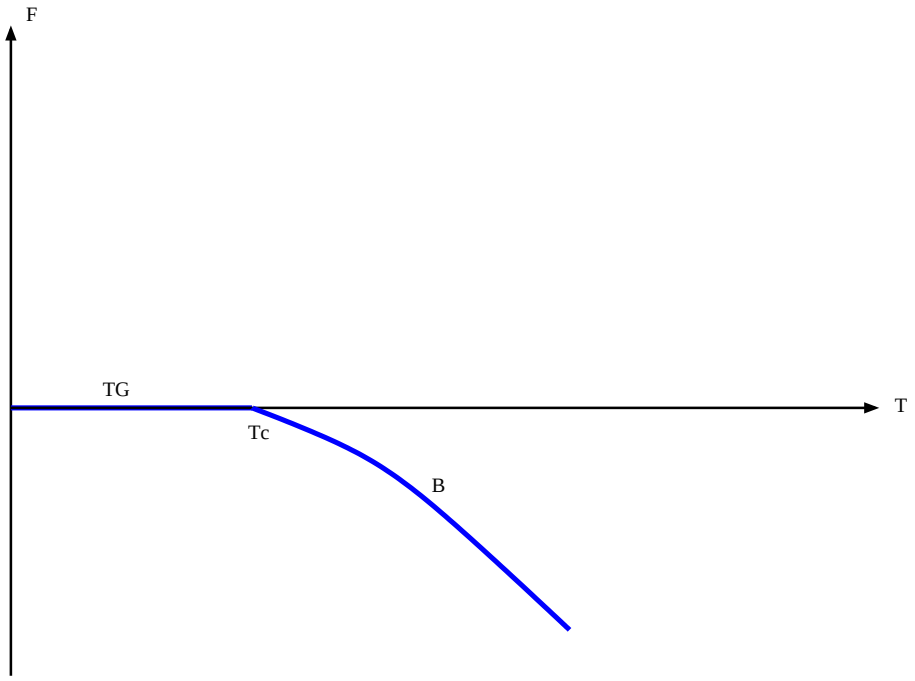

Figure 7. A schematic plot of the free energy in the typical case of a confining geometry. "B" and "TG" denote the big black-hole and the thermal gas respectively. At T_c there is a first order transition. This plot corresponds to evaluating $F(T)$ of figure 4 on the minimum energy configuration.

small and big BHs form at a temperature $T_{\rm min}$, where the minimum energy configuration is still the thermal gas, and as T is kept increasing, the big black-hole takes over the thermal gas phase at a higher temperature T_c. The true free energy of the system, i.e. the function $F(T)$ *evaluated on the minimum energy configuration*, is shown schematically in figure 7.

JHEP05(2009)033

On the other hand, for the non-confining theories (see the case $\alpha < 1$ in figures 5 and 6), $T(\lambda_h)$ is always monotonically decreasing. This is because, in the UV $T \propto \exp[1/b_0\lambda_h]$. Hence it is monotonically decreasing in the UV and there exists no extremum of this function. Therefore its derivative cannot change sign. From (5.35), it follows that $\mathcal{F}(\lambda_h) < 0$ for all λ_h and that there is *no phase transition for the non-confining potentials* at any finite-T.

We have so far proven part i. of the proposition. Parts ii. and iii. are proven as follows. The order of the phase transition is determined by the latent heat:

$$L_h = E(\lambda_c) = S(\lambda_c)T(\lambda_c). \tag{5.39}$$

It follows from (3.26) that, $S(\lambda_c)$ is non-zero unless λ_c coincides with the singularity. Therefore $L_h > 0$ and the phase transition is *first order* for the standard confining geometries. For example, this is the case for $\alpha > 1$ in infinite geometries, (see figures 5 and 6).

On the other hand, in the borderline case $\alpha = 1$, $T_c = T_{\rm min}$ and, at λ_c the entropy vanishes, because λ_c coincides with the singularity and $b(\lambda_c) \to 0$ there. Thus, in this case the transition is of *second order*. It would be interesting to find other examples of second order phase transitions in the Einstein-dilaton system.

The last part of the proposition follows simply from the fact that, for all the non-confining geometries, $\mathcal{F}(\lambda_h) < 0$ for all λ_h and it vanishes only at the singularity. At this point both T and S vanish as the area of the horizon vanishes. Thus there is a trivial second order phase transition at $T = 0^+$ and *the system is always in the black-hole phase* for any finite-T.

5.3.1 Geometries with multiple extrema

We demonstrated our proposition under a single assumption, that the function $T(\lambda_h)$ has at most one single local extremum. We did not find any counter-example to this assumption in our numerical studies, and it is a logical possibility that, with the given assumptions for $V(\lambda)$ (that it is a positive and monotonically increasing function of λ that limits to a constant at $\lambda = 0$ and diverges exponentially as $\lambda \to \infty$), multiple extrema cases never occur. However, we can not rule out these possibilities by analytic arguments, therefore they should be considered in order to complete our demonstration. Moreover, as we discuss below, they bear interesting possibilities for new types of phase transitions.

In general, there may exist theories which admit more than one small and one big black-hole. In these cases, the functions $\mathcal{F}(\lambda_h)$ and $T(\lambda_h)$ are complicated and admit many extrema. As a result $F(T)$, evaluated on the entire set of solutions (not only the lowest energy solution) may be a complicated multi-valued function with many cusps and crossings, see figure 17 in appendix G for an example.

The proof of part i. of the proposition extends without changes to the general case with multiple extrema. To prove points ii. iii. and iv. in full generality, however, we must make an additional assumption on the behavior of the entropy as a function of λ_h: we must assume that a generic black-hole in a given branch has larger entropy than a generic black-hole in the next (with larger λ_h) branch. This is a weak version of monotonicity of

JHEP05(2009)033

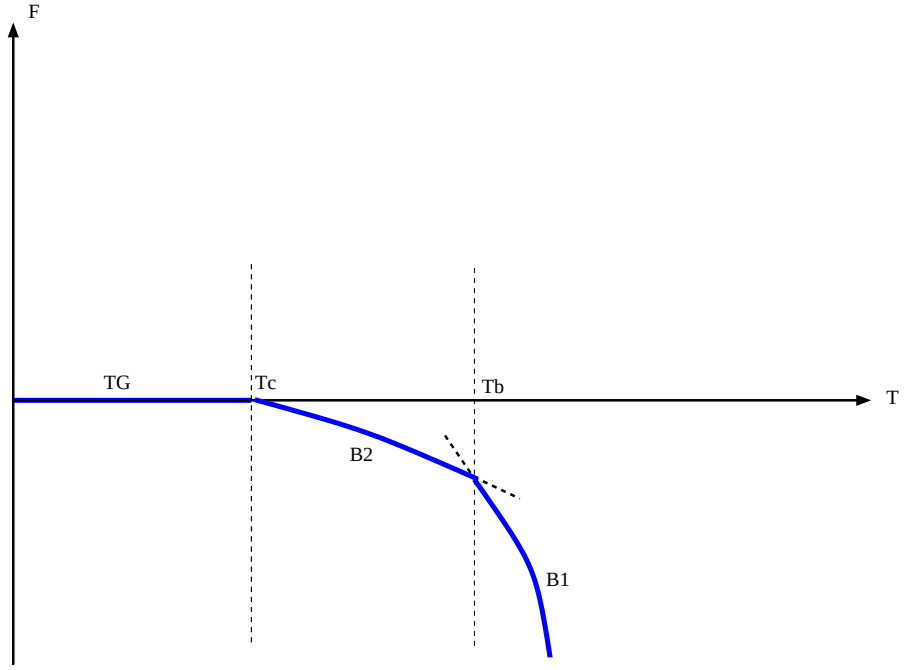

Figure 8. The function $F(T)$ for a multiple extrema case, evaluated on the minimum energy configuration. Here $k = 1$, i.e. there are two big-black-hole geometries denoted by B_1 and B_2 with a first-order transition between them at T_b. TG denotes the thermal gas geometry, that takes over below T_c.

$S(\lambda_h)$, and it is a sufficient condition for the full proposition to hold, although it might not be necessary.[25]

The details of the general case are presented in appendix G. The upshot of the analysis in G is that, regardless how complicated the system is, $F(T)$ *evaluated on the minimum energy configuration* always have a similar form to figure 7 as in the single extremum case. Since, in the infinite volume limit, only the lowest energy configuration is relevant for the thermodynamics, our demonstration in the previous subsection directly carries over to cases of multiple extrema. The precise statement is that *regardless how complicated the function* $T(\lambda_h)$ *is, there exists a confinement-deconfinement phase transition if and only if the corresponding zero-T theory confines.*

However, our analysis in appendix G shows another interesting possibility: in the multiple extrema cases, there may exist *first order phase transitions between different deconfined vacua*. The temperature of these transitions are *always higher than the deconfinement temperature* T_c. In general, there may be an arbitrary number k, of such transitions with $T_k > T_{k-1} > \cdots T_1 > T_c$. In the dual geometric picture, these transitions occur between *different big black-hole geometries*. For a number k of such transitions, the function $T(\lambda_h)$ should possess k local minima and $k-1$ local maxima. This means that, there should be k different pairs of small and big black-holes. This is a necessary condition but it is not

[25]Strict monotonicity is too strong a condition, since we have found numerical counterexamples where this is not satisfied.

JHEP05(2009)033

sufficient. The sufficient condition follows from the particular shape of $F(T)$ that leads to such transitions between different big black-hole branches. An example is discussed in appendix G. We present the free energy for the minimum energy configuration, for the case $k = 1$ in figure 8. The fact the these transitions are always first order follows from discontinuity in $F'(T)$ at T_l, as shown in figure 8 and appendix G.

It was argued that there could be a series of phase transitions in large-N_c gauge theory that would correspond to a partial, step-by-step breaking of the center Z_N of the gauge group, [33]. At large N_c there is room for an arbitrary number of such steps. The order parameter corresponding to the l-th such transition would be $\langle \mathrm{Tr}\ \mathcal{P}^l \rangle$, namely the l-th power of the Polyakov loop. It is plausible that such phase transitions may be in the same universality class as the ones described above.

Let us remark however, that, neither in the lattice studies of [33] nor in our numerical investigations, one has encountered such transitions. They may exist as an exotic possibility in our set-up.

5.4 Similarities with the Yang Mills deconfinement transition

We have found that backgrounds which exhibit confinement, also exhibit a deconfinement phase transition at some finite temperature T_c, above which the black-hole phase dominates. The qualitative features of the phase transition and of the thermodynamics of the deconfined phase are remarkably similar to those found in four dimensional pure Yang Mills theory at large N_c.

Below we list some of the model-independent features of the gravity phase transition that match the gauge theory side. We will analyze the quantitative agreement in concrete models in a separate work [36].

- It is a confinement-deconfinement transition. In particular in the high temperature phase the confining string tension vanishes.

- The Polyakov loop is the order parameter for the confinement-deconfinement transition of SU(N_c) YM theory. The vev of the Polyakov loop $\langle \mathcal{P} \rangle$ is zero in the confined phase and it acquires a non-zero expectation value above T_c. Here we see the analogous behavior in the dual geometric picture [4]: Holographically, the Polyakov loop is described by a classical string embedding that wraps the Euclidean time direction. In the thermal gas solution the time circle is non-shrinkable, hence the action of the string is infinite, giving a zero vev for the Polyakov loop. On the other hand, in the black-hole solution, the time circle shrinks to zero size at the horizon and one obtains a non-trivial vev.

- Both in large-N_c Yang-Mills and in the gravity theory the phase transition is first order, with a latent heat that scales as N_c^2. On the gravity side the latent heat per unit volume is given by (see eq. (3.27))

$$L_h = N_c^2 M_p^3 \left(15\mathcal{G}(T_c) + 3\pi T_c b^3(r_c)\right) = N_c^2 \frac{4}{3}\ell^{-3}\mathcal{G}(T_c) = N_c^2 \frac{4\pi}{45}\ell^{-3} T_c b^3(T_c). \quad (5.40)$$

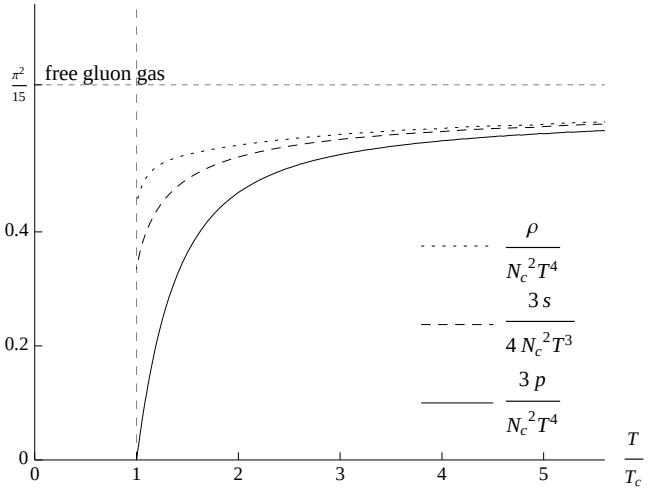

Figure 9. The energy density ρ, entropy density s and pressure p in the black-hole phase for $T_c < T < 5T_c$.

- As in large-N_c Yang-Mills, the quantity $\mathcal{F}/N_c^2$ serves as an order parameter: it is of order one in the deconfined phase, and zero in the confined phase

- The high temperature behavior is the same of a free gluon gas, up to logarithmic corrections. This behavior can be seen in the temperature dependence of the pressure $p = -\mathcal{F}/V_3$, energy density ρ, and entropy density s: from eq. (5.6) and standard thermodynamic relations, and with the choice (5.8) for the Planck scale, we have:

$$\left.\begin{array}{l} \frac{\rho(T)}{T^4} \\ \\ \frac{3p(T)}{T^4} \\ \\ \frac{3}{4}\frac{s(T)}{T^3} \end{array}\right\} \to \frac{\pi^2}{15}N_c^2 \qquad T \to \infty. \tag{5.41}$$

  In figure 9 we present an explicit example of the behavior of these quantities in the deconfined phase, up to a temperature of $5T_c$, derived from our model with a potential of the form (5.28) with $Q = 2/3$ and $P = 1/2$.

  The deviation from conformality is expressed by the trace of the thermal stress tensor:

$$\frac{\rho - 3p}{T^4} \to \begin{cases} L_h/T_c^4 & T \to T_c \\ \\ \frac{4\pi^2 N_c^2}{135}(\log T/T_c)^{-2} & T \to \infty, \end{cases} \tag{5.42}$$

  as can be derived by combining eqs. (4.3) and (5.5). A concrete example of the temperature dependence of this quantity in the black-hole phase is shown in figure (10).

- The speed of sound is given by $c_s^2 \equiv (\partial p/\partial\rho)_S = S/C_v$, where $C_v = \partial E/\partial T$ is the specific heat. As expected in the deconfined phase of pure Yang-Mills in 4D, this quantity approaches from below the conformal value, $c_s^2 \to 1/3$ as $T \to \infty$. This

JHEP05(2009)033

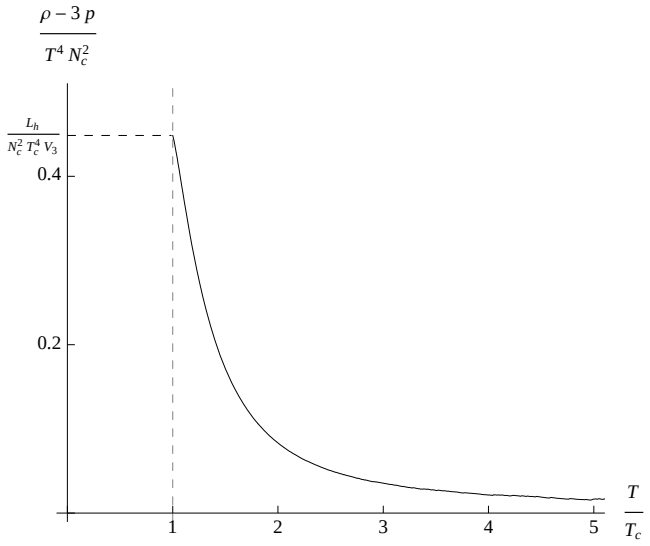

Figure 10. Temperature dependence of the trace of the stress tensor in the black-hole phase for $T_c < T < 5T_c$.

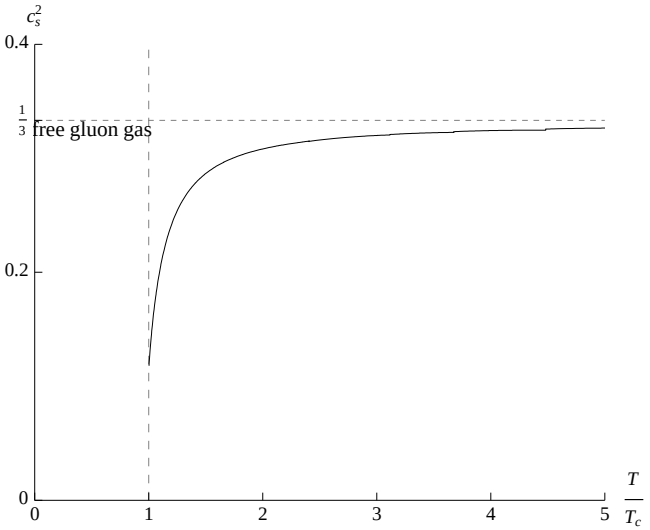

Figure 11. The speed of sound in the black-hole phase for $T_c < T < 5T_c$.

can be seen using the high-temperature expansion of the thermodynamic quantities derived in appendix I. A concrete example in our setup is shown in figure 11.

6 The axion background at finite temperature

The effect of a non-trivial vacuum angle in Yang-Mills is captured by including in the bulk a five-dimensional axion. The axion a is dual to the instanton density $Tr[F \wedge F]$. In particular its UV boundary value is the UV value of the QCD θ-angle. Moreover, its profile $a(r)$ in the vacuum solution may be interpreted as the "running" θ-angle in analogy

JHEP05(2009)033

with the dilaton, that we interpret as the running coupling constant. This was explained and justified in [28].

The axion action is suppressed by $\mathcal{O}(1/N_c^2)$ with respect to the action for the other fields, (2.1):

$$S_{\rm axion} = \frac{M_p^3}{2}\int d^5x\sqrt{-g}\; Z(\lambda)\;\; (\partial_\mu a)^2 \tag{6.1}$$

where $Z(\lambda)$ has the following asymptotic expansions, [28],

$$\lim_{\lambda\to 0} Z(\lambda) = Z_a\left[1+\mathcal{O}(\lambda)\right] \quad , \quad \lim_{\lambda\to\infty} Z(\lambda)\sim \lambda^4 \tag{6.2}$$

The scale Z_a determines the topological susceptibility, while the strong coupling asymptotics are dictated from glueball universality.

At zero temperature the axion solution that is compatible with known properties of large-N_c YM is

$$a(r) = (\theta_{\rm UV}+2\pi k_0)\;\frac{\int_r^{r_0}\frac{dr}{e^{3A}Z(\lambda)}}{\int_0^{r_0}\frac{dr}{e^{3A}Z(\lambda)}} \quad , \quad k_0\in Z \tag{6.3}$$

where $\theta_{\rm UV}$ is the UV value of the θ parameter defined as an angle in the range $[0,2\pi)$, k_0 is an integer that labels oblique confining vacua and is determined by minimizing the θ-dependent vacuum energy

$$E(\theta_{\rm UV},k) = -\frac{M_p^3}{2}\;\frac{(\theta_{\rm UV}+2\pi k)^2}{\int_0^r dr\frac{e^{-3A}}{Z(\lambda)}} \tag{6.4}$$

Finally r_0 is the position of the singularity of the zero-temperature geometry in the radial coordinates.

From this solution we can extract the topological susceptibility and topological density condensate as

$$\chi = \frac{Z(0)M_p^3}{\int_0^{r_0}\frac{dr Z(0)}{e^{3A}Z(\lambda)}} \quad , \quad \langle Tr[F\wedge F]\rangle = -\frac{32\pi^2}{\ell^3}\frac{(\theta_{\rm UV}+2\pi k_0)}{\int_0^{r_0}dr\frac{Z(0)}{e^{3A}Z(\lambda)}} \tag{6.5}$$

At finite temperature, below the deconfining phase transition the situation is similar to $T=0$, since it is the same vacuum solution describing the physics. Above T_c however, once should switch to the black-hole solution. In the black-hole solution the axion background satisfies,

$$\ddot{a}+\left(3\dot{A}+\frac{\dot{f}}{f}+(\partial_\lambda\log Z)\dot{\lambda}\right)\dot{a}=0 \tag{6.6}$$

an equation that can be integrated once to

$$\dot{a} = \frac{C_a}{f\; e^{3A}\; Z(\lambda)} \tag{6.7}$$

where C_a is a constant. Integrating once more we obtain

$$a(r) = \theta_{\rm UV} + C_a\int_0^r\frac{dr'}{f\; e^{3A}\; Z(\lambda)} \tag{6.8}$$

JHEP05(2009)033

Unlike the zero temperature solution, the non-trivial solution here has a singularity at the horizon. Indeed, $f(r) \sim f_0(r-r_h)$ while both $Z(\lambda)$ and e^A are regular there. Therefore the function $\int_0^r \frac{dr'}{f\ e^{3A}\ Z(\lambda)}$ diverges logarithmically as $r \to r_h$. Since the background solution must be regular everywhere, we must necessarily impose $C_a = 0$.

Therefore in the deconfined phase, the axion background is constant

$$a(r) = \theta_{\rm UV} \tag{6.9}$$

and the topological density condensate (proportional to C_a) vanishes

$$\langle F \wedge F \rangle_{\rm deconfined} = 0 \tag{6.10}$$

In fact this can be generalized to higher derivative terms containing the axion. This shows that in the deconfined phase, at large N_c all moments of the topological density vanish. This is in agreement with general expectations at large N_c, since in the deconfined phase such moments obtain contributions only from instantons, that give vanishing e^{-N_c} contributions as $N_c \to \infty$. This expectation is in accordance with lattice calculations , [41].

7 Reduction and solution of the system in scalar variables

Einstein's equations are hard to solve for a generic dilaton potential. This is the case even in numerical evaluation. Here we shall present a method to reduce the degree of the system of equations from 5 to 2 by introducing variables that are explicitly invariant under general coordinate transformations.

There are a number of nice features of this reduction. First, the thermodynamics will only depend on the reduced system. Therefore all thermodynamic observables are determined by solving a coupled system of first order equations. This also clarifies the number of physical parameters in the theory, see section 7.6. It also allows us to find analytic solutions (appendix J).

Aa another bonus, the UV expansion of the finite temperature metric and dilaton used throughout the paper, eqs. (3.13)–(3.14) , are most easily derived with this formalism. This is done in Subsection 7.2.

Finally, this form of Einstein's equation is used in appendix H.4 to show the existence of black-hole solutions with arbitrary λ_h and AdS UV asymptotics.

This section can be read independently of the rest of the paper. All of the ingredients necessary to derive the thermodynamics from the Einstein's equations in a diffeomorphism-invariant manner are presented in this section in a self-contained way.

7.1 Scalar variables

The basic idea was introduced in [28] for the zero-T case and reviewed in section 2. Here we present a generalization of [28] to the black-hole ansatz. We propose to solve the Einstein's equations by introducing the following scalar variables:

$$X(\Phi) = \frac{\Phi'}{3A'}, \qquad Y(\Phi) = \frac{g'}{4A'}. \tag{7.1}$$

JHEP05(2009)033

Note X and Y are invariant under radial coordinate transformations. These variables obey the following first order equations:

$$\frac{dX}{d\Phi} = -\frac{4}{3}(1 - X^2 + Y)\left(1 + \frac{3}{8X}\frac{d\log V}{d\Phi}\right), \tag{7.2}$$

$$\frac{dY}{d\Phi} = -\frac{4}{3}(1 - X^2 + Y)\frac{Y}{X}. \tag{7.3}$$

As shown in section 7.4, the thermodynamics of the dual field theory are completely determined by knowledge of X and Y as a function of Φ. Roughly speaking, Y is dual to the entropy and X to the energy of the gluon fluid.

It is crucial that the system above always admits a special solution, $Y = 0$. This corresponds to the *thermal gas solution* (or the zero-T solution for non-compact time), that is present for any V. This is because, for the solution $Y = 0$, the equation (7.2) reduces to the corresponding zero-T equation (2.10) whose only solution with fixed IR asymptotics is the thermal gas.

The metric functions are given in terms of X and Y by integrating eqs. (7.1). Let us introduce a cut-off Φ_0, that plays the role of the regularized UV boundary. We call the value of the scale factor A at this point as A_0. On the other hand, the black-hole asymptotics requires that g vanishes ($f \to 1$) on the boundary. With these initial conditions, integration of (7.1) gives

$$A = A_0 + \int_{\Phi_0}^{\Phi} \frac{1}{3X} d\tilde{\Phi}, \tag{7.4}$$

$$g = \int_{\Phi_0}^{\Phi} \frac{4}{3}\frac{Y}{X} d\tilde{\Phi}. \tag{7.5}$$

We note that one does not need the cut-off Φ_0 in solving (7.2), (7.3). As we prove in the sequel, the physical observables only depend on the functions X and Y. Therefore they will be independent of the cut-off Φ_0.

In appendix H.1 we prove that the reduced X-Y system solves the full equations of motion (A.17)–(A.20) in the original u-variable. There, we also provide formulas for the derivatives of the metric functions A', g' and Φ' in eqs. (H.1), (H.2) and (H.3), hence completing the full five-degree system of equations.

Let us finally note that, one can invert the equations (7.2) and (7.3) for the dilaton potential:

$$V(\Phi) = V_0(1 + Y - X^2)e^{-\frac{8}{3}\int_{-\infty}^{\Phi} dt\left(X - \frac{Y}{2X}\right)}. \tag{7.6}$$

This equation will be useful later on. We note that for $Y = 0$ it reduces to the corresponding zero-T equation in [28].

7.2 UV asymptotics

In what follows we prefer working in the $\lambda = \exp(\Phi)$ variable instead of Φ.[26] The black-hole deformation is obtained by turning on Y near the boundary. In other words Y should

[26] For notational simplicity, we shall allow for an abuse of notation by referring to, in fact, *different* functions when we write e.g. $V(\lambda)$ and $V(\Phi)$, related by $V(x) \to V(e^x)$.

JHEP05(2009)033

vanish as one approaches the boundary. In addition, the condition that the BH solution approaches the thermal gas solution requires that $X \to X_0$ on the boundary. We recall that the UV asymptotics of the function X_0 is presented in eq. (2.11). Let us now write,

$$X(\lambda) = X_0(\lambda) + \delta X(\lambda), \qquad \lambda \to 0, \tag{7.7}$$

where $\delta X \ll X_0$ for small λ. Studying the small λ asymptotics of the explicit solution for Y, given in eqs. (H.9, H.10), one learns that Y vanishes non-perturbatively in λ; to be precise $Y \sim e^{-4/b_0\lambda}\lambda^{-4b}$. This can also be seen by assuming that Y is exponentially small and than solving (7.3) in the vicinity of $\lambda = 0$. Then, it follows from (7.2) that δX also vanishes with the same exponential factor.

One derives the asymptotic behavior of the functions Y and δX by solving (7.3) and (7.2) near $\lambda = 0$. We spare the details of this calculation to appendix H.5. The result is

$$Y(\lambda) = \mathbf{Y_0}\, e^{-\frac{4}{b_0\lambda}}(b_0\lambda)^{-4b}, \tag{7.8}$$

$$\delta X(\lambda) = \left[\frac{\mathbf{Y_0}/2 - \mathbf{C_0}}{X_0} + \mathbf{C_0} X_0\right] e^{-\frac{4}{b_0\lambda}}(b_0\lambda)^{-4b}. \tag{7.9}$$

Here $\mathbf{Y_0}$ and $\mathbf{C_0}$ are integration constants. They retain finite values as the cut-off is removed by sending $\lambda_0 \to 0$. These values can be computed by matching the solutions above to the full solution of (7.2) and (7.3). Generally these integration constants are non-trivial functions of temperature and this dependence is determined by the regularity condition at the horizon. This is explained in section 7.3 below.

The physical meaning of these integration constants will become clear below: $\mathbf{C_0}$ *determines the energy,* $\mathbf{Y_0}$ *determines the entropy and the combination,*

$$\mathbf{G_0} = \mathbf{C_0} - \frac{\mathbf{Y_0}}{2}, \tag{7.10}$$

determines the vev of the gluon condensate in the gluon plasma.

Finally, we would like to know the UV expansions of the metric functions A, f and Φ in the radial variable u or r. These can be determined using the asymptotic expressions for X and Y given by (7.8) and (7.9) in the formulae for the derivatives A', f' and Φ' given by (H.1), (H.2), (H.3).

To make use of these equations, we first define the fluctuations in A and Φ in the domain wall frame as,

$$\delta A(u) = A(u) - A_o(u), \qquad \delta\Phi(u) = \Phi(u) - \Phi_o(u). \tag{7.11}$$

One then finds:

$$\delta A = \frac{1}{2}\mathbf{G_0} e^{-\frac{4}{b_0\lambda}}(b_0\lambda)^{-4b} + \cdots = \frac{1}{2}\mathbf{G_0}(\Lambda\ell)^4 e^{4u/\ell}(-u/\ell)^{-16/9} + \cdots \tag{7.12}$$

$$f = 1 - \mathbf{Y_0} e^{-\frac{4}{b_0\lambda}}(b_0\lambda)^{-4b} + \cdots = 1 - \mathbf{Y_0}(\Lambda\ell)^4 e^{4u/\ell}(-u/\ell)^{-16/9} + \cdots \tag{7.13}$$

$$\delta\Phi = \frac{9}{4}\mathbf{G_0} e^{-\frac{4}{b_0\lambda}}(b_0\lambda)^{-4b-1} + \cdots = \frac{9}{4}\mathbf{G_0}(\Lambda\ell)^4 e^{4u/\ell}(-u/\ell)^{-16/9+1} + \cdots. \tag{7.14}$$

JHEP05(2009)033

In the last equations we used the results in appendix H.1 to convert the expression in the u variable, with the scale Λ defined in eq. (2.18).

Finally, we want to write an expression for the fluctuation in the conformal frame scale factor and dilaton. To this end, we can use the relation (valid close to the UV boundary $r \to 0$):

$$\frac{r}{\ell} = e^{u/\ell} \left(-u/\ell\right)^{-4/9}, \tag{7.15}$$

see appendix H.1. However, it is not enough to just re-express eq. (7.12) and (7.14) in terms of r through (7.15): as shown in appendix (A.4) one gets an extra shift in δA when changing the frame. The final result is:

$$\delta A(r) = \frac{2}{5}\mathbf{G_0}(\Lambda r)^4, \quad \delta\Phi = \frac{9}{4}\mathbf{G_0}(\Lambda r)^4 \log r\Lambda, \quad f(r) = 1 - \mathbf{Y_0}(\Lambda r)^4 \tag{7.16}$$

Comparison of these expansions to (3.15) and (3.13) relates the coefficients $\mathbf{Y_0}$ and $\mathbf{C_0}$ defined quantities $\mathcal{G}$ and C that enter in the free energy, eq (3.25) as

$$\mathbf{Y_0} = \frac{C\ell}{4(\ell\Lambda)^4}, \qquad \mathbf{G_0} = \frac{5}{2}\frac{\mathcal{G}\ell}{(\Lambda\ell)^4}. \tag{7.17}$$

7.3 Asymptotics near the horizon

The dependence on T on the constants $\mathbf{C_0}$ and $\mathbf{Y_0}$ is determined by the geometry of the black-hole near the horizon. Near the horizon, the black-hole solution should be regular. In particular one requires that the various metric functions and the dilaton behave as,

$$f(r) = f_1(r_h - r) + \mathcal{O}(r_h - r)^2 \tag{7.18}$$

$$A(r) = A_h + A_1(r_h - r) + \mathcal{O}(r_h - r)^2 \tag{7.19}$$

$$\Phi(r) = \Phi_h + \Phi_1(r_h - r) + \mathcal{O}(r_h - r)^2 \tag{7.20}$$

In terms of Y and X, the requirement of regular horizon translates into the following conditions:

$$Y(\Phi) = \frac{Y_h}{\Phi_h - \Phi} + Y_1 + \mathcal{O}(\Phi_h - f), \tag{7.21}$$

$$X(\Phi) = -\frac{4}{3}Y_h + X_1(\Phi_h - \Phi) + \mathcal{O}(\Phi_h - f)^2, \tag{7.22}$$

where Y_1 and X_1 are yet undetermined constants and

$$Y_h = -\frac{\Phi_1}{4A_1}. \tag{7.23}$$

When one solves the coupled system of eqs. (7.2) and (7.3) near any point Φ_i, the solution will generally be parameterized by two integration constants. At first sight, it seems that these two parameters can be taken as Y_h and Φ_h. However a more careful look at the system of equations reveals that demanding a regular horizon reduces the number of parameters to a single one, that fixes Y_h in terms of Φ_h. This can easily be seen by substituting (7.21) and (7.22) in (7.2). One obtains:

$$Y_h = \frac{9}{32}\frac{V'(\Phi_h)}{V(\Phi_h)}. \tag{7.24}$$

JHEP05(2009)033

Similarly X_1, Y_1, etc. are determined from the sub-leading terms in the expansion near the horizon. See appendix H.8. One finds the higher order coefficients in the expansion of (7.21) and (7.22) order by order. The important point is that there is no room for an arbitrary integration constant, the requirement of a regular horizon completely determines all of the coefficients in terms of Φ_h. This shows that we have a single parameter family of solutions of the X-Y system, parameterized by the location of the horizon Φ_h.

The near horizon solution presented here is continuously connected to the near UV solution that is presented in section 7.2. This fact can easily be derived by using the analytic structure of the equations of motion (7.3) and (7.2). See appendix H.4.

7.4 Thermodynamic functions and relations

The thermodynamics is completely determined in terms of the integration constants $\mathbf{C_0}$ and $\mathbf{Y_0}$. In the following, we present the derivations one by one.

Temperature. The temperature of the dual gauge theory is given by the derivative of f at the horizon,

$$T = \frac{|\dot{f}(r_h)|}{4\pi}. \tag{7.25}$$

Here, we shall express it in terms of the solution of the $X - Y$ system. The computation is straightforward and the details are presented in appendix H.9. One finds,

$$T = \frac{\Lambda}{\pi} \ (\Lambda \ \ell)^3 \ \frac{\mathbf{Y_0}(\lambda_h)}{b^3(\lambda_h)}. \tag{7.26}$$

where $b(\lambda)$ is determined from X by (7.4). This equation gives T in the physical units of Λ.

Entropy. The entropy of the field theory is determined by the area of the horizon as in (3.26):

$$S = 4\pi\sigma b^3(\lambda_h), \tag{7.27}$$

where $b(\lambda)$ is again determined from X by (7.4).

We note that, the equations (7.26) and (7.27) combine to yield the entropic contribution to the free energy density as follows,

$$ST = 4\sigma \mathbf{Y_0} \ell^3 \Lambda^4. \tag{7.28}$$

This equation clarifies the physical meaning of the integration constant $\mathbf{Y_0}$.

Free energy and energy. One can obtain an exact expression for the free energy in terms of the scalar variables. This is done by converting the eq. (3.17) in λ using the equations (H.1), (H.2), (H.3). This calculation is explained in detail in the appendix H.6. The result is expressed very simply in terms of the constants of motion defined in the previous section:

$$\mathcal{F} = -pV_3 = \sigma\Lambda^4\ell^3 \left(6\mathbf{C_0} - 4\mathbf{Y_0}\right), \tag{7.29}$$

where the second equation relates pressure to the free energy of the system. Using eq. (7.10) and (7.17), the above expression coincides with (3.25)

The energy follows directly from (7.29) and (7.28) as,

$$E = \rho V_3 = 6\sigma \mathbf{C_0} \Lambda^4 \ell^3, \tag{7.30}$$

where we defined the *energy density* as ρ. This clarifies the physical meaning of the integration constant $\mathbf{C_0}$.

Specific heat. The specific heat is given by,

$$C_v = \frac{dE}{dT} = 6\sigma\Lambda^4\ell^3 \frac{d\mathbf{C_0}}{dT} = 4\sigma\Lambda^4\ell^3 \left(\frac{d\mathbf{Y_0}}{dT} - \frac{\mathbf{Y_0}}{T} \right). \tag{7.31}$$

where we used (7.35), see below.

Speed of sound. The speed of sound in the medium is defined by $c_s^2 = dp/d\rho$, where the pressure p is given in eq. (7.29). By using thermodynamic relations, one can show that:

$$c_s^2 = \frac{S}{C_v}. \tag{7.32}$$

Using (7.31) we can derive a relation for c_s directly in terms of $\mathbf{Y_0}$:

$$\frac{1}{c_s^2} = \frac{d\log \mathbf{Y_0}}{d\log T} - 1. \tag{7.33}$$

Using the high-T asymptotics of $\mathbf{Y_0}$ given in eq. (7.36), we see that $c_s^2 \to 1/3$ for $T/T_c \gg 1$ as required from the conformality in this limit.

We refer the reader to the results presented in appendix I for the high temperature behavior of the thermodynamical functions discussed in this section.

A relation between $\mathbf{C_0}$ and $\mathbf{Y_0}$. One can also relate $\mathbf{C_0}$ and $\mathbf{Y_0}$, by using the definition of the entropy,

$$S = -\frac{d\mathcal{F}}{dT}. \tag{7.34}$$

It follows from (7.34), (7.29) and (3.26) that,

$$\mathbf{C_0}(T) = \frac{2}{3}\mathbf{Y_0}(T) - \frac{2}{3}\int_{T_c}^{T} \frac{\mathbf{Y_0}(t)}{t} dt. \tag{7.35}$$

Therefore, knowledge of $\mathbf{Y_0}$ as a function of T determines the coefficient $\mathbf{C_0}$ analytically.

Equation (7.35) also helps us determine the thermodynamics at high-T. As T increases, λ_h approaches zero, hence the geometry of the black-hole becomes the geometry of an AdS black-hole. For the AdS black-hole one has, $b = \ell/r$, $f = 1 - (r/r_h)^4$ and $T = 1/\pi r_h$. Therefore from the definition of Y in (7.1), of $\mathbf{Y_0}$ in (H.21) and the conversion between λ and r coordinates near the boundary (H.7) we obtain,

$$\mathbf{Y_0}(T) \to \left(\frac{\pi T}{\Lambda}\right)^4 \qquad \frac{T}{T_c} \gg 1. \tag{7.36}$$

JHEP05(2009)033

Using this in (7.35) one obtains,

$$\frac{\mathbf{C_0} - \mathbf{Y_0}/2}{T^4} \to 0 \qquad \frac{T}{T_c} \gg 1. \tag{7.37}$$

We present the explicit high-T behavior of this function in appendix I. We also show that this implies, through eq. (7.10), that the gluon condensate divided by T^4 vanishes at high-T.

7.5 Matching the zero-T solution

As we discussed above, the zero-T solutions of the X-Y system correspond to the special case $Y = 0$. We analyzed the entire set of solutions in this case, in appendix H.3. The conclusion of this analysis is a rephrasing, in terms of the scalar variables, of the general classification in terms of the superpotential that we have discussed in section 5.2.1 and in appendix E. For any dilaton potential asymptotic freedom in the UV i.e. $V(\lambda) \to V_0 + V_1\lambda + \cdots$, as $\lambda \to 0$ and which exhibits exponential asymptotics in the IR, $V(\lambda) \to \lambda^{2Q} (\log \lambda)^P$ as $\lambda \to \infty$, there are three different classes of solutions to X, with different IR behavior (as $\lambda \to \infty$):

i. Solutions with "special" type of IR asymptotics: $X \to -3Q/4$. We denote it $X_*(\Phi)$,

ii. Solutions with "generic" type of IR asymptotics: $X \to -1$,

iii. Solutions with "bouncing" type of IR asymptotics: $X \to 0$.

The second case is not desired because the fluctuations of the bulk fields fall into the singularity, hence it is not of repulsive type, whereas the last case corresponds to λ being a non-monotonic function of the RG scale, hence it can not yield a sensible RG flow. Therefore we based our holographic construction on the special class, case i.

Now, we consider the black-hole solutions to the same potential, with $Y \neq 0$. *A priori*, there is no guarantee that a regular black-hole solution does not correspond to cases ii or iii as the deformation is taken away i.e. $Y \to 0$ (by sending the BH horizon to the singularity). However, as presented in section 5.2.1, we have the following:

> **No-go theorem:** *The only vacuum solutions of Einstein-dilaton gravity, with exponential asymptotics given above, that can be continuously lifted to a regular black-hole correspond to the special class of solutions, case i.*

In the language of scalar variables, the proof is simple. In the previous subsection, we gave the condition for regularity of the horizon, eq. (7.24). We can write this in terms of $X(\Phi)$ using eq. (7.22)

$$X(\Phi_h) = -\frac{3}{8}\frac{V'(\Phi_h)}{V(\Phi_h)}. \tag{7.38}$$

For all regular BHs one should be able to push the horizon down to the singularity of the zero-T solution r_0, by continuously sending $r_h \to r_0$. First, we rule out case iii: Since

$V(\Phi)$, $V'(\Phi) > 0$ for all Φ, one finds from (7.38) that $X(\Phi_h) < 0$. On the other hand, in the region close to the singularity in case iii, one finds $X > 0$, see appendix H.3. Thus, it is not possible that regular black-holes can be continuously connected to case iii, as the horizon is taken close to the singularity, $\Phi_h \to \infty$. In this limit, (7.38) clearly fixes $X \to -3Q/4$. Therefore, the function X exhibits the desired asymptotics of case i.

On the other hand, one can solve for Y in this asymptotic region, using the analytic solution of (H.10). One finds,

$$Y(\Phi) \to \frac{e^{c\Phi}}{C_1 - \frac{d}{c}e^{c\Phi}}, \qquad as \;\; \Phi_h \gg 1 \tag{7.39}$$

Here $c > 0$ and $d > 0$ are given in terms of Q and the location of the horizon is given by the integration constant C_1 as

$$C_1 = \frac{d}{c}e^{c\Phi_h}.$$

We can show that, in the limit $\Phi_h \to \infty$ the entire Y function becomes a spike centered at $\Phi = \infty$: From (7.3) we observe that the r.h.s. is positive definite, hence Y is a monotonically increasing function of Φ. From (7.39), it is also clear that $Y(\Phi_h) \to 0$ as $\Phi_h \to \infty$, for any $\Phi \gg 1$ but $\Phi < \infty$, in the asymptotic region. Combining these two facts, we learn that $Y(\Phi)$ should vanish for *all* $\Phi \neq \infty$, including the UV region. On the other hand, it diverges exactly at $\Phi_h = \infty$.[27]

Thus we proved that, in the limit $\Phi_h \to \infty$ of *any regular BH*, X limits to X_* and $Y(\Phi) \to 0$ for any $\Phi < \infty$. This corresponds to the zero-T solution $Y = 0$, with the integration constant of X equation tuned to $X(\infty) = -3Q/4$. In other words, $X(\Phi) \to X_*(\Phi)$ in the entire range of Φ as $\Phi_h \to \infty$.

7.6 Parameters of the solutions

Here we examine the integration constants in the Einstein equations for a generic black-hole solution. We solve the system by requiring the asymptotic behavior of X and Y near the horizon, as discussed in section 7.3. This solution flows in the UV to $X \to X_0$ and $Y \to 0$ as described in Subsection 7.2. Thus one has a single integration constant Φ_h from eqs. (7.2) and (7.3). It determines the temperature by eq. (7.26).

After X and Y are determined, the metric and dilaton are obtained using eqs. (H.1)-(H.3). The condition $g \to 0$ near the boundary fixes the integration constant in (H.3). The two remaining constants are λ_0 and A_0. As described in [28], these combine to determine the mass scale Λ of the physical system, (2.18). This combination can be viewed as one integration constant of the two equations (H.1) and (H.2). (The other one is irrelevant due to a shift symmetry in r, see ([28]).) As we require that the finite-T solution approaches to the zero-T on near the boundary, the value of $\Lambda\ell$ is determined by the corresponding value at zero T.

Thus, we conclude that *one has only two parameters in the solutions, Λ and λ_h which corresponds to the $\Lambda_{\rm QCD}$ and the temperature.* Furthermore, one of them i.e. Λ is completely

[27] In fact, one can prove that $Y(\Phi)$ becomes proportional to $\delta(\Phi_h - \Phi)$ in the limit $\Phi_h \to \infty$ by using a limit representation of the delta function. We will not need this here however.

fixed by the zero-T solution. It is practically set by the mass of the lowest glueball in the spectrum, see [28].

8 Outlook

In this paper we have analyzed in detail the equilibrium thermodynamics of the 5D Einstein-dilaton system that was proposed in [28] as a phenomenological holographic dual of 4D large-N_c pure Yang Mills. There is a variety of possible directions to extend our work.

An example of an explicit background with similar asymptotics, in critical (IIB compactified to 5D) or a non-critical string theory would be desirable. In addition to justifying our phenomenological set-up based on the principles of AdS/CFT correspondence, this would allow more detailed studies on the α' corrections and how they can affect our results especially in the UV. For the thermodynamics of QCD, the higher derivative corrections are desirable also for a phenomenological reason: It is well-known [50] that η/s is constant in any gravitational theory based on a two-derivative action. However, this quantity is expected to be a non-trivial function of T in QCD that becomes asymptotically large for large temperatures. The higher derivative corrections may provide the desired T dependence.

Having set the general construction in this paper, a natural step forward is to compute dynamical observables (bulk viscosity, drag force, jet quenching parameter) that are important for the physics of the RHIC collider and the upcoming LHC collider . We will address this problem in the near future, [34]. Another related issue is the computation of the various Debye screening masses, where a better comparison with lattice data can emerge.

Another important direction involves the meson sector, that should be introduced through probe D_4+$\overline{D_4}$ branes in the background. Introduction of baryon chemical potential is the next very interesting step to analyze. We expect that this will involve the study of charged black-holes under the overall U(1) gauge field of the flavor branes.

Acknowledgments

We would like to thank Ofer Aharony, Luis Alvarez-Gaumé, Adi Armoni, Massimo Bianchi, Francesco Bigazzi, Richard Brower, Aldo Cotrone, Frank Ferrari, Steve Gubser, Gary Horowitz, Thomas Hertog, Edmond Iancu, Frithjof Karsch, David Kutasov, Hong Liu, Biagio Lucini, David Mateos, Carlos Nunez, Andrei Parnachev, Ioannis Papadimitriu, Edward Shuryak, Kostas Skenderis, Dam Son, Jacob Sonnenschein, Shigeki Sugimoto, Marika Taylor, Michael Teper, Mithat Unsal, Urs Wiedemann, and Lawrence Yaffe for discussions. This work was partially supported by ANR grant NT05-1-41861, RTN contracts MRTN-CT-2004-005104 and MRTN-CT-2004-503369, CNRS PICS 3059 and 3747, Marie Curie Intra-European Fellowships MEIF-CT-2006-039962 and MEIF-CT-2006–039369, INFN, and by the VIDI grant 016.069.313 from the Dutch Organisation for Scientific Research (NWO).

Elias Kiritsis is on leave of absence from CPHT, Ecole Polytechnique (UMR du CNRS 7644).

JHEP05(2009)033

A Various forms of Einstein's equations

We use a metric signature $(-,+,+,+,+)$. We start from the action:

$$S_5 = -M^3 \int d^5x\sqrt{g}\left[R - \frac{4}{3}(\partial\Phi)^2 + V(\Phi)\right] + 2M^3 \int_{\partial M} d^4x\sqrt{h}\ K \tag{A.1}$$

with

$$K_{\mu\nu} \equiv -\nabla_\mu n_\nu = \frac{1}{2}n^\rho \partial_\rho h_{\mu\nu} \quad , \quad K = h^{ab}K_{ab} \tag{A.2}$$

where h_{ab} is the induced metric on the boundary and n_μ is the (outward directed) unit normal to the boundary. e.g. if r denotes the AdS conformal coordinate,

$$n^\mu = -\frac{1}{\sqrt{g_{rr}}}\left(\frac{\partial}{\partial r}\right)^\mu = \frac{\delta^\mu{}_r}{\sqrt{g_{rr}}}. \tag{A.3}$$

The sign of the bulk term is chosen in such a way that 1) in the Euclidean regime, the scalar field kinetic term is positive definite and 2) the curvature of Euclidean AdS is negative. With this choice, the sign of the Gibbons-Hawking term is fixed, as usual, by the requirement that the variation of the action does not contain metric derivatives.

Einstein's equations are:

$$E_{\mu\nu} - \frac{4}{3}\left[\partial_\mu\Phi\partial_\nu\Phi - \frac{1}{2}(\partial\Phi)^2 g_{\mu\nu}\right] - \frac{1}{2}g_{\mu\nu}V = 0, \tag{A.4}$$

$$\Box_5\Phi + \frac{\partial V}{\partial\Phi} = 0, \tag{A.5}$$

with the Einstein tensor defined as,

$$E_{\mu\nu} = R_{\mu\nu} - \frac{1}{2}Rg_{\mu\nu}. \tag{A.6}$$

A.1 Conformal frame

Consider the following ansatz for the metric and dilaton:

$$ds^2 = b(r)^2\left[\frac{dr^2}{f(r)} - f(r)dt^2 + dx^i dx^i\right], \qquad \Phi = \Phi(r). \tag{A.7}$$

with Einstein tensor,

$$E_{rr} = \frac{3\dot{b}(4f\dot{b} + b\dot{f})}{2b^2 f} \quad , \quad E_{tt} = -\frac{3f(\dot{b}\dot{f} + 2f\dot{b})}{2b}, \quad , \quad E_{ij} = \frac{6\dot{b}\dot{f} + 6f\ddot{b} + b\ddot{f}}{2b}\delta_{ij}, \tag{A.8}$$

Laplacian,

$$\Box\Phi = \frac{f}{b^2}\ddot{\Phi} + \frac{f}{b^2}\left(\frac{\dot{f}}{f} + 3\frac{\dot{b}}{b}\right)\dot{\Phi}, \tag{A.9}$$

and Dilaton stress tensor,

$$T_{rr} = \frac{2}{3}\dot{\Phi}^2 + \frac{b^2}{2f}V \quad , \quad T_{tt} = \frac{2f^2}{3}\dot{\Phi}^2 - \frac{b^2 f}{2}V \quad , \quad T_{ij} = -\frac{2f}{3}\dot{\Phi}^2 + \frac{b^2}{2}V. \tag{A.10}$$

The equations of motion are:

$$6\frac{\dot{b}^2}{b^2}+3\frac{\ddot{b}}{b}+3\frac{\dot{b}}{b}\frac{\dot{f}}{f}=\frac{b^2}{f}V, \quad , \qquad 6\frac{\dot{b}^2}{b^2}-3\frac{\ddot{b}}{b}=\frac{4}{3}\dot{\Phi}^2, \tag{A.11}$$

$$\frac{\ddot{f}}{\dot{f}}+3\frac{\dot{b}}{b}=0 \quad , \qquad \ddot{\Phi}+\left(\frac{\dot{f}}{f}+3\frac{\dot{b}}{b}\right)\dot{\Phi}+\frac{3}{8f}b^2\frac{dV}{d\Phi}=0. \tag{A.12}$$

The second equation in (A.12) is not independent of the other three, and it can be dropped.

The Ricci scalar is:

$$R=-\frac{2}{3}E=-\frac{f}{b^2}\left[\frac{\ddot{f}}{f}+8\frac{\ddot{b}}{b}+8\frac{\dot{b}}{b}\frac{\dot{f}}{f}+4\frac{\dot{b}^2}{b^2}\right] \tag{A.13}$$

A.2 Domain-wall frame

We define,

$$b=e^A, \qquad f=e^g, \tag{A.14}$$

and use the domain-wall parametrization of the metric,

$$dr=e^{-A}du. \tag{A.15}$$

In this coordinate frame the metric has the following form:

$$ds^2=e^{2A}\left(-fdt^2+dx^2\right)+\frac{du^2}{f}. \tag{A.16}$$

The equations of motion (3.5) and (3.6) in the variable u take the following form:

$$12A'^2+3A'g'-\frac{4}{3}\Phi'^2-e^{-g}V=0, \tag{A.17}$$

$$A''+\frac{4}{9}\Phi'^2=0, \tag{A.18}$$

$$g'+\frac{g''}{g'}+4A'=0, \tag{A.19}$$

$$\Phi''+4A'\Phi'+g'\Phi'+\frac{3}{8}e^{-g}\frac{dV}{d\Phi}=0. \tag{A.20}$$

A.3 Dilaton frame

This frame uses Φ (or $\lambda\equiv\exp\Phi$) as the radial coordinate, and it is in some sense "maximally gauge fixed," since only the physical integration constants of Einstein's equations appear in the metric. To change variables from u to λ it is useful to define a *superpotential* $W(\Phi)$, such that eq. (A.18) is written as:

$$A'=-\frac{4}{9}W(\Phi), \qquad \Phi'=\frac{dW}{d\Phi}. \tag{A.21}$$

The coordinate change $u=u(\Phi)$ is obtained by inverting the second equation in (A.21). The existence and properties of the superpotential in the zero-temperature and black hole

case will be extensively discussed in appendices E and F respectively. The solution of Einstein's equation in this frame is:

$$ds^2 = \frac{e^{-g(\Phi)}d\Phi^2}{(\partial_\Phi W)^2} + e^{2A(\Phi)}\left(-e^{g(\Phi)}dt^2 + dx^2\right), \tag{A.22}$$

where with a slight abuse of notation we have written $g(u(\Phi)) \equiv g(\Phi)$ and $A(u(\Phi)) \equiv A(\Phi)$. One interesting property of the setup we are discussing is that two different dilaton potentials $V(\Phi)$ and $\tilde{V}(\Phi)$, related by $\tilde{V}(\Phi) = V(\Phi + K)$ for some constant K give essentially the same set of solutions and the same physics. First, given a solution $(A(u), g(u), \Phi(u))$ of eqs. (A.17)–(A.20) with potential $V(\Phi)$, it is straightforward to show that the functions $(\tilde{A}(u), \tilde{g}(u), \tilde{\Phi}(u)) = (A(u), g(u), \Phi(u) - K)$ solve the system with potential $\tilde{V}(\Phi)$. The two solutions are physically equivalent (except for a change in initial conditions, which as we know [28] only affects the overall scale). This is easily seen writing the second solution in the $\tilde{\Phi}$-frame:

$$d\tilde{s}^2 = \frac{e^{-\tilde{g}(\tilde{\Phi})}d\tilde{\Phi}^2}{(\partial_{\tilde{\Phi}}\tilde{W})^2} + e^{2\tilde{A}(\tilde{\Phi})}\left(-e^{\tilde{g}(\tilde{\Phi})}dt^2 + dx^2\right), \tag{A.23}$$

where $\tilde{W}$ is the appropriate superpotential. However, since $\tilde{A}(u) = A(u)$ and $\tilde{g}(u) = g(u)$, it follows that

$$\tilde{A}(\tilde{\Phi}) = A(\Phi), \quad \tilde{W}(\tilde{\Phi}) = W(\Phi), \quad \tilde{g}(\tilde{\Phi}) = g(\Phi). \tag{A.24}$$

Thus, after a change of coordinates $\tilde{\Phi} \to \Phi = \tilde{\Phi} + K$ the metric (A.23) becomes identical to the solution of the original system with potential $V(\Phi)$, eq. (A.22). The initial conditions for the two systems, such that the solutions coincide, are related by $\tilde{A}(\Phi_0 - K) = A(\Phi_0)$.

Thus, there is an "accidental degeneracy" in the classification of Einstein-dilaton gravity by the dilaton potential, since the two potentials $V(\lambda)$ and $V(\kappa\lambda)$ lead to the same physical results. For this reason, the value of the proportionality constant between the dilaton λ and the physical Yang-Mills coupling λ_t is irrelevant.

A.4 Relating fluctuations in different frames

In this appendix we work out the relation between the scale factor and dilaton fluctuations close to the boundary in different frames. For simplicity we set $\ell = 1$. Suppose we start with the zero-temperature and black-hole metrics, both in the domain wall frame:

$$ds^2 = \frac{du^2}{f} + e^{2A^u}\left(f dt^2 + dx_3^2\right), \quad ds_o^2 = du^2 + e^{2A_o^u}\left(dt^2 + dx_3^2\right) \tag{A.25}$$

For clarity, we have added a label (u) to the warp factor. If the two solutions obey the same boundary conditions at $u = -\infty$, then as shown in section 7.2 the two scale factors are related, to lowest order, by:

$$\delta A^u \equiv A^u(u) - A_o^u(u) \simeq \mathcal{G}^u\, e^{4u} \tag{A.26}$$

for some constant $\mathcal{G}^u$. The difference between the dilatons, $\delta\Phi^u \equiv \Phi^u(u) - \Phi_o^u(u)$, can be related to δA by perturbing equation (A.18), which gives:

$$(\delta A^u)'' + \frac{8}{9}(\Phi_o^u)'(\delta\Phi^u)' \tag{A.27}$$

which can be integrated to give:

$$\delta\Phi^u \simeq \frac{9}{2}\,\mathcal{G}^u\,(-u)e^{4u}, \tag{A.28}$$

in agreement with eq. (7.14).

Now we want to obtain the same quantities, namely $A - A_o$ and $\Phi - \Phi_o$, in conformal coordinates. Naively, one may think that it should be enough to make the replacement $u \to \log r$ in eqs. (A.26) and (A.28), since any correction to the relation between u and r would only affect higher orders in δA and $\delta\Phi$. This is however incorrect, as a careful analysis reveals.

What we want to obtain is the difference $\delta A^r = A^r(r) - A^r_o(r)$, where the conformal warp factors are such that the metrics have the form:

$$ds^2 = e^{2A^r}\left(\frac{dr^2}{f} + f dt^2 + dx_3^2\right), \quad ds_o^2 = e^{2A^r_o}\left(dr^2 + dt^2 + dx_3^2\right). \tag{A.29}$$

Now, it is clear that to bring the two metrics in this form one needs two *different* coordinate transformations. We can first define $e^{-A^u(u)}du = dr$: if we perform this coordinate transformation on both metrics we get:

$$\begin{aligned} ds^2 &= e^{2A^u(u(r))}\left(\frac{dr^2}{f} + f dt^2 + dx_3^2\right), \\ ds_o^2 &= e^{2A^u_o(u(r))+2\delta A^u(u(r))}dr^2 + e^{2A^u_o(u(r))}\left(dt^2 + dx_3^2\right). \end{aligned} \tag{A.30}$$

So the black-hole metric is in the conformal form, but the zero-temperature one is not. From the above expression we read off that the function $A^r(r)$ in (A.29) is given by $A^u(u(r))$, but a similar relation does not hold for A^r_o.

Let us define $\tilde{A}^r_o(r) \equiv A^u_o(u(r))$. To get the correct scale factor we have to perform a further coordinate transformation to bring ds_o^2 in conformal form. We thus define:

$$(1 + \delta A^u(u(r)))\,dr = d\tilde{r} \quad \Rightarrow \quad \tilde{r} = r + \frac{1}{5}\,\mathcal{G}^u\,r^5. \tag{A.31}$$

This transformation brings the metric ds_o^2 in conformal frame, parametrized by the coordinate $\tilde{r}$, with scale factor given $A^r_o(\tilde{r}) = \tilde{A}^r_o(r(\tilde{r}))$. Using the explicit form of $r(\tilde{r})$, we can write this as:

$$A^r_o(\tilde{r}) = \tilde{A}^r_o(\tilde{r} - \mathcal{G}^u\tilde{r}^5/5) \simeq \tilde{A}^r_o(\tilde{r}) - \frac{\mathcal{G}^u}{5}\,\tilde{r}^5\partial_{\tilde{r}}\tilde{A}^r_o(\tilde{r}) = A^u_o(u(\tilde{r})) + \frac{\mathcal{G}^u}{5}\tilde{r}^4 \tag{A.32}$$

In the last step we have used the fact that, to lowest order, $\tilde{A}^r_o(\tilde{r}) \sim -\log r$. The first and last steps of the above equality mean that there is an extra shift in A_o, compared to the naive change of variables. Renaming $\tilde{r} \to r$ in (A.32), we finally have:

$$\delta A^r \equiv A^r(r) - A^r_o(r) = A^r(r) - A^u_o(u(r)) - \frac{\mathcal{G}^u}{5}r^4 = \frac{4}{5}\mathcal{G}^u r^4 \tag{A.33}$$

This result could have been guessed from the fact that δA is not invariant under linearized diffeomorphisms $r \to r + \xi$, but rather it transforms as $\delta A \to \delta A + \dot{A}_o\xi$. For $\xi = \mathcal{G}^u r^5/5$, this gives exactly eq. (A.33)

JHEP05(2009)033

Following the same procedure, one can write $\delta\Phi$ in conformal coordinates, and one would find that this time the leading order is simply given by the change of variables $u \to \log r$. The reason is that, under $r \to r+\xi$, the dilaton fluctuation transforms as $\delta\Phi \to \delta\Phi + \dot{\Phi}_o \xi = \delta\Phi + G(r^4/5)(\log r)^{-1}$. Thus the shift induced by the extra diffeomorphism is subleading with respect to the first term, which behaves as $r^4 \log r$. Thus, we have to leading order:

$$\delta\Phi^r(r) \simeq \delta\Phi^u(u(r)) = \frac{9}{2}\mathcal{G}^u r^4 \log r\Lambda. \tag{A.34}$$

Finally, to connect this discussion with the definition of $\mathcal{G}$ given in section 3, let us define $\mathcal{G} \equiv 4\mathcal{G}^u/5$. Then we arrive at:

$$\delta A^r(r) = \mathcal{G} r^4, \qquad \delta\Phi^r = \frac{45}{8}\mathcal{G} r^4 \log r\Lambda. \tag{A.35}$$

For consistency, one can check that the above fluctuations solve the linearized Einstein's equations in conformal coordinates, obtained by perturbing eq. (A.11).

B The AdS_5 case revisited

In this appendix we will reconsider the Einstein system plus a scalar in the conformal case, with a view of exploring all potential boundary conditions at infinity and their effect in the bulk physics both at zero and finite temperature. This situation is simpler than the one we are studying but some of the lessons are similar. Although what we present here is mostly understood in the literature (see for example [42, 43]), they are not widely known and we would like to put them in the right perspective.

B.1 Zero temperature

We reconsider the zero temperature field equations (in the conformal coordinate system) of the Einstein-dilaton system with a potential

$$6\frac{\dot{b}^2}{b^2} + 3\frac{\ddot{b}}{b} = b^2 V(\Phi) \quad , \quad 6\frac{\dot{b}^2}{b^2} - 3\frac{\ddot{b}}{b} = \frac{4}{3}\dot{\Phi}^2 \tag{B.1}$$

$$\ddot{\Phi} + 3\frac{\dot{b}}{b}\dot{\Phi} + \frac{3}{8}b^2\frac{dV}{d\Phi} = 0 \tag{B.2}$$

We will set the potential to be a constant $V = \frac{12}{\ell^2}$ and we will find the UV asymptotics of solutions for arbitrary initial conditions.

The first equation can be integrated once to yield

$$\dot{b} = -\sqrt{\frac{C^2}{b^4} + \frac{b^4}{\ell^2}} \tag{B.3}$$

where we have chosen the minus sign branch so that b decreases with increasing r, and C^2 is an integration constant that we set to be positive. When $C = 0$ the solution is AdS_5

$$b = \frac{\ell}{r - r_0} \tag{B.4}$$

JHEP05(2009)033

The constant C, and two extra boundary conditions for the two first order equations (B.3) and the second one in (B.1) viewed as a first order equation for the dilaton are the full set of boundary conditions necessary near the boundary.

For general C, the first order equation (B.3) can be integrated as

$$\int_{\frac{1}{b_*}}^{\frac{1}{b}} \frac{du}{\sqrt{1+C^2\ell^2u^8}} = \frac{r-r_0}{\ell} \tag{B.5}$$

giving

$$\frac{1}{b}F\left[\frac{1}{8},\frac{1}{2},\frac{9}{8},-\frac{\ell^2C^2}{b^8}\right] = \frac{1}{b_*}F\left[\frac{1}{8},\frac{1}{2},\frac{9}{8},-\frac{\ell^2C^2}{b_*^8}\right] + \frac{r-r_0}{\ell} \tag{B.6}$$

where F is the standard hypergeometric function and $b_* = b(r_0)$. The equation for the dilaton becomes

$$\begin{aligned}\dot{\Phi} = \frac{3C}{b^3} \rightarrow \Phi(r) = \Phi_* + 3C\int_{r_0}^{r}\frac{dr'}{b^3} = \Phi_* - 3C\ell\int_{b_*}^{b}\frac{db/b}{\sqrt{\ell^2C^2+b^8}} \\ \rightarrow \Phi = \Phi_* + \frac{3}{4}\text{ArcTanh}\sqrt{1+\frac{b^8}{(\ell C)^2}}\Bigg|_{b_*}^{b}\end{aligned} \tag{B.7}$$

where the sign ambiguity is hidden in the sign of C. Note that for the AdS solution the dilaton is constant. The three integration constants C, b_*, Φ_0 are in one-to-one correspondence with the three boundary conditions at the boundary. As explained in [28], one of them, that we can take to be b_* is a gauge artifact, related to the position of the boundary in the radial coordinate. We will therefore choose $r_0 = 0$ to be the position of the boundary, $b_* = \infty$. Then the solution becomes

$$\frac{1}{b}F\left[\frac{1}{8},\frac{1}{2},\frac{9}{8},-\frac{\ell^2C^2}{b^8}\right] = \frac{r}{\ell} \quad , \quad \Phi(r) = \Phi_* + \frac{3}{4}\text{ArcSinh}\frac{C\ell}{b^4} \tag{B.8}$$

Near the boundary $\frac{b^8}{(C\ell)^2} \rightarrow \infty$ and we can expand F around zero to find

$$b \simeq \frac{\ell}{r}\left[1 - \frac{C^2r^8}{18\ell^6} + \mathcal{O}\left(r^{16}\right)\right] \tag{B.9}$$

valid when $r \rightarrow 0$. In the same region

$$\Phi = \Phi_* + \frac{3}{4}\frac{C}{\ell^3}r^4 + \mathcal{O}\left(r^{12}\right) \tag{B.10}$$

Therefore for non-zero C there is a non-zero vev of the operator dual to the scalar Φ.

Consider now the region $b \rightarrow 0$. We use the transformation rule

$$F\left[\frac{1}{8},\frac{1}{2},\frac{9}{8},-\frac{\ell^2C^2}{b^8}\right] = \frac{\Gamma\left[\frac{1}{8}\right]\Gamma\left[\frac{3}{8}\right]}{8\Gamma\left[\frac{1}{2}\right]}\frac{b}{(C\ell)^{\frac{1}{4}}} - \frac{1}{3}\frac{b^4}{C\ell}F\left[\frac{1}{2},\frac{3}{8},\frac{11}{8},-\frac{b^8}{\ell^2C^2}\right] \tag{B.11}$$

to obtain

$$b \simeq (3C(\hat{r}_0 - r) + \cdots)^{\frac{1}{3}} \quad , \quad \hat{r}_0 = \frac{\Gamma\left[\frac{1}{8}\right]\Gamma\left[\frac{3}{8}\right]}{8\Gamma\left[\frac{1}{2}\right]}\ell(C\ell)^{-\frac{1}{4}} \tag{B.12}$$

JHEP05(2009)033

The scalar there diverges as

$$\Phi \sim \log(\hat{r}_0 - r) \tag{B.13}$$

We may use the relations

$$\frac{\ddot{b}}{b} = \frac{2b^2}{\ell^2} - \frac{2C^2}{b^6} \quad , \quad \frac{\dot{b}^2}{b^2} = \frac{b^2}{\ell^2} + \frac{C^2}{b^6} \tag{B.14}$$

to calculate the curvature invariant for the metric. We obtain

$$R = -\frac{1}{b^2}\left[4\frac{\dot{b}^2}{b^2} + 8\frac{\ddot{b}}{b}\right] = \frac{12C^2}{b^8} - \frac{12}{\ell^2} \tag{B.15}$$

Near the boundary, $b \to \infty$ and we obtain constant negative curvature as expected. In the interior, as $b \to 0$, we observe that the space has a curvature singularity, if $C \neq 0$ at a distance $\delta r \sim (C\ell)^{-\frac{1}{4}}$ from the boundary. Imposing regularity in the bulk imposes $C = 0$. Therefore the dynamics of the theory does not allow for a non-trivial vev associate to the operator dual to Φ.

B.2 The black-hole solution

We will now solve again the equations with constant potential seeking a black-hole type solution.

$$6\frac{\dot{b}^2}{b^2} + 3\frac{\ddot{b}}{b} + 3\frac{\dot{b}}{b}\frac{\dot{f}}{f} = \frac{12b^2}{\ell^2 f} \quad , \qquad 6\frac{\dot{b}^2}{b^2} - 3\frac{\ddot{b}}{b} = \frac{4}{3}\dot{\Phi}^2 \tag{B.16}$$

$$\frac{\ddot{f}}{\dot{f}} + 3\frac{\dot{b}}{b} = 0 \quad , \qquad \ddot{\Phi} + \left(\frac{\dot{f}}{f} + 3\frac{\dot{b}}{b}\right)\dot{\Phi} = 0 \tag{B.17}$$

We may integrate once the two last equations as

$$\dot{f} = -\frac{8C}{b^3} \quad , \quad \dot{\Phi} = \frac{3D}{b^3 f} \tag{B.18}$$

and we will take the two constants of integration to be positive $D > 0, C > 0$. Using this may derive the following equations for b

$$\left(8\frac{\dot{b}^3}{b^3} - \frac{\dot{b}\ddot{b}}{b^2} - \frac{\dddot{b}}{b}\right) = \frac{2C\ell^2}{b^5}\left(\frac{\dot{b}^2\ddot{b}}{b^3} - 2\frac{\ddot{b}^2}{b^2} + \frac{\dot{b}\dddot{b}}{b^2}\right) \tag{B.19}$$

$$f\left(2\frac{\dot{b}^2}{b^2} + \frac{\ddot{b}}{b}\right) = 8C\frac{\dot{b}}{b^4} + \frac{4b^2}{\ell^2} \quad , \quad f^2\left(2\frac{\dot{b}^2}{b^2} - \frac{\ddot{b}}{b}\right) = \frac{4D^2}{b^6} \tag{B.20}$$

We now introduce an auxiliary variable

$$\zeta = \sqrt{1 + \frac{4D^2\dot{b}^2}{\left(\frac{b^6}{\ell^2} + 2C\dot{b}\right)^2}} \quad , \quad \sqrt{\zeta^2 - 1} = -\frac{2D\dot{b}}{\left|\frac{b^6}{\ell^2} + 2C\dot{b}\right|} = \frac{2\epsilon D\dot{b}}{\left(\frac{b^6}{\ell^2} + 2C\dot{b}\right)} \tag{B.21}$$

where $\epsilon = 1$ iff $\frac{b^6}{\ell^2} + 2C\dot{b} < 0$ and $\epsilon = -1$ if $\frac{b^6}{\ell^2} + 2C\dot{b} > 0$, ($\dot{b}$ is always negative). In terms of this new variable we obtain

$$\frac{\ddot{b}}{b} = 2\frac{\dot{b}^2}{b^2}\left[\frac{4}{\zeta+1} - 1\right] \quad , \quad \dot{b} = \frac{b^6\sqrt{\zeta^2-1}}{2\ell^2(\epsilon D - C\sqrt{\zeta^2-1})} \tag{B.22}$$

which may translated as a first order equation for ζ

$$b\zeta' = \frac{8}{D}(1-\zeta)(D - \epsilon C\sqrt{\zeta^2-1}) \tag{B.23}$$

where the prime stands for derivative with respect to b. This can be integrated as

$$\frac{(D - \epsilon C\sqrt{\zeta^2-1})}{\zeta-1}\left(\frac{\sqrt{C^2+D^2} - \epsilon C - D\sqrt{\frac{\zeta-1}{\zeta+1}}}{\sqrt{C^2+D^2} + \epsilon C + D\sqrt{\frac{\zeta-1}{\zeta+1}}}\right)^{\frac{\epsilon C}{\sqrt{C^2+D^2}}} = \tilde{C}b^8 \tag{B.24}$$

Using the relation

$$\left(\sqrt{C^2+D^2} - \epsilon C - D\sqrt{\frac{\zeta-1}{\zeta+1}}\right)\left(\sqrt{C^2+D^2} + \epsilon C + D\sqrt{\frac{\zeta-1}{\zeta+1}}\right) = \frac{2D}{\zeta+1}(D - \epsilon C\sqrt{\zeta^2-1}) \tag{B.25}$$

the solution can be written in the following alternative form

$$\frac{1}{2D}\frac{\zeta+1}{\zeta-1}\frac{\left(\sqrt{C^2+D^2} - \epsilon C - D\sqrt{\frac{\zeta-1}{\zeta+1}}\right)^{1+\frac{\epsilon C}{\sqrt{C^2+D^2}}}}{\left(\sqrt{C^2+D^2} + \epsilon C + D\sqrt{\frac{\zeta-1}{\zeta+1}}\right)^{-1+\frac{\epsilon C}{\sqrt{C^2+D^2}}}} = \tilde{C}b^8 \tag{B.26}$$

In particular, for $\epsilon = 1$

$$\frac{1}{2D}\frac{\zeta+1}{\zeta-1}\left(\sqrt{C^2+D^2} - C - D\sqrt{\frac{\zeta-1}{\zeta+1}}\right)^{a_+}\left(\sqrt{C^2+D^2} + C + D\sqrt{\frac{\zeta-1}{\zeta+1}}\right)^{a_-} = \tilde{C}b^8 \tag{B.27}$$

with

$$a_+ = 1 + \frac{C}{\sqrt{C^2+D^2}} \geq 0 \quad , \quad a_- = 1 - \frac{C}{\sqrt{C^2+D^2}} \geq 0 \tag{B.28}$$

while for $\epsilon = -1$

$$\frac{1}{2D}\frac{\zeta+1}{\zeta-1}\left(\sqrt{C^2+D^2} + C - D\sqrt{\frac{\zeta-1}{\zeta+1}}\right)^{a_-}\left(\sqrt{C^2+D^2} - C + D\sqrt{\frac{\zeta-1}{\zeta+1}}\right)^{a_+} = \tilde{C}b^8 \tag{B.29}$$

We will now investigate several special cases of this general solution.

B.2.1 $C = 0$

The solution becomes

$$\frac{D}{\zeta-1} = \tilde{C}b^8 \tag{B.30}$$

JHEP05(2009)033

which using (B.21) becomes

$$\dot{b}^2 = \frac{1}{4\tilde{C}^2\ell^4}\frac{1}{b^4} + \frac{1}{2\tilde{C}D\ell^4}b^4 \tag{B.31}$$

Compatibility with the other equations determines $\tilde{C} = \frac{1}{2D\ell^2}$. This solution has no horizon (f=1). It is the same solution found in the previous subsection, where D plays the role of the Φ condensate.

B.2.2 $D = 0$

The equation (B.26) becomes the trivial one $\zeta = 1$. From (B.20) we obtain $\frac{\ddot{b}}{b} = 2\frac{\dot{b}^2}{b^2}$ which is solved by the AdS scale factor $b \sim \frac{1}{r}$. Finally the rest of the equations give

$$b = \frac{\ell}{r} \quad , \quad f = 1 - \frac{2Cr^4}{\ell^3} \tag{B.32}$$

This is the standard AdS black-hole solution with a flat horizon.

The two previous cases indicate that the constant C controls the temperature of the solution while the constant D controls the Φ condensate.

B.3 Analysis of the general solution

The function f is given by

$$f = \frac{2D\ell^2(D - \epsilon C\sqrt{\zeta^2-1})}{b^8(\zeta-1)} \tag{B.33}$$

The boundary $b \to \infty$, is always at $\zeta = 1$. To test whether we have a regular horizon we need the the trace of the Einstein tensor which is given by

$$E = -\frac{f}{b^2}\left[\frac{\ddot{f}}{f} + 8\frac{\ddot{b}}{b} + 8\frac{\dot{b}}{b}\frac{\dot{f}}{f} + 4\frac{\dot{b}^2}{b^2}\right] = \frac{2}{\ell^2}\frac{D(3\zeta-13) + 10\epsilon C\sqrt{\zeta^2-1}}{D - \epsilon C\sqrt{\zeta^2-1}} \tag{B.34}$$

To continue we distinguish two cases:

B.3.1 $\epsilon = -1$

There is no horizon in this case as f never vanishes. There is also no singularity as E never blows up. The scale factor becomes a constant asymptotically

B.3.2 $\epsilon = 1$

The horizon ($f = 0$) is at

$$\zeta_h = \sqrt{1 + \frac{D^2}{C^2}} \tag{B.35}$$

It is singular unless $D = 0$. At the horizon $b \to 0$. Therefore, even at finite temperature the Φ condensate must vanish in order to have a regular solution.

JHEP05(2009)033

C The black hole action and ADM mass

C.1 The on-shell action

We want to compute the regularized action evaluated on a solution of Einstein's equations, (A.4). We start from eq. (2.1):

$$\begin{aligned} S_5 &= S_E + S_{GH}, \\ S_E &= -M^3 \int d^5x\sqrt{g}\left[R - \frac{4}{3}(\partial\Phi)^2 + V(\Phi)\right], \\ S_{GH} &= 2M^3 \int_{\partial M} d^4x\sqrt{h}\; K. \end{aligned} \tag{C.1}$$

We work in conformal frame, with the metric given by eq. (A.7).

Taking the trace of equation (A.4) we obtain for the Ricci scalar:

$$R = \frac{4}{3}(\partial\Phi)^2 - \frac{5}{3}V. \tag{C.2}$$

This leads to the on-shell Einstein action:

$$\begin{aligned} S_E &= \frac{2}{3}M^3 \int d^5x\sqrt{g}\;\; V(\Phi) = \frac{2}{3}M^3V_3 \int_0^\beta dt \int_0^{r_h} dr\; b^5 \;\; V(\Phi) \\ &= 2M^3V_3 \int_0^\beta dt \int_0^{r_h} dr\; \frac{d}{dr}(fb^2\dot{b}) \end{aligned} \tag{C.3}$$

From (A.3) the components of the unit normal to the boundary are $n_r = -b/\sqrt{f}$, $n_i = 0$. The trace of the extrinsic curvature is:

$$K = \frac{\sqrt{f}}{2b}\left[8\frac{\dot{b}}{b} + \frac{\dot{f}}{f}\right] \tag{C.4}$$

We find:

$$\mathcal{S}^\epsilon_E = 2M^3V_3 \int_0^\beta dt \int_\epsilon^{r_h} dr\; \frac{d}{dr}(fb^2\dot{b}) = 2\beta M^3V_3(f(r_h)b^2(r_h)\dot{b}(r_h) - f(\epsilon)b^2(\epsilon)\dot{b}(\epsilon)) \tag{C.5}$$

$$\begin{aligned} \mathcal{S}^\epsilon_{GH} &= 2M^3V_3 \int_0^\beta dt \frac{b^3(\epsilon)f(\epsilon)}{2}\left[8\frac{\dot{b}}{b} + \frac{\dot{f}}{f}\right]_\epsilon = 2M^3V_3\beta\;\frac{b^3(\epsilon)f(\epsilon)}{2}\left[8\frac{\dot{b}}{b} + \frac{\dot{f}}{f}\right]_\epsilon \\ &= 2M^3V_3\beta\;\frac{b^3(\epsilon)f(\epsilon)}{2}\left[8\frac{\dot{b}}{b} + \frac{\dot{f}}{f}\right]_\epsilon \end{aligned} \tag{C.6}$$

Putting together eqs. (C.5) and (C.6) we obtain for the full result:

$$\mathcal{S}^\epsilon = \mathcal{S}^\epsilon_E + \mathcal{S}^\epsilon_{GH} = 2\beta M^3V_3\left[3b^2(\epsilon)f(\epsilon)\dot{b}(\epsilon) + \frac{1}{2}\dot{f}(\epsilon)b^3(\epsilon)\right] \tag{C.7}$$

where we used that $f(r_h) = 0$.

JHEP05(2009)033

The calculation for the zero-temperature background is exactly the same, except that the integral of the Einstein-Hilbert action extends on the region $(0, r_0)$, where r_0 is the singularity. Thus in evaluating (C.5) one gets:

$$\mathcal{S}_E^\epsilon = 2\beta M^3 V_3 (b_o^2(r_0)\dot{b}_o(r_0) - b_o^2(\epsilon)\dot{b}_o(\epsilon)) \tag{C.8}$$

The IR contribution vanishes whenever $b_o^2\dot{b}_0 \to 0$ as $r \to r_0$. This is always true for good singularities.

C.2 Evaluation of the free energy

We start from eq. (3.24), which we rewrite below:

$$\mathcal{F} = \sigma \left\{ 6b^2(\epsilon)\sqrt{f(\epsilon)} \left[\dot{b}(\epsilon)\sqrt{f(\epsilon)} - \frac{b^2(\epsilon)}{b_o^2(\tilde{\epsilon})}\dot{b}_o(\tilde{\epsilon}) \right] + \dot{f}(\epsilon) b^3(\epsilon) \right\} \tag{C.9}$$

where the limit $\epsilon \to 0$ is understood. In terms of $\delta b = b - b_o$, and $\delta\epsilon = \tilde{\epsilon} - \epsilon$, the previous equation reads:

$$\frac{\mathcal{F}}{\sigma} = 6b^2(\epsilon)\sqrt{f(\epsilon)} \left[(\dot{b}_o + \dot{\delta b})(\epsilon)\sqrt{f(\epsilon)} - \frac{(b_o + \delta b)^2(\epsilon)}{(b_o + \delta\epsilon\, \dot{b}_o)^2(\epsilon)} (\dot{b}_o + \delta\epsilon\, \ddot{b}_o)(\epsilon) \right] + \dot{f}(\epsilon)(b_o + \delta b)^3(\epsilon). \tag{C.10}$$

For small ϵ, $b_o(\epsilon) \sim \epsilon/r$, and by eqs. (3.13), (3.15) and (3.21) we have:

$$\delta b(\epsilon) \simeq \mathcal{G}\frac{\epsilon^3}{\ell^2}, \quad \dot{\delta b}(\epsilon) \simeq \mathcal{G}\frac{3\epsilon^2}{\ell^2}, \quad f(\epsilon) \simeq 1 - \frac{C}{4}\frac{\epsilon^4}{\ell^3}, \quad \delta\epsilon = -\frac{45}{8}\frac{\mathcal{G}}{\ell^3}\epsilon^5 (\log \epsilon\Lambda)^2. \tag{C.11}$$

We see that the only divergent contribution inside the square brackets, i.e. $\dot{b}_o$, cancels. What is left is of order ϵ^2 times eventually some logarithmic corrections. Therefore, to this order we can replace the overall prefactor $b^2(\epsilon)\sqrt{f(\epsilon)}$ by ℓ^2/ϵ^2. Thus, to lowest non-vanishing order:

$$\frac{\mathcal{F}}{\sigma} = 6\frac{\ell^2}{\epsilon^2} \left[\left(5\mathcal{G} + \frac{C}{8} \right) \frac{\epsilon^2}{\ell^2} + b_o(\epsilon)\delta\epsilon \left(2\frac{\dot{b}_o^2}{b_o^2}(\epsilon) - \frac{\ddot{b}_o}{b_o}(\epsilon) \right) \right] - C \tag{C.12}$$

The last term in the parenthesis requires more care: due to the extra logarithm in $\delta\epsilon$ we cannot just replace $b_o(r)$ by ℓ/r. On the other hand we can use the zeroth order Einstein's equation (A.11) to write it as:

$$b_o(\epsilon)\delta\epsilon \left(2\frac{\dot{b}_o^2}{b_o^2}(\epsilon) - \frac{\ddot{b}_o}{b_o}(\epsilon) \right) = b_o(\epsilon)\, \delta\epsilon\, \frac{4}{9}\dot{\Phi}_o^2(\epsilon) = -\frac{5}{2}\, \mathcal{G}\, \frac{\epsilon^2}{\ell^2} \tag{C.13}$$

where in the last line we used $\dot{\Phi}_o(\epsilon) = -(\epsilon \log \epsilon\Lambda)^{-1}$ (cfr. eq. (2.17)). Notice that the logarithm in $\delta\epsilon$ has canceled. Finally, we get:

$$\frac{\mathcal{F}}{\sigma} = 15\, \mathcal{G} - \frac{C}{4} \tag{C.14}$$

JHEP05(2009)033

C.3 The black-hole mass

The mass of a solution, with respect to a reference background, can be defined following the procedure: first consider a time slicing of the 5-dimensional metric, of the ADM form

$$ds^2 = -N^2 dt^2 + \gamma_{ij}(dx^i - N^i dt)(dx^j - N^j dt) \qquad i,j = r,1,2,3 \tag{C.15}$$

where γ_{ij} is the induced metric on each 4D slice Σ_t. Then the mass of the solution, with respect to a reference background with the same asymptotic behavior at spatial infinity, is given by [46]

$$E = -\frac{1}{8\pi G_5}\int_{\Sigma_\infty} N\left(\sqrt{\gamma^{\rm ind}}\,{}^{(3)}K - \sqrt{\gamma_o^{ind}}\,{}^{(3)}K_o\right) \tag{C.16}$$

where Σ_∞ is a 3-dimensional surface at spatial infinity embedded in the 4D constant-time slice Σ_t, γ_{ind} is the three-dimensional induced metric, ${}^{(3)}K$ is its extrinsic curvature, and $\gamma_o^{\rm ind}$ and ${}^{(3)}K_o$ the analogous quantities for the reference background. The latter should be chosen so that the geometry of the 3-dimensional surface at infinity and the value of the scalar field on that surface match.

In our case, the 5D solutions are static and in conformal coordinates they are of the form:

$$ds^2 = b(r)^2\left(-f(r)dt^2 + \frac{dr^2}{f(r)} + dx^m dx_m\right), \quad ds_o^2 = b_o(r)^2\left(-dt^2 + dr^2 + dx^m dx_m\right). \tag{C.17}$$

The boundary at infinity is at $r = \epsilon$, with $\epsilon \to 0$. Thus, we have:

$$N = b(r)\sqrt{f}, \qquad \gamma_{ij}dx^i dx^j = b(r)^2\left(\frac{dr^2}{f(r)} + dx^m dx_m\right), \tag{C.18}$$

and on the surface $r = \epsilon$ we have

$$\gamma_{mn}^{\rm ind} = b(\epsilon)^2\delta_{mn}, \qquad n^i = -\frac{\sqrt{f}(\epsilon)}{b(\epsilon)}\left(\frac{\partial}{\partial r}\right)^i \tag{C.19}$$

The 3D extrinsic curvature is given by:

$${}^{(3)}K = \nabla_i n^i = \frac{1}{\sqrt{\gamma}}\partial_j\left(\sqrt{\gamma}\gamma^{ij}n_j\right) = -3\sqrt{f(\epsilon)}\frac{\dot{b}(\epsilon)}{b^2(\epsilon)}. \tag{C.20}$$

The reference background has $f = 1$, boundary at $\tilde{\epsilon} = \epsilon + \delta\epsilon$ (as in 3.21) so that $\lambda(\epsilon) = \lambda_o(\tilde{\epsilon})$, and rescaled volume $\tilde{V}_3 = V_3 b^3(\epsilon)/b_o(\tilde{\epsilon})$. Also, the time slicing has to be the same, i.e. $N(\epsilon) = N_o(\tilde{\epsilon})$ in the ADM decomposition. Thus from eq. (C.16) we obtain:

$$E = \frac{3V_3}{8\pi G_5}b^2(\epsilon)\sqrt{f(\epsilon)}\left(\sqrt{f}(\epsilon)\dot{b}(\epsilon) - \frac{b^2(\epsilon)}{b_o^2(\tilde{\epsilon})}\dot{b}_o(\tilde{\epsilon})\right) \tag{C.21}$$

Using eqs. (C.11) and performing similar steps to those that led to eq. (C.14) we obtain:

$$E = M_p^3 N_c^2 V_3\left(15\mathcal{G} + \frac{3}{4}C\right) \tag{C.22}$$

where we have used $16\pi G_5 = M_p^{-3}N_c^{-2}$.

JHEP05(2009)033

D The gluon condensate asymptotics

We want to show that the gluon condensate $\mathcal{G}$ obeys to the asymptotics (5.5) at high temperatures. To do this we need to compute explicitly the relation between T and r_h in the UV limit $r_h \to 0$.

Temperature. Knowing that the expansion for the metric reads as in (2.16) (this is the zero temperature solution, however the r^4 correction of the finite temperature solution is subleading w.r.t. logarithms) we find that the expansion for the thermal factor $f(r)$ in the UV is given by solving the second equation in (3.5)

$$f(r) = 1 - \frac{r^4}{r_h^4}\left[1 + \frac{4}{3}\frac{\log\frac{r}{r_h} - \frac{4}{3}}{\log \Lambda r \, \log \Lambda r_h} + \mathcal{O}\left(\frac{\log(-\log \Lambda r)}{\log^2 \Lambda r}\right)\right] \tag{D.1}$$

The derivative of f w.r.t. r then evaluates to

$$\dot{f}(r) = -4\frac{r^3}{r_h^4}\left[1 + \frac{4}{3}\frac{\log\frac{r}{r_h} - \frac{4}{3}}{\log \Lambda r \, \log \Lambda r_h} + \frac{1}{3}\frac{1 + \mathcal{O}\left(\frac{1}{\log \Lambda r}\right)}{\log \Lambda r \, \log \Lambda r_h} + \mathcal{O}\left(\frac{\log(-\log \Lambda r)}{\log^2 \Lambda r}\right)\right] \tag{D.2}$$

The temperature is obtained by evaluating the above expression at the horizon

$$T = \frac{|\dot{f}(r_h)|}{4\pi} = \frac{1}{\pi r_h}\left[1 - \frac{4}{9}\frac{1}{\log^2 \Lambda r_h} + \mathcal{O}\left(\frac{\log(-\log \Lambda r)}{\log^3 \Lambda r}\right)\right] \tag{D.3}$$

Entropy. We now want to calculate the entropy density $s = 4\pi M^3 b^3(r_h)$. Inverting this relation we get r_h as a function of the temperature

$$r_h = \frac{1}{\pi T}\left[1 - \frac{4}{9}\frac{1}{\log^2 \frac{\Lambda}{\pi T}} + \mathcal{O}\left(\frac{\log(-\log \frac{\Lambda}{\pi T})}{\log^3 \frac{\Lambda}{\pi T}}\right)\right] \tag{D.4}$$

Plugging this expression into the expansion for the scale factor (5.5) we obtain b as a function of the temperature

$$b(T) = \pi \ell T\left[1 + \frac{4}{9}\frac{1}{\log \frac{\Lambda}{\pi T}} + \mathcal{O}\left(\frac{\log(-\log \frac{\Lambda}{\pi T})}{\log^2 \frac{\Lambda}{\pi T}}\right)\right] \tag{D.5}$$

The subleading term $\mathcal{O}\left(\log^{-2}(\Lambda/\pi T)\right)$ will not enter into the leading calculation of the gluon condensate asymptotics. The entropy density evaluates to

$$s(T) = 4\pi^4 \ell^3 T^3\left[1 + \frac{4}{3}\frac{1}{\log \frac{\Lambda}{\pi T}} + \mathcal{O}\left(\frac{\log(-\log \frac{\Lambda}{\pi T})}{\log^2 \frac{\Lambda}{\pi T}}\right)\right] \equiv 4\pi^4 \ell^3 T^3 \xi(T) \tag{D.6}$$

where the last equality is the definition of the function $\xi(T)$.

JHEP05(2009)033

Gluon condensate asymptotics. Putting together the information relating the gluon condensate to the free energy on the one hand through eq. (3.25) and, on the other hand, the free energy to the entropy through $\mathcal{F} = -\partial S/\partial T$ we arrive to an equation for the gluon condensate

$$12\mathcal{G}(T) = \frac{Ts(T)}{4} - \int_{T_c}^{T} \mathrm{d}t\; s(t) \tag{D.7}$$

$$= \pi^4 \ell^3 T^4 \xi(T) - 4\pi^4 \ell^3 \int_{T_c}^{T} \mathrm{d}t\; t^3 \xi(t) \tag{D.8}$$

$$= \pi^4 \ell^3 \int_{T_c}^{T} \mathrm{d}t\; t^4 \xi'(t)\ . \tag{D.9}$$

The last line uses integration by parts. The expansion of the derivative of the function $\xi(T)$ reads

$$\xi'(T) = \frac{4}{3}\frac{1}{T}\frac{1}{\log^2 \frac{\Lambda}{\pi T}}\,(1 + \dots) \tag{D.10}$$

The ellipsis indicates subleading terms in the log expansion.

So that finally the gluon condensate expansion at high temperatures $T \gg \Lambda$ at leading order can be written as

$$\mathcal{G}(T) \approx \frac{\pi^4}{36}\ell^3 \frac{T^4}{\log^2 \frac{\Lambda}{\pi T}} \tag{D.11}$$

E The superpotential at zero-T

Here we analyze the general solution of the zero-temperature superpotential equation, eq. (2.7), (below, $\lambda = e^{\Phi}$).

$$-\frac{4}{3}\lambda^2 (W'(\lambda))^2 + \frac{64}{27} W^2(\lambda) = V(\lambda). \tag{E.1}$$

we assume $V(\lambda) > 0$ First let us observe some general properties:

1. The solution can only exist as long as $|W(\lambda)| > \sqrt{(27/64)V(\lambda)}$;
2. The equation has a symmetry $W \to -W$, so we can limit the analysis to $W > 0$.
3. For any $\lambda_0 \neq 0$, there are two solutions of (E.1), $W_+(\lambda), W_-(\lambda)$ passing through the point λ_0, such that $W_+(\lambda_0) = W_-(\lambda_0)$, and $W'_+\lambda_0) = -W'_-(\lambda_0)$. In other words there are two branches of solutions: one where W and W' have the same sign (i.e. $W'_+(\lambda) > 0$) , another where they have opposite sign ($W_+(\lambda) < 0$)
4. At any $\lambda_* \neq 0$ where $|W(\lambda_*)| = \sqrt{27/64 V(\lambda_*)}$, $W' = 0$.
5. A solution can go past such a point λ_* *only* if $V'(\lambda_*) = 0$. Indeed, suppose that $V'(\lambda_*) > 0$. if the solution exists for $\lambda < \lambda_*$, at the point λ_* we have:

$$W(\lambda_*) = \sqrt{(27/64)V(\lambda_*)};\;\; W'(\lambda_*) = 0\;\; ; V'(\lambda_*) > 0$$
$$\Rightarrow \quad W(\lambda_* + \epsilon) < \sqrt{(27/64)V(\lambda_* + \epsilon)} \tag{E.2}$$

therefore the solution does not exists for $\lambda > \lambda_*$.

6. By the same argument, if $V(\lambda_*) < 0$, the solution does not exist for $\lambda < \lambda_*$.

7. It follows from points 3,4 and 5 that, if $V(\lambda)$ is positive and monotonic, the two branches $W_+(\lambda)$ and $W_-(\lambda)$ (see point 4) are completely disconnected, since neither W' nor W can change sign. However two solutions belonging to different branches can be glued together at a point $W' = 0$.

8. All solutions that reach $\lambda = 0$ have either $W(0) = \sqrt{(27/64)V(0)}$, or $W'(0) = \infty$.

In what follows we assume $V(\lambda) > 0$ and without loss of generality we take $W(\lambda) > 0$.

E.1 Solution close to a critical point

Let us see how the solution approaches the critical points $W'(\lambda_*) = 0$. For definiteness, consider $V(\lambda)$ monotonically increasing, and $W(\lambda) > 0$ (as in our model). The solution exists only for $\lambda < \lambda_*$. As we said there are two disconnected branches with opposite sings of W'. Let us are analyze them separately.

W_- Branch

In this case, $W'(\lambda) < 0$ for all $\lambda < \lambda_*$. Then eq. (E.1) can be written as:

$$W'(\lambda) = -\frac{4}{3\lambda}\sqrt{W^2 - \frac{27}{64}V} \tag{E.3}$$

Let us look at this equation close to a point $\lambda_* \neq 0$ where $W^2(\lambda_*) = 27/64V(\lambda_*) \equiv W_*^2$. Write $W = W_* + w(\lambda)$, with $w(\lambda_*) = 0$, and expand (E.3) to linear order in $w(\lambda)$:

$$w'(\lambda) = -\frac{4}{3\lambda_*}\sqrt{2W_* w(\lambda) - V'(\lambda_*)(\lambda - \lambda_*)} \tag{E.4}$$

this is still hard to solve explicitly, but we can carry out the analysis by making further assumptions about the possible behavior of $w(\lambda)$ close to λ_*. There are only three possibilities:

1. $|w(\lambda)| > O(\lambda - \lambda_*)$ as $\lambda \to \lambda_*$.
   then we can neglect the second term under the square root, and the equation becomes

   $$w'(\lambda) = -\frac{4}{3\lambda_*}\sqrt{2W_* w(\lambda)} \tag{E.5}$$

   which is solved by $w(\lambda) \sim (\lambda - l_*)^2$. This is inconsistent with the assumption $|w(\lambda)| > O(\lambda - \lambda_*)$, so this case is ruled out.

2. $|w(\lambda)| \simeq -w_1(\lambda - \lambda_*)$ as $\lambda \to \lambda_*$, with $w_1 > 0$.

   Eq. (E.4) becomes:

   $$w'(\lambda) = -\frac{4}{3\lambda_*}\sqrt{(2W_* w_1 + V'(\lambda_*))(\lambda_* - \lambda)}, \tag{E.6}$$

   which is solved, for $\lambda < \lambda_*$, by $w \simeq const(\lambda_* - \lambda)^{3/2}$, in contradiction with our assumption. So this case is ruled out too.

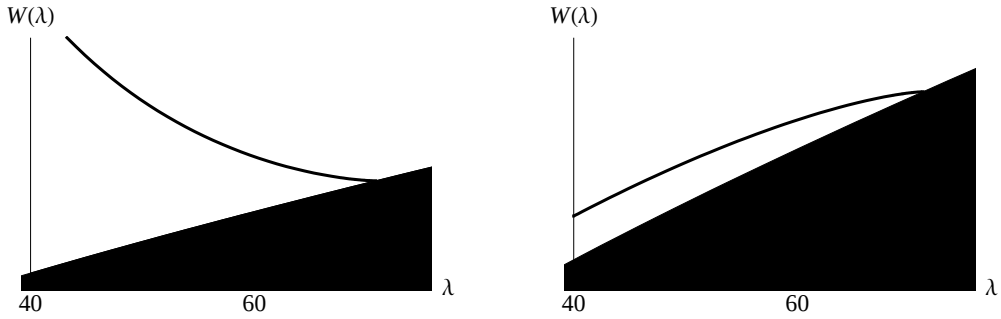

Figure 12. Superpotential on (a) the W_- branch and (b) the W_+ branch, close to a critical point. The black area is the "forbidden" region below the critical curve $\sqrt{27V/64}$, where W' would become imaginary. The solution stops where it meets the critical curve.

3. $|w(\lambda)| < O(\lambda - \lambda_*)$ as $\lambda \to \lambda_*$.
   In this case we can neglect the first term in the square root, and obtain:

$$w'(\lambda) = -\frac{4}{3\lambda_*}\sqrt{V'(\lambda_*)(\lambda_* - \lambda)} \tag{E.7}$$

   which integrates to:

$$w(\lambda) \sim \frac{8}{9\lambda_*}\sqrt{V'(\lambda_*)}(\lambda_* - \lambda)^{3/2} \qquad \lambda < \lambda_* \tag{E.8}$$

   This time the solution is consistent with the hypothesis.

The three possibilities listed above exhaust all possible behaviors of $W(\lambda)$ close to a critical point λ_*, and the only one which does not lead to a contradiction is the last one. Thus, we can conclude that the behavior close to a critical point is given by eq. (E.8). in other words, $W_-(\lambda)$ is positive and decreasing for $\lambda < \lambda_*$, and it reaches a finite value W_* at the critical point, where it behaves like

$$W_-(\lambda) \sim W_* + W_1(\lambda_* - \lambda)^{3/2}, \qquad W_1 > 0 \tag{E.9}$$

The behavior of $W_-(\lambda)$ close to a critical point is exemplified in figure 12 (a)

W_+ branch. The analysis is the same as for the W_- branch: the solution is defined only for $\lambda \leq \lambda_*$, except that $W(\lambda)$ is increasing and close to λ_* we have:

$$W_+(\lambda) \sim W_* - W_1(\lambda_* - \lambda)^{3/2}, \qquad W_1 > 0 \tag{E.10}$$

this type of solution is shown in figure 12 (b)

Metric and dilaton close to a critical point. Although $W'(\lambda_*) = 0$, the metric is *not* AdS close to λ_*. In fact, the equation for $A(\lambda)$ reads:

$$\lambda\frac{dA}{d\lambda} = -\frac{3}{X(\lambda)}, \qquad X = -\frac{3}{4}\lambda\frac{W'}{W}. \tag{E.11}$$

JHEP05(2009)033

Close to the critical point λ_*, $X \sim \mp(3W_1/2W_*)(\lambda_* - \lambda)^{1/2}$, so the scale factor close to λ_* is finite, and behaves as

$$A_\pm(\lambda) \sim A_* \pm A_1(\lambda_* - \lambda)^{1/2}, \qquad A_1 > 0 \tag{E.12}$$

Notice that the upper sign corresponds to the W_+ branch ($X < 0$), in which the scale factor *decreases* towards the endpoint λ_*, which is therefore in the IR.The other branch $W_-(\lambda)$ ($X > 0$) has $\lambda = \lambda_*$ as the UV.

Finally, we can integrate the dilaton equation as a function of the coordinate r,

$$\frac{\dot\lambda}{\lambda} = \lambda \frac{dW}{d\lambda} e^A. \tag{E.13}$$

Using the form of $A(\lambda)$ and $W(\lambda)$ close to λ_*, eqs. (E.12), we arrive at:

$$\lambda(r) \sim \lambda_* - \lambda_1(r_* - r)^2, \quad A_\pm(r) \sim A_* \pm A_1|r_* - r|, \qquad \lambda_1 > 0, A_1 > 0 \tag{E.14}$$

Here the upper sign holds for $r < r_*$, the lower for $r > r_*$. From the last equation, we see that in the r coordinate the point r_* where $\lambda(r_*) = \lambda_*$ is perfectly regular, and we can obtain a full solution describing both branches by simply removing the absolute value,

$$\lambda(r) \sim \lambda_* - \lambda_1(r_* - r)^2, \quad A(r) \sim A_* + A_1(r_* - r), \qquad \lambda_1 > 0, A_1 > 0 \tag{E.15}$$

At the critical point the dilaton reaches its maximum value λ_*, then reverts the direction of running, and is not a good coordinate globally. Instead $A(r)$ is monotonic along the full solution. The UV corresponds to $r < r_*$, the IR to $r > r_*$.

E.2 Solutions close to $\lambda = 0$

Here we still have two branches, but we have two completely different behaviors in each branch. Assume $V > 0$, $V' > 0$ close to $\lambda = 0$, and a power expansion of the form:

$$V = V_0 + V_1\lambda + V_2\lambda^2 + \dots \tag{E.16}$$

***W_* branch.** In this case the general solution of eq. (E.1) close to $\lambda = 0$ is:

$$W_-(\lambda) \sim W_0 \left(\frac{C}{\lambda^{4/3}} + \frac{\lambda^{4/3}}{C} + W_1 \frac{\lambda^{4/3+1}}{C} + \dots \right), \quad C > 0 \tag{E.17}$$

where W_0 and W_1 are completely fixed by the expansion coefficients of $V(\lambda)$ around zero. Since W_- is a decreasing function for small λ, from our general considerations we know that if $V(\lambda)$ is monotonic then $W_-(\lambda)$ is monotonically decreasing globally, therefore the solution will hit a critical point at some $\lambda_* > 0$ and terminate.

Solving the metric and dilaton equations in the region $\lambda \sim 0$ with the superpotential (E.17) gives a singularity at a finite value $r = r_0$ of the conformal coordinate, where both the scale factor $a(r) \to 0$ and the dilaton $\lambda \to 0$.

$$e^{A(r)} \sim (r_0 - r)^{\frac{1}{3}}, \qquad \lambda(r) \sim (r_0 - r)^{\frac{1}{2}}. \tag{E.18}$$

We see that $e^{A(r)}$ decreases to zero as $\lambda(r) \to 0$, and $\dot l/\dot A > 0$. With our holographic dictionary, ($\log A \leftrightarrow E$ and $\beta(\lambda) = \dot l/\dot A$, we conclude that Therefore in this case the small λ region is in the IR, and the theory is IR-free.

JHEP05(2009)033

W_+ branch. In this branch, any solution of (E.1) necessarily satisfies

$$W_+(0) = \sqrt{\frac{27}{64}V_0} \tag{E.19}$$

(one can show that any ansatz with $W'(0) = +\infty$ cannot solve the equation).

Moreover, if W is written as a power series expansion around $\lambda = 0$,

$$W(\lambda) = W_0 + W_1\lambda + W_2\lambda^2 + \dots \tag{E.20}$$

then *all the coefficients W_i are uniquely determined by the expansion coefficients V_i of $V(\lambda)$*. However, it is incorrect to conclude that that the solution in this branch is unique. To see this, take any function $\hat{W}(\lambda)$ that solves (E.1) to all orders in powers of λ. Then, consider a function $W(\lambda)$ that, close to $\lambda = 0$, behaves as

$$W(\lambda) = \hat{W}(\lambda) + w(\lambda), \qquad \frac{w(\lambda)}{\hat{W}(\lambda)} \to 0 \ as \ \lambda \to 0. \tag{E.21}$$

Inserting this in the eq. (E.1), and expanding to linear order in $w(\lambda)$ gives, close to $\lambda = 0$:

$$-\frac{4}{3}2\lambda^2\hat{W}'(0)w'(\lambda) + \frac{64}{27}2\hat{W}(0)w(\lambda) = 0 \tag{E.22}$$

i.e. a homogeneous, linear equation, whose general solution is

$$w_C(\lambda) = C\lambda^{16/9-4b}\exp\left[-\frac{16}{9}\frac{\hat{W}(0)}{\hat{W}'(0)}\frac{1}{\lambda}\right] \tag{E.23}$$

Therefore, also in the $W' > 0$ branch we have a one-parameter family of solutions, that close to $\lambda = 0$ all have the same power expansion, and look like:

$$W(\lambda) = \hat{W} + w_c(\lambda) + \dots \tag{E.24}$$

where $\hat{W}$ is a fixed power series (say, with no exponential part), $w_c(\lambda)$ is given in eq. (E.23), and the dots represent even more subleading terms ($\sim w^2$).

Due to the expasion (E.20), the solution close to $\lambda = 0$ is, to leading order, an AdS_5 spacetime with logarithmic running,

$$b(r) = \frac{\ell}{r}\left[1 + \frac{4}{9}\frac{1}{\log r\Lambda} + \dots\right], \quad \lambda(r) = -\frac{1}{b_0\log r\Lambda} + \dots \tag{E.25}$$

Notice that the exponent in (E.23) is fixed by the first two expansion coefficients of $V(\lambda)$, and one can easily show that, in terms of the β-function coefficient b_0:

$$\frac{16}{9}\frac{\hat{W}(0)}{\hat{W}'(0)} = \frac{4}{b_0} \quad \Rightarrow \quad w_c \sim \lambda^{16/9-4b}e^{-\frac{4}{b_0\lambda}}, \tag{E.26}$$

Using the perturbative asymptotics $b_0\lambda \sim (\log r)^{-1}$, this corresponds to a power-law correction to the logarithm expansion in (E.25), that scales like r^4 close to the AdS boundary $r = 0$. Since the power series expansion of $W(\lambda)$ around $\lambda = 0$ is independent of the integration constant C in (E.23), we conclude that metric that correspond to different solutions on the W_+ branch differ only by *non-perturbative* $O(r^4)$ terms, which correspond to different values for the gluon condensate.

JHEP05(2009)033

E.3 Solutions close to $\lambda = \infty$

Finally we analyze the solution of (E.1) in the asymptotic region of large λ. We assume for the potential a power-law behavior

$$V(\lambda) \sim V_\infty \lambda^{2Q} (\log \lambda)^P \qquad \lambda \to \infty \tag{E.27}$$

for some constant V_∞ and $Q > 0$. We are interested in $V_\infty > 0$, since this case corresponds to a potential which is bounded from below. There are two kinds of solutions:

1. a continuous one-parameter family of the form:

$$W_C(\lambda) = W_\infty \left[C\lambda^{4/3} + \frac{C^{-1}}{(4-3Q)} \lambda^{2Q-4/3} (\log \lambda)^P + \dots \right], \qquad W_\infty = \sqrt{\frac{27 V_\infty}{64}} \tag{E.28}$$

   where C is an arbitrary constant of integration;

2. a *single* solution that asymptotes as

$$W_s(\lambda) = \tilde{W}_\infty \lambda^Q (\log \lambda)^{P/2}, \qquad \tilde{W}_\infty = \sqrt{\frac{27 V_\infty}{4(16-9Q^2)}} \tag{E.29}$$

Notice if $V_\infty > 0$, both types of solutions exist only if $Q < 4/3$: for $Q > 4/3$ the l.h.s. of the differential equation is asymptotically negative. In this case there is no solution that reaches arbitrarily large values of λ, but rather all solutions to (E.1) are of the type described in section (E.1): they reach a maximum value λ_* where a W_+ and a W_- solutions join.

With the restriction $Q < 4/3$ the first term in eq. (E.28) is the dominant one, and the singular solution grows slower than any of the solutions in the continuous family.

For all superpotentials in the continuous family the metric and dilaton exhibit the same kind of IR singularity at finite r (where $a(r) \to 0$, $\lambda(r) \to \infty$) , regardless of the value of Q and P:

$$a(r) \sim (r_0 - r)^{1/3}, \qquad \lambda(r) \sim \frac{1}{(r_0 - r)^{1/2}}. \tag{E.30}$$

This is similar to the singularity in eq. (E.18), up to $\lambda \to 1/\lambda$. These singularity always fall in the pathological class, as discussed in ([28]): the singularity is not screened from physical fluctuations, and one can have an infalling flux of particles. Moreover, as shown in appendix F, these singularity do not appear as continuous limits of black-hole solutions with regular horizons.

On the ohter hand the singular solution (E.29) is the most interesting from a physical point of view: the singularity is repulsive for $Q < 2\sqrt{2}/3$ and it can be cloaked by a horizon. Solutions of this kinds are the ones that give rise to the most interesting holographic constructions from the QCD perspective.

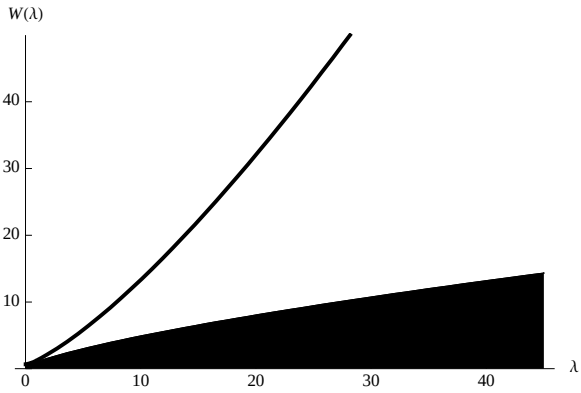

Figure 13. Superpotential of the "generic" kind. The black area is the forbidden region below the curve $\sqrt{27V/64}$

E.4 General classification of the solutions

The results of this appendix can be summarized as follows: For any positive and monotonic potential $V(\lambda)$ with the asymptotics:

$$\begin{aligned} V(\lambda) &= V_0 + V_1\lambda + V_2\lambda^2 + \dots & V_0 > 0, \qquad \lambda \to 0 \\ V(\lambda) &= V_\infty \lambda^{2Q} (\log \lambda)^P, & V_\infty > 0, \qquad \lambda \to \infty \end{aligned}$$

the zero-temperature superpotential equation has three types of solutions, that we name the *Generic*, the *Special*, and the *Bouncing* types: :

1. A continuous one-parameter family that has a fixed power-law expansion near $\lambda = 0$, and reaches the asymptotic large-λ region where it grows as

$$W \simeq C_b \lambda^{4/3} \qquad \lambda \to \infty \tag{E.31}$$

   where C_b is an arbitrary positive real number These solutions lead to backgrounds with "bad" (i.e. non-screened) singularities at finite r_0, where $b(r) \to 0$ and $\lambda \to \infty$ as

$$a(r) \sim (r_0 - r)^{1/3}, \qquad \lambda(r) \sim (r_0 - r)^{-1/2} \tag{E.32}$$

   We call this solution *generic*. An example is shown in figure 13

2. A unique solution, which also reaches the large-λ region, but slower:

$$W(\lambda) \sim W_\infty \lambda^Q (\log \lambda)^{P/2}, \qquad W_\infty = \sqrt{\frac{27 V_\infty}{4(16 - 9Q^2)}} \tag{E.33}$$

   This leads to a repulsive singularity, provided $Q < 2\sqrt{2}/3$ [28]. We call this the *special* solution. An example is shown in figure 14

JHEP05(2009)033

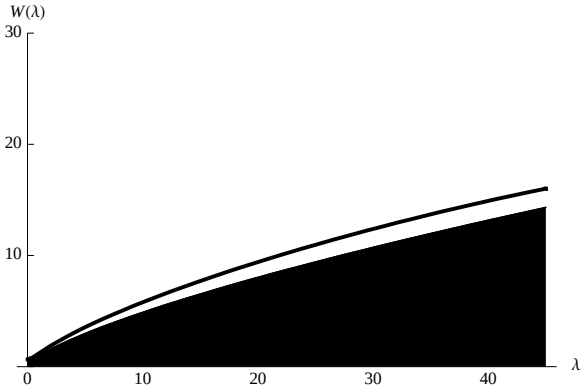

Figure 14. Superpotential of the "special" solution. The black area is the forbidden region below the curve $\sqrt{27V/64}$

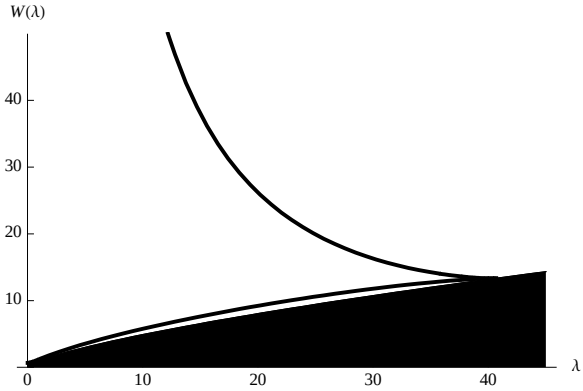

Figure 15. Superpotential of the "bouncing" kind. The black area is the forbidden region below the curve $\sqrt{27V/64}$

3. A second continuous one-parameter family where $W(\lambda)$ does not reach the asymptotic region. These solutions have two branches that both reach $\lambda = 0$ (one in the UV, the other in the IR) and merge at a point λ_* where $W(\lambda_*) = \sqrt{27V(\lambda_*)/64}$. The IR branch is again a "bad" singularity at a finite value r_0, where $W \sim \lambda^{-4/3}$, and

$$b(r) \sim (r_0 - r)^{1/3}, \qquad \lambda(r) \sim (r_0 - r)^{1/2}. \tag{E.34}$$

We call this solution *bouncing*. An example is shown in figure 15

Notice that, as two solutions with positive derivative cannot cross, the special solution (figure 14) marks the boundary between the generic solutions, that reach the asymptotic large-λ region as $\lambda^{4/3}$ (figure 13) and the bouncing ones, that don't reach it, figure 15. Notice that, if $Q > 4/3$, only bouncing solutions exist.

In all types of solutions the UV corresponds to the region $\lambda \to 0$ on the W_+ branch. There the behavior of W_+ is universal: a power series in λ with *fixed* coefficients, plus a

JHEP05(2009)033

subleading non-analytic piece which depends on an arbitrary integration constant C_w:

$$W = \sum_{i=1}^{\infty} W_i \lambda^i + C_w \lambda^{16/9} e^{-\frac{16W_0}{9W_1}} [1 + O(\lambda)] \tag{E.35}$$

All the power series coefficients W_i are completely determined by the coefficients in the small λ expansion of $V(\lambda)$, the first few being:

$$W_0 = \frac{\sqrt{27V_0}}{8}, \quad W_1 = \frac{V_1}{16}\sqrt{\frac{27}{V0}}, \quad W_2 = \frac{\sqrt{27}(64V_0V_2 - 7V1^2)}{1024V_0^{3/2}} \tag{E.36}$$

F The superpotential at finite T

F.1 The thermal superpotential

A useful way of counting the integration constants and to parametrize the different black-hole solution is to extend the notion of superpotential to the black-hole backgrounds. We will call the resulting *thermal superpotential* $W(\Phi)$, and its zero-temperature precursor $W_o(\Phi)$.

First, we define

$$b = e^A, \qquad f = e^g, \tag{F.1}$$

and use the domain-wall parametrization of the metric,

$$dr = e^{-A} du. \tag{F.2}$$

In this coordinate frame the metric has the following form:

$$ds^2 = e^{2A}\left(-e^g dt^2 + dx_m dx^m\right) + e^{-g} du^2. \tag{F.3}$$

The equations of motion (3.5) and (3.6) in the variable u take the following form (a prime denotes derivative w.r.t. u):

$$A'' + \frac{4}{9}\Phi'^2 = 0, \tag{F.4}$$

$$g' + \frac{g''}{g'} + 4A' = 0, \tag{F.5}$$

$$12A'^2 + 3A'g' - \frac{4}{3}\Phi'^2 - e^{-g}V = 0, \tag{F.6}$$

Equation (F.4) is the same as in the zero-temperature system, cfr. eqs. (2.6). This has an interesting consequence: we recall that (F.4) is the equation that guarantees a well-defined arrow of the RG flow in the gauge theory. Here we see that one can define the RG flow in the same way in the gauge theory at finite-T. In other words, the conclusion that $A(u)$ is monotonically decreasing still holds at finite temperature.

Since eq. (F.4) takes the same form as when $g(r) = 0$, we can use this equation to define a superpotential just as for $T = 0$: the second order equation (F.4) can be replaced

JHEP05(2009)033

by the two first order equations, and the system becomes:

$$A' = -\frac{4}{9}W(\Phi), \qquad \Phi' = \frac{\mathrm{d}W(\Phi)}{\mathrm{d}\Phi}, \tag{F.7}$$

$$\frac{g'' + g'^2}{g'} = \frac{16}{9}W(\Phi) \tag{F.8}$$

$$-\frac{4}{3}\left(\frac{\mathrm{d}W(\Phi)}{\mathrm{d}\Phi}\right)^2 + \frac{64}{27}W(\Phi)^2 - \frac{4}{3}W(\Phi)\,g' = \mathrm{e}^{-g}V(\Phi). \tag{F.9}$$

Equations (F.7) provide the definition of the thermal superpotential $W(\Phi)$.

F.2 Counting integration constants: uniqueness properties of BH solutions

The system (F.7)–(F.9) has to be solved for the functions A, Φ, g, W once $V(\Phi)$ is given as input. As in the $T = 0$ case, once $W(\Phi)$ is given the scale factor and dilaton are uniquely fixed up to a single physical integration constant (a choice of scale) However, now $W(\Phi)$ is not simply a solution of a first order equation, as in (2.7). Since we cannot decouple the equation for W, we cannot choose it as an input as we did in the $T = 0$ case.

As it turns out, the most natural place where to fix the integration constants is the horizon, rather than the boundary. In other words, the general solution of the fifth order system (F.7)–(F.9) is most easily parametrized by the horizon value of the functions involved.

Consider a black-hole with a regular horizon located at $u = u_h$. As we approach the horizon, $u \to u_h$, the dilaton, the scale factor and the superpotential have regular expansions,

$$\begin{aligned} &A \to A_h - (u_h - u)A'(u_h) + \ldots, \quad \lambda \to \lambda_h - (u_h - u)\lambda'(u_h) + \ldots, \\ &W \to W_h - (u_h - u)\lambda'(u_h)\partial_\lambda W(\lambda_h), \end{aligned} \tag{F.10}$$

where $W_h \equiv W(\lambda_h)$. On the other hand close to the horizon we must have have:

$$g = \log(u_h - u) + g_h + O\left((u_h - u)^2\right), \qquad u \to u_h \tag{F.11}$$

where $g_h = \log[-f'(u_h)]$. Substituting these values in equation (F.9) we see that regularity at the horizon requires the condition:

$$W_h = \frac{1}{3}e^{-g_h}V(\lambda_h). \tag{F.12}$$

On the other hand, the quantities A_h, λ_h and g_h are free. The differential equation determines the following terms in the expansion around u_h in terms of these quantities, and of $V(\lambda)$ and its derivatives at λ_h.

We can use the horizon quantities to fix all integration integration constants of the system (F.7)–(F.9). The system is first order in $A(u)$,$\Phi(u)$ and $W(u)$, and second order in $g(u)$, therefore it contains five integration constants. One of them is un-physical, and it is due to reparametrization invariance. It can be eliminated by using λ in place of u as a coordinate, or it can be fixed by setting u_h to an arbitrary value. The four quantities λ_h, A_h, g_h, W_h provide the remaining four integration constants. For an arbitrary choice

the solution will be singular at the horizon, whereas regularity is assured by imposing the constraint (F.12).

Notice that the value of the potential at the horizon has to be positive in order to get a well-behaved black-hole solution. This is similar to Gubser's criterion identifying good singularities [29].

What we have shown above means that the theory has a three-parameter family of regular black-hole solutions, characterized by the three real numbers λ_h, A_h, g_h. However, since the initial conditions were set at the horizon, these solutions will not all have the same UV asymptotics. To understand what happens in the UV, $u \to -\infty$ in these coordinates), notice that close to u_h we have $W(u) > 0$, $g'(u) < 0$. Moreover by eq. (F.8), $g''(u) < 0$ as long as $g'(u) < 0$ and $W > 0$. Thus, $|g'(u)|$ decreases as we go further away from the horizon. As a consequence, the extra term $-Wg'$ in (F.9), that did not appear in the zero-temperature equation (2.7), become less and less important as we move away from the horizon towards the asymptotic region. At the same time due to the relative signs of g' and g'', $g(u)$ approaches a constant value g_0, and the r.h.s. of eq. (F.9) approaches the r.h.s. of (2.7) up to a multiplicative constant. Therefore the solution will get closer and closer to one of the zero-temperature solutions, up to a rescaling of $W(\Phi)$: $W(\lambda) \to e^{g_0/2} W_o(\lambda)$ as $\lambda \to 0$. The existence of a solution that connects the horizon to the UV boundary will be proved more rigorously in appendix H.4.

This is not the end of the story, since we want the the black-hole solution to have the same UV asymptotics as the zero-temperature solutions. Notice however that eqs. (F.7)–(F.9) are invariant under the two following independent transformations:

$$\lambda(u), A(u), g(u), W(u) \to \lambda(ue^{-\delta_1}), A(ue^{-\delta_1}), g(ue^{-\delta_1}) - 2\delta_1, e_1^{\delta} W(ue^{-\delta_1}) \quad \text{(F.13)}$$

$$\lambda(u), A(u), g(u), W(u) \to \lambda(u), A(u) + \delta_2, g(u), W(u) \quad \text{(F.14)}$$

where $\delta_{1,2}$ are arbitrary real numbers. These transformations map a solution into another solution, and also preserve the regularity condition (F.12). Therefore one can use these transformations to move in the space of solutions, and reach the one with the desired asymptotics. Specifically, one can construct a regular UV black-hole solution with UV asymptotics matching a given $T = 0$ background in the following way:

1. choose an arbitrary horizon position u_h and fix arbitrary values for the initial data at the horizon, namely A_h, g_h, λ_h

2. fix the fourth initial data, W_h, according to the regularity condition.

3. Evolve the solution from the horizon to the UV. In general, as $u \to -\infty$, $g(u)$ will go to a constant $g_{\rm UV} \neq 0$.

4. Use a symmetry transformation with parameter $\delta_1 = g_{\rm UV}/2$. In the new solution g goes to the correct UV limit (namely, zero).

5. Use a δ_2 transformation to reset the overall scale of the solution to the desired value (e.g. to match a given $T = 0$ solution). (This does not affect $g(u)$)

JHEP05(2009)033

At the end of this procedure, the only free parameter remains the initial choice of λ_h. Thus, for each λ_h, the solution with given UV boundary conditions is unique. For a given choice of UV asymptotics, the black-hole metric and temperature depends only on λ_h, which can then be used as an unambiguous quantity to parametrize the different solutions.

F.3 Asymptotic form of the solution

Here we determine the behavior of the solution of the finite-T generalization of the superpotential equations, (F.9), in the small λ and large-λ region, respectively.

The nontrivial part of eqs. (F.7)–(F.9) is the one that determines W and g; then, A and Φ follow as in the zero-temperature case. We can decouple the $W-g$ system from the rest, as follows: First using (F.7), we rewrite eqs. (F.8) and (F.9) keeping Φ as the independent variable. In this way, the four equations (F.7)–(F.9) split in two independent sets of equations. For the scale factor we have (as for zero-temperature)

$$\partial_\Phi A = -\frac{4}{9}\frac{W}{\partial_\Phi W}; \tag{F.15}$$

for $W(\Phi)$ and $g(\Phi)$ we find:

$$\left(\partial_\Phi g + \frac{\partial_\Phi^2 g}{\partial_\Phi g}\right)\partial_\Phi W + \partial_\Phi^2 W = \frac{16}{9}W \tag{F.16}$$

$$-\frac{4}{3}W(\partial_\Phi W)(\partial_\Phi g) - \frac{4}{3}(\partial_\Phi W)^2 + \frac{64}{27}W^2 = e^{-g}V(\lambda) \tag{F.17}$$

Eq. (F.16) can be integrated to a closed expression for $g(\Phi)$ in terms of $W(\Phi)$. Write

$$\partial_\Phi\left[g + \log(-\partial_\Phi g)\right] = \frac{\frac{16}{9}W - \partial_\Phi^2 W}{\partial_\Phi W} \equiv F_W(\Phi) \tag{F.18}$$

Thus,

$$g + \log(-\partial_\Phi g) = \int d\Phi\, F_W(\Phi), \tag{F.19}$$

and exponentiating:

$$(-\partial_\Phi g)e^g = e^{\int d\Phi\, F_W(\Phi)}. \tag{F.20}$$

Integrating one more time we obtain an explicit expression for $g(\Phi)$ in terms of the (still unknown) function $F_W(\Phi)$:

$$g(\Phi) = \log\int d\Phi e^{\int d\Phi' F_W(\Phi')}. \tag{F.21}$$

F.3.1 Solution of the $W(\Phi)$-$g(\Phi)$ system in the $\lambda \to 0$ limit

As usual, we assume a power series expansion of $V(\lambda)$ as $\lambda \to 0$. We take a power series ansatz for $W(\lambda)$ as well, as for its zero temperature counterpart,

$$W(\lambda) = \tilde{W}_0 + \tilde{W}_1\lambda + \tilde{W}_2\lambda^2 + \ldots \tag{F.22}$$

where the expansion coefficients $\tilde{W}_i$ are *a priori* temperature dependent.

Using this ansatz in eq. (F.21), written in terms of $\lambda = e^{\Phi}$, we can obtain the form of $g(\lambda)$ for small λ. We have from eq (F.18)

$$F_W(\lambda) = \frac{16\tilde{W}_0}{9\tilde{W}_1}\frac{1}{\lambda} + \frac{1}{9}\left(7 - 32\frac{\tilde{W}_0\tilde{W}_2}{\tilde{W}_1{}^2}\right) + O(\lambda), \qquad \lambda \to 0. \tag{F.23}$$

Using this expression in eq. (F.21) we obtain:

$$g(\lambda) = \log\left\{g_1 + g_2\lambda^{\gamma}e^{-\frac{16\tilde{W}_0}{9\tilde{W}_1}\frac{1}{\lambda}}\left[1 + O(\lambda)\right]\right\} \qquad \gamma \equiv \frac{16}{9} - 32\frac{\tilde{W}_0\tilde{W}_2}{\tilde{W}_1{}^2} \tag{F.24}$$

where g_1 and g_2 are integration constants. To recover the UV boundary condition $g(\lambda) \to 0$ as $\lambda \to 0$, we must fix $g_1 = 1$. g_2 ultimately determines the temperature of the solution, and is only required to be negative.

Next, we insert the asyptotics (F.24) in the equation (F.17), in order to determine the coefficients. For small λ it reads:

$$\begin{aligned} -\frac{4}{3}g_2 W(\partial_\lambda W)\lambda^{\gamma+2}e^{\frac{-16\tilde{W}_0}{9\tilde{W}_1}\frac{1}{\lambda}}\left[1 + O(\lambda)\right] - \frac{4}{3}\lambda^2\left(\partial_\lambda W\right)^2 + \frac{64}{27}W^2 \\ = V(\lambda)\left[1 - g_2\lambda^{\gamma}e^{\frac{-16\tilde{W}_0}{9\tilde{W}_1}\frac{1}{\lambda}} + \dots\right] \end{aligned} \tag{F.25}$$

To any finite order in powers of λ, *this equation is the same as the zero-temperature superpotential equation*, (E.1). It follows that the power series expansion of $W(\lambda)$ is not affected by the temperature, and all the coefficients are the same as in the zero temperature solution: $\tilde{W}_i = W_i$. The difference between the finite-T and zero-T solutions are of order $\lambda^{\gamma}e^{-4/(b_0\lambda)} \sim r^4$, and imply a temperature dependent value for the gluon condensate, cfr. appendix E.

Since the series coefficients of $W(\lambda)$ completely determine the UV series in inverse logarithms of r of the metric and dilaton, it follows that such series has the same form for any temperature.

F.3.2 Solution of the $W(\Phi)$-$g(\Phi)$ system in the asymptotic large Φ region

Next we want to solve the system of eqs (5.12)–(5.13), for in the asymptotic region of large Φ. This is defined as the region beyond some Φ_0 where the potential can be well approximated by its leading asymptotic,[28]

$$V(\Phi) \simeq e^{2Q\Phi}\Phi^P \qquad \Phi \gg \Phi_0. \tag{F.26}$$

We assume the horizon is situated in this region, i.e. we work in the limit $\Phi_h \geq \Phi > \Phi_0$. The IR asymptotics of the zero temperature superpotential $W_o(\Phi)$ giving rise to the well behaved solutions with the repulsive singularity are of the form:

$$W_o \sim \Phi^{P/2}\, e^{Q\,\Phi}, \Phi \gg \Phi_0. \tag{F.27}$$

[28] the actual value of Φ_0 is immaterial, and will depend on the specific choice for the potential.

JHEP05(2009)033

Let us try the ansatz for the large Φ behavior of W:

$$W(\Phi) \sim e^{\tilde{Q}\Phi}\Phi^{\tilde{P}/2}, \qquad \Phi \gg \Phi_0. \tag{F.28}$$

With this ansatz we can directly calculate the r.h.s. of eq. (F.18). To leading and first subleading order we have:

$$F_W(\Phi) \simeq K + \frac{R}{\Phi} + O\left(\frac{1}{\Phi^2}\right), \quad K \equiv \left(\frac{16}{9\tilde{Q}} - \tilde{Q}\right), \quad R \equiv -\frac{\tilde{P}}{2}\left(1 + \frac{16}{9\tilde{Q}^2}\right), \tag{F.29}$$

and from eq. (F.20) we obtain:

$$g(\Phi) = \log\left\{C_2 - C_1\Phi^R e^{K\Phi}\left[1 + O\left(\frac{1}{\Phi}\right)\right]\right\}, \tag{F.30}$$

where C_1 and C_2 are two integration constants. This solution is supposed to be valid in the whole region $\Phi_0 \ll \Phi \leq \Phi_h$, and we can relate Φ_h to the integration constants by going to the horizon, $g \to -\infty$:

$$C_2 - C_1(\Phi_h)^R e^{K\Phi_h} = 0 \tag{F.31}$$

so we can write eq. (F.30) as:

$$g(\Phi) = \log C_2\left\{1 - \left(\frac{\Phi}{\Phi_h}\right)^R e^{K(\Phi-\Phi_h)}\left[1 + O\left(\frac{1}{\Phi}\right)\right]\right\}. \tag{F.32}$$

Finally, requiring $g \simeq 0$ for $1 \ll \Phi \ll \Phi_h$, fixes $C_2 = 1$.

The appropriate solution for $f \equiv \mathrm{e}^g$ is therefore:

$$f(\Phi) = 1 - \left(\frac{\Phi}{\Phi_h}\right)^R e^{-K(\Phi_h-\Phi)}. \tag{F.33}$$

which correctly interpolates between the desired behavior at $\Phi \ll \Phi_h$ and $\Phi = \Phi_h$. This solution is valid in the whole region $\Phi \gg \Phi_0$ up to the horizon $\Phi = \Phi_h$.[29]

Now let us look at equation (5.13). Using (F.33), and neglecting $O(1/\Phi^2)$ terms, it becomes:

$$\begin{aligned}
&\left\{\frac{4}{3}\left(\tilde{Q} + \tilde{P}/2\Phi\right)\left(K + \frac{R}{\Phi}\right)\frac{\left(\frac{\Phi}{\Phi_h}\right)^R e^{K(\Phi-\Phi_h)}}{1 - \left(\frac{\Phi}{\Phi_h}\right)^R e^{K(\Phi-\Phi_h)}} - \frac{4}{3}\left(\tilde{Q}^2 + \frac{\tilde{P}}{2\Phi}\right)^2 + \frac{64}{27}\right\} e^{2\tilde{Q}\Phi}\Phi^{\tilde{P}} \\
&= \frac{1}{1 - \left(\frac{\Phi}{\Phi_h}\right)^R e^{K(\Phi-\Phi_h)}}\left\{-\frac{4}{3}\left(Q^2 + \frac{P}{2\Phi}\right)^2 + \frac{64}{27}\right\} e^{2Q\Phi}\Phi^P.
\end{aligned} \tag{F.34}$$

For $\Phi \ll \Phi_h$ this requires:

$$\tilde{Q} = Q, \quad \tilde{P} = P, \tag{F.35}$$

[29] For $\Phi > \Phi_h$ the solution is the same, but the definition of g changes: $f = -e^{-g}$.

JHEP05(2009)033

i.e. the superpotential must have the same large Φ asymptotics as the zero-temperature special solution. *Then, eq. (F.34) is equivalent to the Φ-independent algebraic equations*:

$$-\frac{4}{3}QK = -\frac{4}{3}Q^2 + \frac{64}{27}, \qquad \left(\frac{PK}{2} + RQ\right) = -QP \tag{F.36}$$

which are identically satisfied, due to the definitions of K and R in (F.29)!

Therefore the asymptotic solution with horizon at $\Phi = \Phi_h$ is , to this order:

$$W(\Phi) \simeq W_o(\Phi) \simeq e^{Q\Phi}\Phi^{P/2} \tag{F.37}$$

$$f(\Phi) \simeq 1 - \left(\frac{\Phi}{\Phi_h}\right)^R \exp[-K(\Phi_h - \Phi)], \tag{F.38}$$

valid in the whole asymptotic region $\Phi_h > \Phi \gg \Phi_0$.

In the particular case of power-law behavior, $A_o(r) \sim -Cr^\alpha$, corresponding to $Q = 2/3$, $P = (\alpha - 1)/\alpha$ (see [28]), the solution in r-coordinates is, for large r:

$$A(r) \sim -Cr^\alpha, \tag{F.39}$$

$$\Phi(r) \simeq \frac{3}{2}Cr^\alpha + \frac{3}{4}(\alpha - 1)\log r, \tag{F.40}$$

$$f \sim \Phi^{-\frac{5}{2}P}e^{2\Phi} \sim r^{-\frac{5}{2}(\alpha-1)}e^{3Cr^\alpha + \frac{3}{2}(\alpha-1)\log r} \sim r^{1-\alpha}e^{3Cr^\alpha} \tag{F.41}$$

The horizon position is obtained by inverting $\Phi(r_h) = \Phi_h$.

We can verify directly that these asymptotics solve eqs. (3.5)–(3.6), for $V \sim \mathrm{e}^{\frac{4}{3}\Phi}$. Using the asymptotic form $b(r) = b_0\mathrm{e}^{-Cr^\alpha}$, we get, integrating eq (3.7)

$$\begin{aligned} f(r) &\sim C_2 + C_1\int^r \mathrm{d}t\, b^{-3}(t) = C_2 + \frac{C_1}{\alpha C}\int^{3Cr^\alpha} \mathrm{d}s\, s^{\frac{1}{\alpha}(1-\alpha)}\mathrm{e}^s \\ &\simeq C_2 + \frac{C_1}{3\alpha C}r^{1-\alpha}\mathrm{e}^{3Cr^\alpha} \end{aligned} \tag{F.42}$$

Substituting into the equation for the potential yields

$$\begin{aligned} V(r) &= \frac{3}{b^2}\left\{f\left[2\frac{\dot b^2}{b^2} + \frac{\ddot b}{b}\right] + \dot f\frac{\dot b}{b}\right\} \\ &\simeq \frac{3}{b^2}\left\{\left(C_2 + \frac{C_1}{3\alpha C}r^{1-\alpha}\mathrm{e}^{3Cr^\alpha}\right)\left(3\alpha^2C^4r^{2(\alpha-1)}\right) + C_1\mathrm{e}^{3Cr^\alpha}\left(-\alpha Cr^{\alpha-1}\right)\right\} \\ &\simeq \frac{9\alpha^2C^2}{b_0n^2}C_2r^{2(\alpha-1)}\mathrm{e}^{2r^\alpha} \sim \Phi^{\frac{\alpha-1}{\alpha}}e^{\frac{4}{3}\Phi}. \end{aligned} \tag{F.43}$$

This is the expected leading behavior for the potential. The contributions proportional to $C_1\mathrm{e}^{5Cr^\alpha} \simeq C_1\mathrm{e}^{\frac{10}{3}\Phi}$ cancel between the two terms containing f and $\dot f$ respectively. V is independent of C_1, which encodes the horizon position. Furthermore, comparing eq. (F.43) with the expression for $V(r)$ one obtains with $f \equiv 1$, we see that C_2 must be set to $C_2 = 1$ if the potential has to be the same as in the zero-temperature solution, in agreement with eq. (5.19).

JHEP05(2009)033

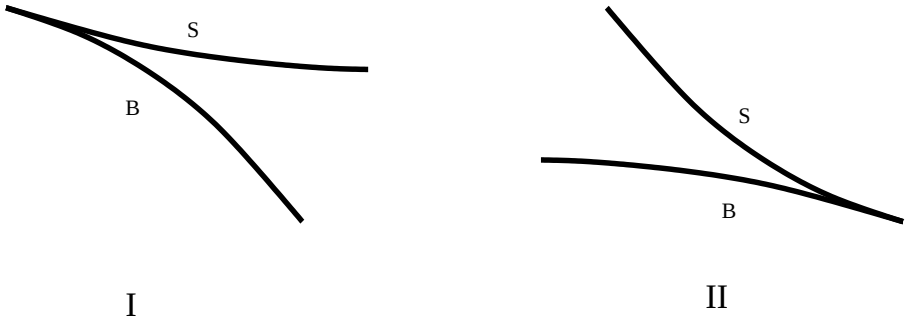

Figure 16. Two possible types of cusps at which the small and big BH in pair can merge. These are denoted by "S" and "B" , respectively. The full curve $F(T)$ should be constructed by various combinations of these vertices.

G Multiple big black-holes

In this section we generalize the proposition of section 5.3 to a much larger class of geometries, for which the functions $F(\lambda_h)$ and $T(\lambda_h)$ may acquire multiple extrema,[30] see figures 18 and 19 for an example. In these cases there are more than just two BHs. However for the generic confining theories,[31] they still come in pairs of one small ($T'(\lambda_h) > 0$) and one big ($T'(\lambda_h) < 0$) BH, connected at an extremum of $T(\lambda_h)$. Therefore there is an even number of BHs in total. This follows from the fact that there always exists an asymptotically AdS big BH for $\lambda_h \to 0$ and a small BH for $\lambda_h \to \infty$ and one extremum of $T(\lambda_h)$ creates two branches (a small and a big), by definition.

In particular we want to prove the following:

1. Existence of a deconfinement phase transition,
2. Finite latent heat (first order transition),
3. Continuity of F as a function of T,
4. Uniqueness of the deconfinement transition.

We shall first present a graphical proof of these points. For illustration purposes we make the following additional assumption (that seems natural and satisfied by a large class of potentials): $C_v = TdS/dT$ is negative (positive) for small (big) BHs.[32] After the graphical demonstration below, we provide an analytic proof which applies to cases when this additional assumption is weakened. The assumption about the specific heat is actually not needed for point 1 in the above list, so that the main result (the existence of a phase transition) is valid for an arbitrary behavior of the specific heat. The function $F(T)$ is determined from $F(\lambda_h)$ and $\lambda_h(T)$. Since the latter is generally multi-valued, so is $F(T)$. As a multivalued function it can have a very complicated form with cusps and crossings, see figure 17 for an example. Although complicated, the form of $F(T)$ is restricted by certain rules:

[30] We assume that these functions are C^∞ in λ_h.
[31] except the borderline case of $\alpha = 1$.
[32] as in the case of the AdS_5 BH with spherical horizon.

JHEP05(2009)033

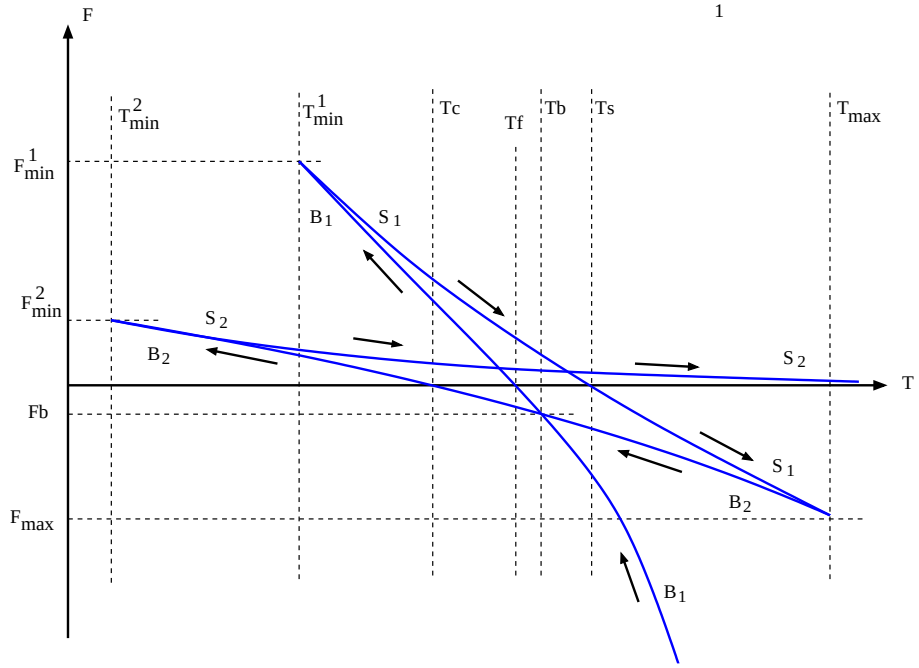

Figure 17. Example of a curve $F(T)$ that exhibits multiple extrema. S_1 and S_2 denote small BHs whereas B_1 and B_2 denote big BHs. The arrows represent direction of increasing λ_h.

1. On every piece of the $F(T)$ curve, $F'(T) < 0$. This follows from the positivity of entropy.

2. On the small black-hole branches $F''(T) > 0$, and on the big black-hole branches $F''(T) < 0$. This follows from our assumption above and from $F'' \propto -C_v$.

3. There should always be a big black-hole branch (which asymptotically becomes the AdS black-hole at high-T) in the high-T (small λ_h) region, on which $F(T) \to -\infty$ as $T \to \infty$.

4. There should always be a small black-hole branch in the high-T (large λ_h) region, on which $F(T) \to 0$. This follows from the discussion in section 5.2.

5. The small and the big BHs always come in pairs, hence there are equal numbers of branches on the $F(T)$ curve, with negative and positive $F''(T)$. This is clear from the fact that one small and one big black-hole branches off at an extremum of $T(\lambda_h)$.

6. These merging points of a pair of big and small BHs are represented by a cusp. There are two possible types of cusps as shown in figure 16. These particular shapes follow from the first two properties above. Since at the merging points the entropy is the same, $\mathcal{F}'$ is the same on the two branches of the cusp.

For an example of a curve $F(T)$ with these properties, see figure 17. Given these properties, it is not hard to show that the *minimum energy configuration* for $T > T_c$[33]

[33]There may be more than one T_c on which F vanishes and our statement applies to all of these points.

JHEP05(2009)033

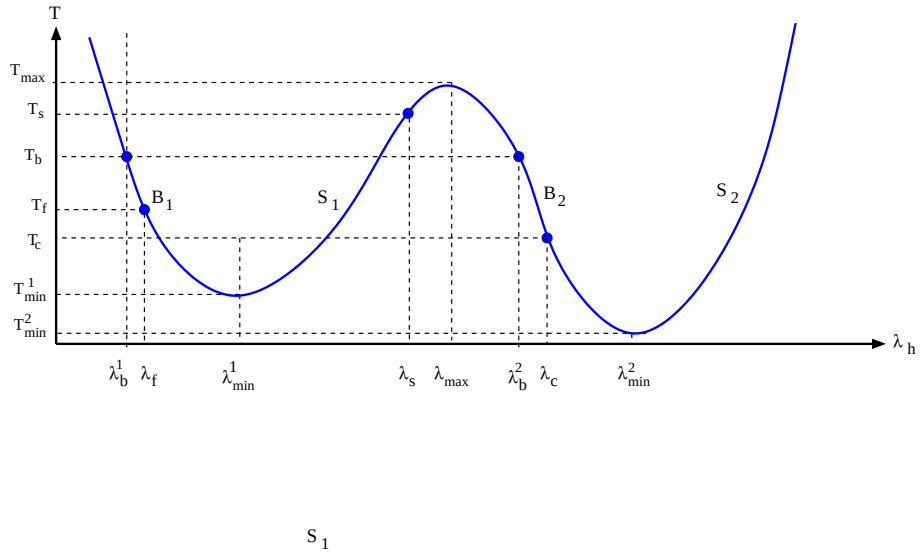

Figure 18. T as a function of λ_h in the example of figure 17.

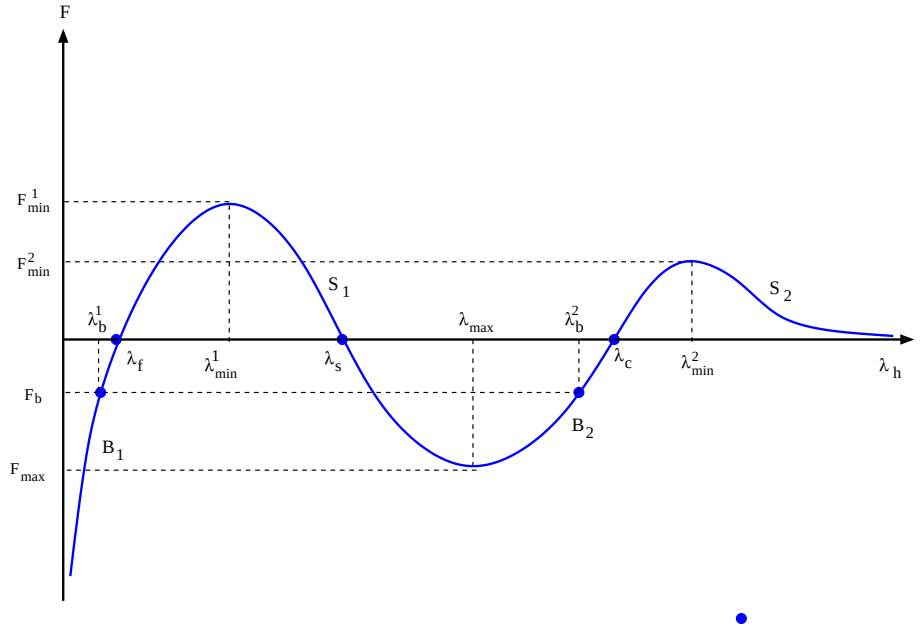

Figure 19. F as a function of λ_h in the example of figure 17.

is always a big BH. This is because, the entire curve $F(T)$ should be formed out of the vertices given in figure 16 connected with small and big BH legs. Clearly for any small BH, there exist a big BH that stems from the same vertex which has lower energy. Therefore, in the entire curve for $F < 0$, the lowest energy configuration should be a big black-hole.

Of course, below $T = T_c$ the lowest energy configuration becomes the thermal gas and the curve $F_{\rm min}(T)$ for the minimum energy configuration always looks like in figure 7. For the example given in fig 17, the corresponding free energy diagram is constructed in 8. The reason that $F(T)$ should cross zero (point 1 in the list above), hence exhibit a phase

JHEP05(2009)033

transition, follows from the 2nd and the 3rd properties above. Similarly, the points 2, 3 and 4 simply follow from the fact that one cannot draw a function $F(T)$ that violates these points with the properties listed above. Thus, we demonstrated what we wanted: *the proposition of section 5.3 apply to the multiple extrema cases as well.*

Before going into the analytic proof of these statements, let us analyze the example of figure 17 in more detail. In this particular case, there are two small and big BH pairs that are denoted by (S_1, B_1) and (S_2, B_2). The black-holes in each pair merge at two local minima of $T(\lambda_h)$ (that are denoted by $T^1_{\rm min}$ and $T^2_{\rm min}$)) and the two pairs are connected at a local maxima of $T(\lambda_h)$ (denoted by $T_{\rm max}$). See figure 18 which plots $T(\lambda_h)$, that corresponds to figure 17 for a clear demonstration of these facts. We also present the function $F(\lambda_h)$ that corresponds to this example in figure 19. Given figure 18 and figure 19, figure 17 follows by solving for F as a function of T parametrically. The arrows in figure 17 point to the direction of increasing λ_h.

Figure 17 exhibits various *first order* transitions between different branches. First of all there are transitions between thermal gas (with $F(T) = 0$) and B_1, B_2 and S_1. We denote these points as T_f, T_c and T_s respectively in figure 17. However, not all of these points correspond to actual phase transitions. In order to obtain the true free energy of the system, one should draw $F(T)$ *on the minimum energy configuration.* This looks is much simpler and the one corresponding to figure 17 is given by figure 8. In particular, we see that out of T_f, T_c and T_s, only T_c is a real phase transition. It is in fact the confinement-deconfinement phase transition in this example. T_f corresponds to a "fake" deconfinement transition, because B_1 has higher energy than B_2 at the point it crosses $F = 0$. Similarly, at T_s, there is a fake transition between a *small* BH and the thermal gas geometry. Although these are fake transitions, hence uninteresting for the dual field theory point of view, they may bear some interest on the bulk as they describe possible transitions between various different geometries in asymptotically AdS spaces. The fake transitions described here parallels the transitions found in R^4 and F^4 corrected AdS geometry in [51]. In addition, there are various transitions among small and big BHs (S_2 and B_1 in the figure) and different small black-holes (S_1 and S_2 in the figure).

However there is another interesting possibility that is also present in this example: *a first order transition between two different big black-holes at T_b.* This transition is not "fake" as others, because it corresponds to first order transition between two minimum energy configurations, B_1 and B_2 in fig 17. See also figure 8. It will be interesting to investigate whether or not a dilaton potential $V(\lambda)$ with this property exists; if so, whether or not this corresponds to a meaningful phase transition in the dual gauge theory.

G.1 Analytic demonstration

Suppose the function $T(\lambda_h)$ has an arbitrary number n of minima, with n (even) odd for (non-)confining IR asymptotics,[34] corresponding to certain values λ_i, $i = 1 \ldots n$. Then, there will be $n + 1$ black-hole branches, each corresponding to the ranges $(\lambda_i, \lambda_{i+1})$, with $\lambda_0 \equiv 0$ and $\lambda_{n+1} \equiv +\infty$. In each branch the free energy as a function of T is single valued,

[34] except in the borderline confining case where there is also an even number of minima

JHEP05(2009)033

and is given by the first law, $\mathcal{F}_i(T) = -\int S_i(T')dT' + C_i$ where S_i is the entropy function in the ith branch (i.e. in the interval $(\lambda_{i-1}, \lambda_i)$), and C_i are integration constants. We can still write the free energy in compact form as

$$\mathcal{F}(\lambda_h) = \int_{\lambda_h}^{+\infty} d\lambda'\, S(\lambda')\frac{dT}{d\lambda'}, \tag{G.1}$$

as this is the unique continuous function that satisfies $d\mathcal{F}/dT = -S$ on every branch, and vanishes as $\lambda_h \to \infty$. Since S is nowhere vanishing for finite λ, a minimum for $T(\lambda)$ corresponds to a maximum for $\mathcal{F}(\lambda)$. Using the integral expression of the free energy, we can give an analytic proof of the proposition in section 5.3 relating confinement with the existence of phase transitions.

Let us consider confining asymptotics. We want to show that these always exhibit a first order phase transition. In particular we want to prove the following three statements:

1. $\mathcal{F}$ changes sign at some finite λ. Specifically, $\mathcal{F} \to -\infty$ as $\lambda \to 0$, whereas $\mathcal{F}(\lambda_n) > 0$;

2. For every λ_i corresponding to a *minimum* of $T(\lambda)$, either $\mathcal{F}(\lambda_i)$ is positive or it is larger than the free energy of some big black-hole with the same temperature;

3. For every λ_i corresponding to a *maximum* of $T(\lambda)$, $\mathcal{F}(\lambda_i)$ there exists a big black-hole with the same temperature and lower free energy.

Step 1 by itself shows that there is indeed a phase transition. It goes in the right direction, since at small temperature ($T < T_{\rm min}$) there are no black-hole solutions, and moreover in any black-hole branch the free energy is a decreasing function of temperature. Therefore the black-hole free energy crosses from positive to negative (with respect to the vacuum) as the temperature increases.

Steps 2 and 3 imply that the free energy never jumps in either directions: the branching points when a large/small black-hole pair appears or disappears have always higher free energy than some other state in the ensemble (which therefore must have been dominant starting from some lower temperature). If this weren't true, it would be possible to have discontinuous jumps in the free energy, i.e. phase transitions with infinite latent heat. In this step, one needs an extra assumption about the ordering of the black-hole branches. Step 3 also implies that ones the system is in the black-hole phase for some temperature, it stays in a black-hole phase for all higher temperatures, so there cannot be any inverse "reconfining" transition.

The proof of Step 1 is straightforward, and identical to the argument we used in section 5.3 in the case of $n = 1$, i.e. when $T(\lambda_h)$ has a single minimum. Thus, the existence of a deconfining phase transition *per se* is easy to prove. To prove Steps 2 and 3 however, in the general case $n > 1$ we need to make an extra assumption about the nature of the entropy $S(\lambda)$:

Assumption: *the black-hole branches are "ordered" in the sense that* $S_i(\lambda) > S_{i+1}(\lambda')$ *for any* $\lambda \in (\lambda_{i-1}, \lambda_i)$ *and any* $\lambda' \in (\lambda_i, \lambda_{i+1})$.

This still allows some local violation of the monotonicity of $S(\lambda)$ within each branch. Although we cannot exclude violation of this assumption from first principles, it is satisfied in all examples we have studied numerically, where we also found cases with strict monotonicity of $S(\lambda)$ violated (these cases correspond to regions of stable small black-holes, as discussed in section 5.2.2). The above assumption might be relaxed, since it is probably not a necessary condition for the statements 2 and 3 to hold, but it allows the construction of a simple enough proof.

With the above assumption, the proof of the proposition goes as follows.

Step 1. The fact that $\mathcal{F} < 0$ for small enough λ follows from eq. (5.6), whose validity does not depend on the number of extrema of $T(\lambda_h)$; on the other hand, evaluating the free energy on the extremum (a minimum) of $T(\lambda_h)$ with larger λ_h, we obtain:

$$\mathcal{F}(\lambda_n) = \int_{\lambda_n}^{+\infty} S \frac{dT}{d\lambda'} > 0, \tag{G.2}$$

since in the last branch $dT/d\lambda > 0$. This is true without additional assumptions about the function $S(\lambda)$.

Step 2. First, consider the extremum λ_i corresponding to the absolute minimum of $T(\lambda_h)$, $T(\lambda_i) = T_{\min}$. Since the last extremum λ_n is also a minimum, there will be $2k = n - i$ minima and $2k - 1$ maxima in the region $\lambda > \lambda_i$, corresponding to $2k$ maxima and $2k - 1$ minima for $\mathcal{F}(\lambda)$. We are going to show that $\mathcal{F}(\lambda_i) - \mathcal{F}(\lambda_n) > 0$. Let us evaluate the black-hole free energy at the point λ_i:

$$\begin{aligned} \mathcal{F}(\lambda_i) &= \int_{\lambda_i}^{+\infty} S(\lambda') \frac{dT}{d\lambda'} \\ &= \int_{\lambda_i}^{\lambda_{i+1}} S(\lambda') \frac{dT}{d\lambda'} + \int_{\lambda_{i+1}}^{\lambda_{i+2}} S(\lambda') \frac{dT}{d\lambda'} + \ldots \int_{\lambda_{n-1}}^{\lambda_n} S(\lambda') \frac{dT}{d\lambda'} + \mathcal{F}(\lambda_n). \end{aligned} \tag{G.3}$$

Each integral is extended over a different black-hole branch. In every branch, we can use the mean value theorem:

$$\int_{\lambda_j}^{\lambda_{j+1}} S(\lambda') \frac{dT}{d\lambda'} = S_{j+1}(T_{j+1} - T_j), \tag{G.4}$$

where $S_{j+1} \equiv S(\bar{\lambda}_{j+1})$, for some appropriate value $\bar{\lambda}_{j+1}$ with $\lambda_j < \bar{\lambda}_{j+1} < \lambda_{j+1}$.

Then, (G.3) becomes:

$$\mathcal{F}(\lambda_i) - \mathcal{F}(\lambda_n) = S_{i+1}(T_{i+1} - T_i) + S_{i+2}(T_{i+2} - T_{i+1}) + \ldots S_n(T_n - T_{n-1}). \tag{G.5}$$

The sum has alternating sign since, for any $l > 0$, T_{i+2l} are local minima and T_{i+2l+1} are local maxima. By assumption, $S_{i+1} > S_{i+2} > \ldots S_n$, therefore:

$$\begin{aligned} &\mathcal{F}(\lambda_i) - \mathcal{F}(\lambda_n) > S_{i+1}(T_{i+1} - T_i) + S_{i+1}(T_{i+2} - T_{i+1}) + \ldots S_{n-1}(T_n - T_{n-1}) \\ = \;& S_{i+1}(T_{i+2} - T_i) + S_{i+3}(T_{i+4} - T_{i+2}) + \ldots S_{n-1}(T_n - T_{n-1}) \end{aligned} \tag{G.6}$$

Notice that now only temperature corresponding to local *minima* appear. Next, subtract the combination $S_{n-1}(T_n - T_i)$ from both sides of the above inequality:

$$\begin{aligned}
\mathcal{F}(\lambda_i) \; - \; & \mathcal{F}(\lambda_n) - S_{n-1}(T_n - T_i) > S_{i+1}(T_{i+2} - T_i) + S_{i+3}(T_{i+4} - T_{i+2}) + \dots \\
& \dots + S_{n-3}(T_{n-2} - T_{n-4}) + S_{n-1}(T_n - T_{n-2}) - S_{n-1}(T_n - T_i) \\
= \; & S_{i+1}(T_{i+2} - T_i) + S_{i+3}(T_{i+4} - T_{i+2}) + \dots + S_{n-3}(T_{n-2} - T_{n-4}) + S_{n-1}(T_i - T_{n-2}) \\
> \; & S_{i+1}(T_{i+2} - T_i) + S_{i+3}(T_{i+4} - T_{i+2}) + \dots + S_{n-3}(T_{n-2} - T_{n-4}) + S_{n-3}(T_i - T_{n-2}) \\
= \; & S_{i+1}(T_{i+2} - T_i) + S_{i+3}(T_{i+4} - T_{i+2}) + \dots + S_{n-3}(T_i - T_{n-4}) \\
> \; & \dots > S_{i+1}(T_{i+2} - T_i) + S_{i+3}(T_i - T_{i+2}) = (S_{i+1} - S_{i+3})(T_{i+2} - T_i) > 0
\end{aligned} \tag{G.7}$$

In each subsequent step we have used $S_{l+1} > S_{l+3}$ and $(T_{l+2} - T_i) < 0$ since we took T_i to be the absolute minimum. Therefore, from the first and last side of (G.7) we get:

$$\mathcal{F}(\lambda_i) > \mathcal{F}(\lambda_n) + S_{n-1}(T_n - T_i) > 0 \tag{G.8}$$

This shows that at the minimum temperature when a black-hole pair appears, the free energy is positive, and the thermal gas background still dominates the ensemble, so the global free energy of the system does not jump abruptly.

To show that the free energy does not exhibits jump at the creation of subsequent black-hole pairs occurring at $T > T_{\min}$, we proceed as follows. Consider the case when λ_i is a generic local minimum. If all the subsequent minima $\lambda_{i+2} \dots \lambda_n$ have higher temperature, then we can proceed exactly as above and show that $F(\lambda_i) > 0$; Otherwise, if there is a local minimum for some $\lambda_{i+2l} > \lambda_i$, with $T_{i+2l} < T_i$, then there is also a big black-hole with temperature $T_B = T_i$, corresponding to a point $\lambda_B \in (\lambda_{i+2l-1}, \lambda_{i+2l})$. It is easy to show that $\mathcal{F}(\lambda_i) > \mathcal{F}(\lambda_B)$, using the same procedure that led to (G.7):

$$\begin{aligned}
\mathcal{F}(\lambda_i) - \mathcal{F}(\lambda_B) = & \int_{\lambda_i}^{\lambda_B} d\lambda' \, S(\lambda') T'(\lambda') \\
= \; & S_{i+1}(T_{i+1} - T_i) + S_{i+2}(T_{i+2} - T_{i+1}) + \dots S_B(T_B - T_{i+2l-1}) \\
> \; & S_{i+1}(T_{i+2} - T_i) + S_{i+3}(T_{i+4} - T_{i+2}) + \dots S_B(T_B - T_{i+2l-1}) \\
> \; & S_B(T_B - T_i) = 0
\end{aligned} \tag{G.9}$$

Therefore, the black-hole pair that appears at T_i cannot dominate the ensemble right at T_i, and the global free energy of the system does not jump.

Step 3. Finally, we show that there cannot be an increase of the free energy back above zero, for temperatures higher than the critical temperature. Since in each branch the free energy of single black-holes is monotonically decreasing, the only way the global free energy can increase is by jumping up at a point where a small/big black-hole pair disappears, i.e. at a local *maximum* of $T(\lambda_h)$ (i.e. a local *minimum* of $\mathcal{F}(\lambda_h)$). Therefore, it is sufficient to show that for any maximum λ_i of $T(\lambda_h)$, with temperature T_i, there exist a black hole with the same temperature $T_B = T_i$ but lower free energy, so that the system does is not forced to jump at $T = T_i$. Since $T(\lambda \to 0) = +\infty$, there certainly exists at least one big black-hole with $T_B = T_i$ and $\lambda_B < \lambda_i$. Let us consider the closest one to λ_i. λ_i will be

JHEP05(2009)033

separated from λ_B by an odd number of extrema (l minima and $l-1$ maxima). Proceeding along similar lines as in Step 2, we now compute the difference $\mathcal{F}(\lambda_B)-\mathcal{F}(\lambda_i)$ and show it is negative:

$$\begin{aligned}\mathcal{F}(\lambda_B)-\mathcal{F}(\lambda_i) &= \int_{\lambda_B}^{\lambda_i} d\lambda'\, S(\lambda')T'(\lambda') \\ &= S_{i-2k-1}(T_{i-2k-1}-T_B)+S_{i-2k}(T_{i-2k}-T_{i-2k-1})+\ldots+S_i(T_i-T_{i-1}) \\ &< S_{i-2k-1}(T_{i-2k}-T_B)+S_{i-2k+1}(T_{i-2k+2}-T_{i-2k})\ldots+S_{i-1}(T_i-T_{i-2}) \\ &= S_{i-2k-1}(T_{i-2k}-T_i)+S_{i-2k+1}(T_{i-2k+2}-T_{i-2k})\ldots+S_{i-1}(T_i-T_{i-2})\end{aligned} \tag{G.10}$$

In the last line, we replaced T_B with T_i in the first term. Now only temperatures of local maxima appear, of which T_i is the highest one. Using repeatedly the inequalities $S_{i-2k-1}>S_{i-2k+1}>\ldots S_{i-1}$ we have:

$$\begin{aligned}\mathcal{F}(\lambda_B)-\mathcal{F}(\lambda_i) &< S_{i-2k-1}(T_{i-2k}-T_i)+S_{i-2k+1}(T_{i-2k+2}-T_{i-2k})+\ldots+S_{i-1}(T_i-T_{i-2}) \\ &< S_{i-2k-+1}(T_{i-2k}-T_i)+S_{i-2k+1}(T_{i-2k+2}-T_{i-2k})+\ldots+S_{i-1}(T_i-T_{i-2}) \\ &= S_{i-2k+1}(T_{i-2k+2}-T_i)+\ldots+S_{i-1}(T_i-T_{i-2}) \\ &< \ldots < S_{i-1}(T_{i-2}-T_i)+S_{i-1}(T_i-T_{i-2})=0\end{aligned} \tag{G.11}$$

Thus, when a black-hole pair disappears at temperature T_i, the system is already on another big black-hole branch with lower free energy.

So far we have treated the case of confining asymptotics. The converse can also be proven under the same assumptions: non-confining asymptotics do not exhibit a thermal gas/black-hole phase transition,[35] rather the system is in a (big) black-hole phase for any $T>0$. The proof proceeds along the same lines as in the confining case.

H Details of the computations with scalar variables

H.1 Equivalence to Einstein's equations

Here we prove that the reduced system of equations presented in the section 7 are equivalent to the equations of motion in the u-variable in (A.17)–(A.20). For this purpose we should supplement (7.2) and (7.3) by the equations that determine the metric functions. These are given by the following first order equations:

$$A' = -\frac{1}{\ell}e^{-\frac{4}{3}\int_{-\infty}^{\Phi}X}, \tag{H.1}$$

$$\Phi' = -\frac{3X}{\ell}e^{-\frac{4}{3}\int_{-\infty}^{\Phi}X}, \tag{H.2}$$

$$g' = -\frac{4Y}{\ell}e^{-\frac{4}{3}\int_{-\infty}^{\Phi}X}. \tag{H.3}$$

Using $d/du=\Phi'(d/d\Phi)$, (7.2), (7.3) and the three equations above in (A.17)–(A.20), it is straightforward to show that they are all solved.

[35] One cannot talk about a deconfining transition here, since the zero-temperature solution itself is not confining

JHEP05(2009)033

To convert the system (7.2), (7.3), (H.1)–(H.3) to the conformal coordinate system, one uses,

$$\frac{du}{dr} = e^A. \tag{H.4}$$

Now, we use this equation to show how r and λ related near the boundary. Converting (H.2) into the r-variable by (H.4), changing variable to $\lambda = \exp(\Phi)$ and using the equation (7.4), one has:

$$\frac{d\lambda}{dr} = -\frac{3X}{\ell}\lambda e^{A_0+\int_{\lambda_0}^{\lambda}(3X\lambda)^{-1}-\frac{4}{3}\int_0^{\lambda}\frac{X}{\lambda}}. \tag{H.5}$$

We use the expansion of X near the boundary in (2.11) to get,

$$\frac{d(b_0\lambda)}{dr} = \frac{1}{\ell}(b_0\lambda)^2 e^{A_0-\frac{1}{b_0\lambda_0}}(b_0\lambda_0)^{-b}e^{\frac{1}{b_0\lambda}}(b_0\lambda)^b\left(1+\mathcal{O}(\lambda)\right). \tag{H.6}$$

Now, we use the definition of the QCD scale Λ in (2.18) and integrate (H.6) to obtain:

$$r\ \Lambda = e^{-\frac{1}{\lambda b_0}}(b_0\lambda)^{-b}. \tag{H.7}$$

The corresponding relation involving the domain wall coordinates is obtained by integrating eq. (H.2). The result in terms of $\lambda(u)$ reads:

$$\frac{1}{b_0\lambda} + \left(\frac{4}{9}+b\right)\log(b_0\lambda) = -\frac{u}{\ell} - \log\Lambda\ell \tag{H.8}$$

H.2 Solution of eq. (7.3)

Here, we note that (7.3) can be solved in terms of X explicitly. Define,

$$c(\Phi) = \frac{4(X^2-1)}{3X}, \qquad d(\Phi) = -\frac{4}{3X}. \tag{H.9}$$

Then, the solution is,

$$Y(\Phi) = e^{\int^{\Phi}c(\Phi')d\Phi'}\left(C_1 - \int^{\Phi}d\Phi' d(\Phi')e^{\int^{\Phi'}c(\tilde{\Phi})d\tilde{\Phi}}\right)^{-1}. \tag{H.10}$$

This is the general solution of (7.3) for non-zero Y. As already mentioned, $Y = 0$ is also a consistent solution, which corresponds to the thermal gas.

H.3 A fixed point analysis of the X-Y system

In order to understand the number of integration constants in the system, one can perform a fixed point analysis of the XY system given by eqs. (7.3) and (7.2).

It is obvious that $Y = 0$ is a fixed line in the phase space. This line corresponds to the zero temperature solutions discussed in [28]. We focus on this case first. The solution is determined by (7.2) at $Y = 0$. Clearly, there are four fixed points of the system for an arbitrary potential. These are given by $X = \pm 1$ and $\pm\infty$. For the special class of exponential potentials $V \sim \exp(\alpha\Phi)$, there is the additional fixed point $X = -3\alpha/8$. Furthermore, $X = 0$ is also a fixed point for the types of potentials we study in this paper.

We solve the system by specifying the boundary conditions (or the asymptotic behavior) in the IR, for large λ. Suppose $X = X_f$ at $\lambda = \lambda_f$. Let us assume for the moment that $X_f < 0$ (as is the case for the "special" and "generic" solutions discussed in this paper). Then, one obtains the following:

JHEP05(2009)033

1. If $-1 < X_f < 0$, then $X \to 0$ as λ decreases, at $\lambda = 0$.

2. If $-\infty < X < -1$ then $X \to -\infty$ as λ decreases at $\lambda = \lambda_i \neq 0$.

To prove the above statements, let us first show that $X = -1$ is a repulsive fixed point in the direction of decreasing λ. To show this, we substitute $X = -1 + \epsilon$, $1 \gg \epsilon > 0$ in (7.2). One has,

$$\frac{d\epsilon}{d\Phi} = \epsilon(-\frac{8}{3} + \frac{d\log(V)}{d\Phi}), \tag{H.11}$$

with the solution,

$$\epsilon = c\ V(\Phi)e^{-8\Phi/3}. \tag{H.12}$$

As $\Phi \to \infty$ $V \to e^{4\Phi/3}$ in our case. Hence one falls into $X = -1$ as $\Phi \to \infty$. Note that the fixed point would instead be attractive for decreasing λ, were $V \to e^{a\Phi/3}$ with $a > 8/3$. The analysis is the same for $X = -1 - \epsilon$, $1 \gg \epsilon > 0$, as one obtains the same equation, (H.11).

Now let us focus on the vicinity of $X = 0$, by writing $X = -\epsilon$, $1 \gg \epsilon > 0$. One obtains

$$\frac{d\epsilon}{d\Phi} = \frac{4}{3} - \frac{1}{2\epsilon}\frac{d\log(V)}{d\Phi}. \tag{H.13}$$

Let us assume that one can reach $X = 0$ at finite $\Phi = \Phi_f$. Then, one can ignore the first term in the r.h.s. of (H.13) above and obtain the follwing solution:

$$\epsilon^2 = -\log(V(\Phi)/V(\Phi_f)) \tag{H.14}$$

as $\Phi \to \Phi_f$. This shows that $X = 0$ *can never be reached* in the decreasing λ direction, in finite λ-time. *Instead X always runs into $X = 0$, in the direction of decreasing λ.*

On the other, hand (H.14) allows to pass the $X = 0$ point in the direction of *increasing* λ, in finite λ-time. These solutions (as functions of r) continue to the positive X region and hit back to the $X = 1$ fixed point as r increases, see figure 20. However, in these solutions the derivative of $\lambda(r)$ changes sign at the locus $X = 0$. As our purpose is to find solutions dual to field theories with negative definite β-functions, these do not correspond to any reasonable theories.

One can easily carry out a similar analysis in the vicinity of $X = -\infty$. For this purpose, we define $Z = 1/X$, and focus on the vicinity of $Z \to 0^-$ by defining $Z = -\epsilon > 0$. To leading order,

$$\frac{d\epsilon}{d\Phi} = \frac{4}{3} - \frac{\epsilon}{2}\frac{d\log(V)}{d\Phi}, \tag{H.15}$$

with the solution,

$$\epsilon = \frac{4}{3}V[\Phi]^{-\frac{1}{2}}\int_{\Phi_i}^{\Phi_f} V^{\frac{1}{2}}[\Phi']d\Phi' \tag{H.16}$$

where Φ_i finite, is an integration constant. It is clear that, ϵ goes to 0 only at a finite point Φ_i.

This completes the proof of the assertions above. A similar analysis can be carried out in the region of $X > 0$. We summarize the behavior of flows in the direction of decreasing λ in figure 21.

The class of solutions to the X equation of motion for $Y = 0$, are summarized in figure 20. There are five classes:

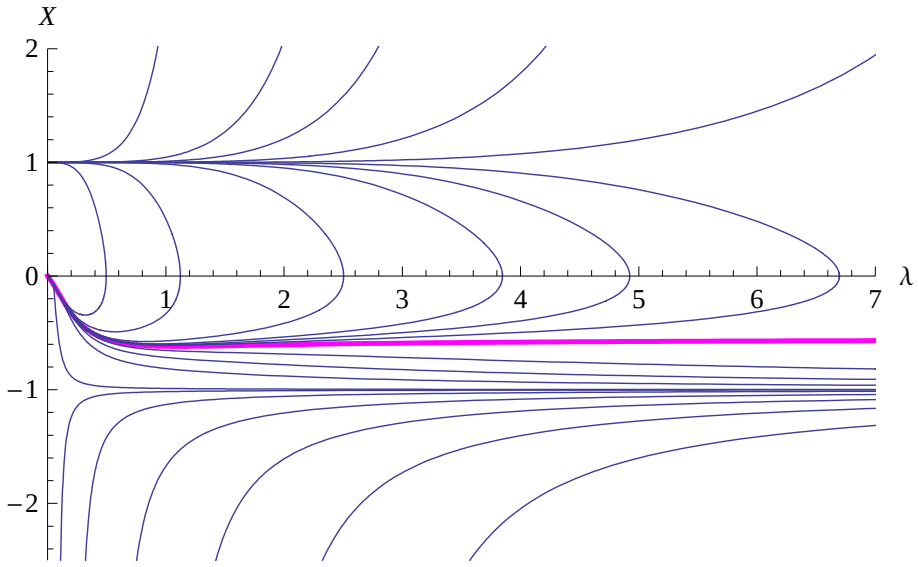

Figure 20. All solutions to the X equation of motion are shown. The thick (red) curve corresponds to our solution X_0, that flows to the fixed point $X = -1/2$. One clearly observes the fixed points $X = \pm 1, \pm\infty$ and $1/2$ in the figure. The direction of flow (as a function of r) is towards the left for $X > 0$ and towards the right for $X < 0$.

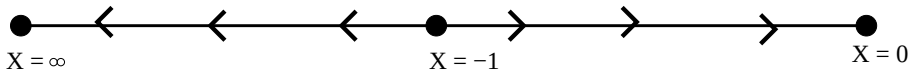

Figure 21. Flow chart of the solutions for $Y = 0$ case. The arrows show the direction of decreasing λ.

- First of all there is our main solution, X_0 that flows to $-1/2$ as l increases. We recall that the fixed point $X = -1/2$ exists only for the potentials that has an asymptotic form $V \to \exp(4\Phi/3)$. This is shown as the thick (red) curve in 20.

- Secondly, there are the solutions $-1 < X < X_0$ that flow to -1. These are also asymptotically AdS in the UV but have differ in the IR from X_0. The solutions described in [43] is an example of this class.

- The solutions $X_0 < X < +1$. They also have an AdS fixed point in the UV. As a function of r the solutions continue in the region of positive X, hence positive β-function. This is not acceptable for an RG-flow in a field theory. The reason that such a behavior can happen in a gravity dual is because $\lambda(r)$ is determined by solving a second order differential equation whereas in the field theory it solves the first-order Gell-Mann-Low equation. Therefore we discard these solutions as un-physical for holographic purposes.

- Finally there are the solutions $-\infty < X < -1$ and $\infty > X > 1$ that posses negative and positive β-functions respectively. They do not exhibit an asymptotically AdS fixed point, hence are not useful for our purposes here.

JHEP05(2009)033

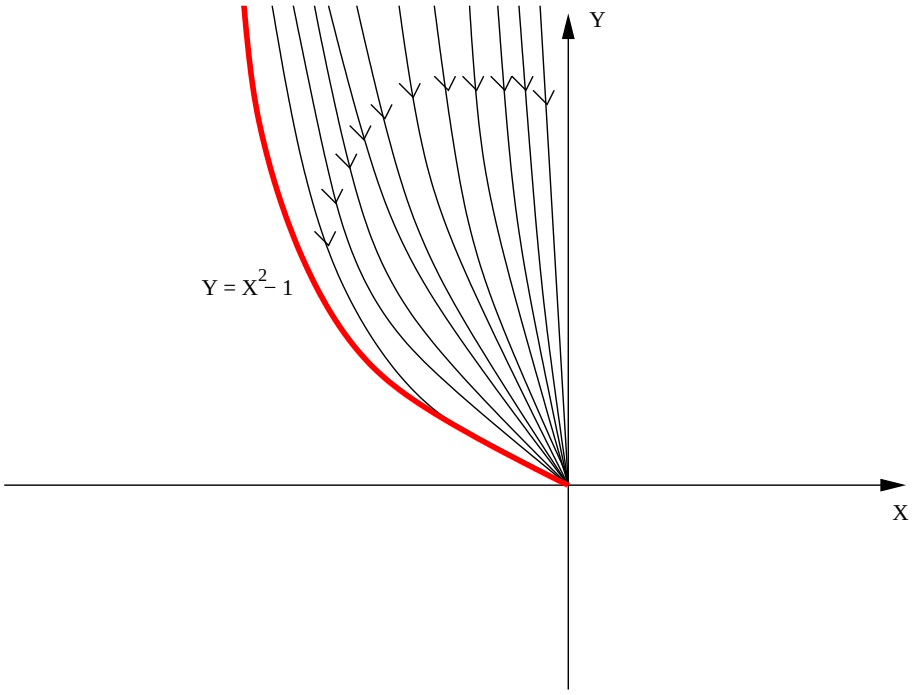

Figure 22. Flow chart of the solutions for the general case for non-zero Y. The arrows show the direction of decreasing λ.

Now, it turns out that the above behavior of solutions easily generalize the case of $Y \neq 0$. For simplicity, we focus only the region of the phase space that we are interested in, i.e. $X < 0$, $Y > 0$ and $Y > X^2 - 1$. In this case, the fixed point $X = -1$ is replaced by the fixed line $X = -\sqrt{1+Y}$. The flow chart in the phase space is shown in figure 22. The thick (red) curve represents the fixed line of the system $1 - X^2 + Y = 0$. As described in section 7.3, Y diverges at the horizon that corresponds to a $X = X_h = -3/8V'(\lambda_h)/V(\lambda_h)$. Therefore each different curve corresponds to a different temperature.

It may be interesting to carry out an analysis as a function of r and obtain a flow chart that generalizes figure 20 to the case of the full X-Y system. This would determine the entire family of solutions to (7.2, 7.3), most of which would be un-physical. We leave this question to future work.

H.4 Near-horizon continuously connects near-boundary

We want to show that the BH solution that is given by the initial conditions for X and Y at the horizon i.e. (7.21), (7.22) continuously extends over the solution near the boundary, i.e. $Y \approx 0$, $X \approx X_0$. As shown by eqs. (7.8) and (7.9), the solution of the system becomes $Y \approx 0$, $X \approx X_0$ as $\Phi \to -\infty$, independently of the initial conditions at the horizon. We shall prove that this asymptotic UV solution is continuously connected to the solution near the horizon. This is achieved by examining the equations is motion (7.2) and (7.3).

First, we see from (7.3) that $X = X_0$, $Y = 0$ cannot be reached at a finite point

$\Phi = \Phi_f$ with $-\infty < \Phi_f < \Phi_h$: Suppose $Y = \epsilon$ near Φ_f. Then, one obtains

$$\frac{d\epsilon}{d\Phi} = -\frac{4(1-X^2)}{3X}\epsilon$$

with the solution

$$\epsilon = C\ e^{-\frac{4(1-X_f^2)}{3X_f}\Phi},$$

where $X_f = X(\Phi_f)$. Thus, $\epsilon = 0$ can only be reached as $\Phi \to -\infty$ (recall that $X < 0$) in contradiction with our assumption. Therefore we learn that Y and X should be finite at an arbitrary mid-point Φ_f.

The only way the near UV ($\Phi < \Phi_f$) and the near horizon ($\Phi > \Phi_f$) solutions are detached would be a divergence in the r.h.s. of (7.2) and/or (7.3) at $\Phi = \Phi_f$ as Φ decreases down from Φ_h. In this region, V is bounded, X is also bounded as $-1 < X < 1$. From the exact solution for Y in (H.10) one finds that Y is also bounded. Hence the only way one can get a divergence is as $X \to 0$ at Φ_*. Now, we write $X = -\epsilon$ in (7.2) and find that ϵ satisfies,

$$-\frac{d\epsilon^2}{d\Phi} = \epsilon_0 \frac{d}{d\Phi}\log(V(\Phi)),$$

where $\epsilon_0 = 1 + Y(\Phi_f) > 0$. The solution is,

$$\epsilon^2 = -\epsilon_0 \log\left(\frac{V(\Phi)}{V(\Phi_f)}\right)$$

which cannot be satisfied for any $\Phi > \Phi_f$, because we assumed $V(\Phi)$ monotonically increasing. Thus we proved that, given the initial conditions for X and Y at the horizon, the solution flows down to $\Phi = -\infty$ and connects continuously to the UV region where $Y \to 0$ and $X \to X_0$.

Note however that $X = 0$ *can* be reached at a finite Φ_f for Φ approaching Φ_f *from below*. This is analogous to the "bouncing" solution studied in the previous appendix. At finite temperature, this possibility is automatically ruled out by imposing the regularity condition at the horizon.

H.5 Near boundary behavior of δX and Y

In order to derive the asymptotic behavior of δX and Y, it proves useful to obtain differential equations satisfied by these perturbations. This is done by expanding (7.2) and (7.3) to first order in the perturbations and making use of (7.6). One obtains:

$$\lambda\frac{dY}{d\lambda} = -\frac{4}{3}\frac{1-X_0^2}{X_0}Y, \tag{H.17}$$

$$\lambda\frac{d\delta X}{d\lambda} = \delta X\left[\frac{4}{3X_0}(X_0^2-1) + \frac{X_0^2+1}{X_0^2-1}\frac{\lambda}{X_0}\frac{dX_0}{d\lambda}\right] + \frac{\lambda}{1-X_0^2}\frac{dX_0}{d\lambda}Y. \tag{H.18}$$

The solution is straightforward:

$$Y(\lambda) = Y(\lambda_0)\, e^{-\frac{4}{3}\int_{\lambda_0}^{\lambda}\frac{d\tilde{\lambda}}{\tilde{\lambda}}\frac{1-X_0^2}{X_0}}, \tag{H.19}$$

$$\delta X(\lambda) = e^{-\frac{4}{3}\int_{\lambda_0}^{\lambda}\frac{d\tilde{\lambda}}{\tilde{\lambda}}\frac{1-X_0^2}{X_0}}\left[\left(\frac{Y(\lambda_0)}{2} - C_0(\lambda_0)\right)\frac{1}{X_0} + C_0(\lambda_0)X_0\right], \tag{H.20}$$

$$Y(\lambda_0) = \mathbf{Y_0}\, e^{-\frac{4}{b_0\lambda_0}}(b_0\lambda_0)^{-4b}, \qquad C_0(\lambda_0) = \mathbf{C_0}\, e^{-\frac{4}{b_0\lambda_0}}(b_0\lambda_0)^{-4b}. \tag{H.21}$$

Here $\mathbf{Y_0}$ and $\mathbf{C_0}$ are integration constants. By expanding the above equations one obtains (7.17).

H.6 Free energy in λ: details

We will compute the free energy in the λ-coordinate frame. In this frame, the metric of the thermal gas and the black-hole are as follows:

$$ds^2_{TG} = B_0^2(\lambda)\left(dt^2 + d\vec{x}^2 + \frac{d\lambda^2}{D_0(\lambda)^2}\right), \tag{H.22}$$

$$ds^2_{BH} = B^2(\lambda)\left(dt^2 F(\lambda) + d\vec{x}^2 + \frac{d\lambda^2}{F(\lambda)D(\lambda)^2}\right). \tag{H.23}$$

Here the various metric functions are defined as follows:

$$B_0(\lambda) = B_0(\lambda_0)e^{\frac{1}{3}\int_{\lambda_0}^{\lambda}\frac{d\tilde{\lambda}}{\tilde{\lambda}}\frac{1}{X_0}}, \qquad D_0(\lambda) = -\frac{3}{\ell}\frac{X_0(\lambda)}{\lambda}B_0(\lambda)e^{-\frac{4}{3}\int_0^{\lambda}\frac{d\tilde{\lambda}}{\tilde{\lambda}}X_0}, \tag{H.24}$$

$$B(\lambda) = B(\lambda_0)e^{\frac{1}{3}\int_{\lambda_0}^{\lambda}\frac{d\tilde{\lambda}}{\tilde{\lambda}}\frac{1}{X}}, \qquad D(\lambda) = -\frac{3}{\ell}\frac{X(\lambda)}{\lambda}B(\lambda)e^{-\frac{4}{3}\int_0^{\lambda}\frac{d\tilde{\lambda}}{\tilde{\lambda}}X}, \tag{H.25}$$

$$F(\lambda) = e^{\frac{4}{3}\int_0^{\lambda}\frac{d\tilde{\lambda}}{\tilde{\lambda}}\frac{Y}{X}}. \tag{H.26}$$

They are obtained directly from the the expressions for the metric functions defined in the text in terms of the radial variable r, viz. (7.4), (7.5) and (H.2). We call the metric functions in λ with the capital letters to distinguish them from the analogous functions of r. The relations are explicitly given by the following formulae:

$$B_0(\lambda) = b_0\left(r_0(\lambda)\right), \qquad B(\lambda) = b\left(r(\lambda)\right), \qquad F(\lambda) = f\left(r(\lambda)\right), \tag{H.27}$$

where r and r_0 are determined by,

$$r_0(\lambda) = \int_0^{\lambda}\frac{d\tilde{\lambda}}{\tilde{\lambda}D_0(\tilde{\lambda})}, \qquad r(\lambda) = \int_0^{\lambda}\frac{d\tilde{\lambda}}{\tilde{\lambda}D(\tilde{\lambda})}. \tag{H.28}$$

The expressions above completely determine the map between the r-frame and the λ-frame.

H.6.1 Einstein contribution

We first compute the Einstein contribution to the free energy. This is generally given by the frame-independent expression,

$$S_E = \frac{2}{3}M^3\int_{\mathcal{M}}\sqrt{g}V. \tag{H.29}$$

JHEP05(2009)033

$\mathcal{M}$ is the manifold with a boundary. We regulate the integral in the λ-frame by placing a cut-off at λ_0. Thus, using the metric functions defined above, one obtains the following expression in the lambda variable, for the thermal gas solution,

$$S_E^{TG} = \frac{2}{3} M^3 \beta' V_3' \int_{\lambda_0}^{\infty} B_0(\lambda)^5 V(\lambda) D_0(\lambda)^{-1}. \tag{H.30}$$

Here β' and V_3' are the circumference of the Euclidean time and the volume of the space-part. They are related to the analogous quantities in the black-hole geometry, by matching the two solutions on the cut-off:

$$\beta' B_0(\lambda_0) = \beta B(\lambda_0)\sqrt{F(\lambda_0)}, \qquad V_3' B_0(\lambda_0)^3 = V_3 B(\lambda_0)^3. \tag{H.31}$$

Now, we use the expression for the potential [28],

$$V(\lambda) = \frac{12}{\ell^2}(1 - X_0^2) e^{\int_0^\lambda X_0(\tilde{\lambda})\frac{d\tilde{\lambda}}{\tilde{\lambda}}}, \tag{H.32}$$

in (H.30) and see that it can be rewritten in the following form:

$$S_E^{TG} = -\frac{8}{3\ell} M \beta' V_3' B_0(\lambda_0)^4 e^{-\frac{4}{3}\int_0^{\lambda_0} X_0 \frac{d\tilde{\lambda}}{\tilde{\lambda}}} \int_{\lambda_0}^{\infty} \frac{d\lambda}{\lambda} \frac{1 - X_0^2}{X_0} e^{\frac{4}{3}\int_{\lambda_0}^{\lambda} \frac{d\tilde{\lambda}}{\tilde{\lambda}} \frac{1-X_0^2}{X_0}}. \tag{H.33}$$

To obtain this expression, we used (H.25), (H.24) and (H.32). We see that the integrand is a total derivative, hence the integral can be carried out exactly. One has,

$$S_E^{TG} = -\frac{2}{\ell} M^3 \beta' V_3' B_0(\lambda_0)^4 e^{-\frac{4}{3}\int_0^{\lambda_0} X_0 \frac{d\tilde{\lambda}}{\tilde{\lambda}}} e^{\frac{4}{3}\int_{\lambda_0}^{\lambda} \frac{d\tilde{\lambda}}{\tilde{\lambda}} \frac{1-X_0^2}{X_0}} \Big|_{\lambda_0}^{\infty}. \tag{H.34}$$

It is easy to see that the contribution from ∞ vanishes, as the expression above scales a λ^{-2} for large λ for our confining IR asymptotics. Thus one only has the contribution at λ_0:

$$S_E^{TG} = \frac{2}{\ell} M^3 \beta' V_3' B_0(\lambda_0)^4 e^{-\frac{4}{3}\int_0^{\lambda_0} X_0 \frac{d\tilde{\lambda}}{\tilde{\lambda}}}. \tag{H.35}$$

This is our final expression for the Einstein term on the TG geometry.

Let us now compute the analogous contribution on the BH geometry. From (H.29) we get,

$$S_E^{BH} = \frac{2}{3} M^3 \beta V_3 \int_{\lambda_0}^{\lambda_h} B(\lambda)^5 V(\lambda) D(\lambda)^{-1}. \tag{H.36}$$

Following the same steps as before, we substitute the expression for $D(\lambda)$, $B(\lambda)$ and $V(\lambda)$ from (H.25), (H.24) and (7.6), and obtain,

$$S_E^{BH} = -\frac{8}{3\ell} M^3 \beta V_3 B(\lambda_0)^4 e^{-\frac{4}{3}\int_0^{\lambda_0} (X - \frac{Y}{X})\frac{d\tilde{\lambda}}{\tilde{\lambda}}} \int_{\lambda_0}^{\lambda_h} \frac{d\lambda}{\lambda} \frac{1 - X^2 + Y}{X} e^{\frac{4}{3}\int_{\lambda_0}^{\lambda} \frac{d\tilde{\lambda}}{\tilde{\lambda}} \frac{1-X^2+Y}{X}}. \tag{H.37}$$

Again, the integrand is a total derivative and one has,

$$S_E^{BH} = -\frac{2}{\ell} M^3 \beta V_3 B(\lambda_0)^4 e^{-\frac{4}{3}\int_0^{\lambda_0} X_0 \frac{d\tilde{\lambda}}{\tilde{\lambda}}} e^{\frac{4}{3}\int_{\lambda_0}^{\lambda} \frac{d\tilde{\lambda}}{\tilde{\lambda}} \frac{1-X^2+Y}{X}} \Big|_{\lambda_0}^{\lambda_h}. \tag{H.38}$$

JHEP05(2009)033

This can be simplified further: using (7.3), one realizes that the integrand in the exponent is a total derivative of $\log Y(\lambda)$. Thus, one has,

$$S_E^{BH} = -\frac{2}{\ell} M^3 \beta V_3 B(\lambda_0)^4 e^{-\frac{4}{3}\int_0^{\lambda_0} X_0 \frac{d\tilde{\lambda}}{\tilde{\lambda}}} \left(\frac{Y(\lambda_0)}{Y(\lambda_h)} - 1 \right). \tag{H.39}$$

But $Y(\lambda_h) = \infty$ by regularity condition at the horizon (see section (7.3)), hence we have the final expression for the Einstein contribution on the BH geometry:

$$S_E^{BH} = \frac{2}{\ell} M^3 \beta V_3 B(\lambda_0)^4 e^{-\frac{4}{3}\int_0^{\lambda_0} (X - \frac{Y}{X}) \frac{d\tilde{\lambda}}{\tilde{\lambda}}}. \tag{H.40}$$

The Einstein contribution to the free energy follows from the difference of (H.35) and (H.40). In order to match the two expressions we use the matching conditions (H.31). Finally we also use (H.26) to obtain:

$$\delta S_E = S_E^{BH} - S_E^{TG} = \frac{2}{\ell} M^3 \beta V_3 B(\lambda_0)^4 \left(e^{-\frac{4}{3}\int_0^{\lambda_0} (X - \frac{Y}{X}) \frac{d\tilde{\lambda}}{\tilde{\lambda}}} - e^{-\frac{4}{3}\int_0^{\lambda_0} (X_0 - \frac{Y}{2X}) \frac{d\tilde{\lambda}}{\tilde{\lambda}}} \right). \tag{H.41}$$

As λ_0 is very small and the integrands in the expression above are very small in that region, one can expand the exponentials and obtain,

$$\delta S_E = \frac{2}{\ell} M^3 \beta V_3 B(\lambda_0)^4 \frac{2}{3} \int_0^{\lambda_0} \left(\frac{Y}{X} - 2\delta X \right). \tag{H.42}$$

The functions Y and δX are given in section (7.2). Using these expressions it is straightforward to carry out the integrals. One obtains,

$$\delta S_E(\lambda_0) = -\frac{2}{\ell} M^3 \beta V_3 C_0 B(\lambda_0)^4 e^{-\frac{4}{b_0 \lambda_0}} (b_0 \lambda_0)^{-4b}. \tag{H.43}$$

Finally we remove the cut-off by sending λ_0 to 0 and using the definition of the integration constant Λ:

$$\lim_{\lambda_0 \to 0} B(\lambda_0) e^{-\frac{1}{b_0 \lambda_0}} (b_0 \lambda_0)^{-b} = \Lambda \, \ell. \tag{H.44}$$

Thus the final expression for the Einstein contribution to the free energy reads,

$$\mathcal{F}_E = -\frac{2}{\ell} C_0 M^3 V_3 (\Lambda \, \ell)^4. \tag{H.45}$$

H.6.2 Gibbons-Hawking contribution

We move on to the Gibbons-Hawking term that is given by the frame-independent expression, the second term in (2.1).

We first define two more functions of λ in addition to (H.25):

$$D_{A0}(\lambda) = -\frac{1}{\ell} B_0(\lambda) e^{-\frac{4}{3}\int_0^{\lambda} \frac{d\tilde{\lambda}}{\tilde{\lambda}} X_0(\tilde{\lambda})}, \qquad D_A(\lambda) = -\frac{1}{\ell} B(\lambda) e^{-\frac{4}{3}\int_0^{\lambda} \frac{d\tilde{\lambda}}{\tilde{\lambda}} X(\tilde{\lambda})}. \tag{H.46}$$

Just as in (H.25) these are obtained from mapping the derivative of the scale factor from r to λ frame:

$$D_{A0}(\lambda) = \frac{dA_0}{dr}(r_0(\lambda)), \qquad D_A(\lambda) = \frac{dA}{dr}(r(\lambda)) \tag{H.47}$$

JHEP05(2009)033

where the functions $r(\lambda)$ and $r_0(\lambda)$ are given in (H.28).

Computing the trace of the extrinsic curvature in the λ-frame on the TG solution (H.22), one obtains,

$$S_{GH}^{TG} = 8M^3\beta' V_3' B_0(\lambda_0)^3 D_{A0}(\lambda_0). \tag{H.48}$$

Using the expressions above and (H.24), one has,

$$S_{GH}^{TG} = -\frac{8}{\ell} M^3\beta' V_3' B_0(\lambda_0)^4 e^{-\frac{4}{3}\int_0^{\lambda_0}\frac{d\tilde{\lambda}}{\tilde{\lambda}}X_0(\tilde{\lambda})} \tag{H.49}$$

Similarly, the Gibbons-Hawking term evaluated on the BH solution reads,

$$S_{GH}^{BH} = M^3\beta V_3 B(\lambda_0)^3 D_A(\lambda_0)\left(8 + 4Y(\lambda_0)\right), \tag{H.50}$$

which gives,

$$S_{GH}^{BH} = -\frac{8}{\ell} M^3\beta V_3 B(\lambda_0)^4 e^{-\frac{4}{3}\int_0^{\lambda_0}\frac{d\tilde{\lambda}}{\tilde{\lambda}}X(\tilde{\lambda})}\left(1 + \frac{1}{2}Y(\lambda_0)\right), \tag{H.51}$$

Just as in the previous subsection, we compute the Gibbons-Hawking contribution to the free energy by taking the difference of (H.49) and (H.51). Following the same steps as outlined above (H.42), one arrives at the following result:

$$\delta S_{GH} = S_{GH}^{BH} - S_{GH}^{TG} = -\frac{8}{\ell} M^3\beta V_3 B(\lambda_0)^4\left(\frac{2}{3}\int_0^{\lambda_0}\left(\frac{Y}{X} - 2\delta X\right) + \frac{1}{2}Y(\lambda_0)\right). \tag{H.52}$$

Evaluating the integrals as before and using the small λ asymptotics of Y (see section 7.2) one arrives at the final expression for the Gibbons-Hawking contribution to the free energy:

$$\mathcal{F}_E = \frac{8}{\ell}(C_0 - Y_0/2) M^3 V_3 (\Lambda\ \ell)^4. \tag{H.53}$$

Thus, the total free energy is obtained from combining (H.45) and (H.53) as,

$$\mathcal{F} = \frac{1}{\ell}(6C_0 - 4Y_0) M^3 V_3 (\Lambda\ \ell)^4. \tag{H.54}$$

H.7 Fluctuations of λ and A in the λ-frame:

In order to compute the gluon condensate, we need to know $\delta\lambda(r) = \lambda(r) - \lambda_0(r)$, near the boundary. This quantity is defined in the r-frame. In the λ-frame the quantities λ and λ_0 are the same, by definition. However one still finds a non-zero value for $\delta\Phi(r)$ after a careful change of variables from r to λ frame.

The quantity $\lambda_0(r)$ maps to $\lambda(r_0(\lambda))$ where r_0 is defined in (H.28). Thus, $\delta\lambda$ in the λ-frame is evaluated by:

$$\delta\lambda \equiv \lambda(r) - \lambda_0(r) = \lambda - \lambda(r_0(\lambda)) = \left.\frac{d\lambda}{dr}\right|_{r_0(\lambda)} \delta r(\lambda) = D_0(\lambda)\delta r(\lambda), \tag{H.55}$$

where D_0 is defined in (H.25) and δr is given by, see (H.28),

$$\delta r(\lambda) = r(\lambda) - r_0(\lambda) = \int_0^{\lambda} d\tilde{\lambda}\left(D(\tilde{\lambda})^{-1} - D_0(\tilde{\lambda})^{-1}\right). \tag{H.56}$$

JHEP05(2009)033

It is straightforward to work out (H.56) from (H.25) and (H.24). Let us define,

$$B(\lambda) = B_0(\lambda)\,(1 + \delta A(\lambda))\,. \tag{H.57}$$

Then, one obtains,

$$\delta r(\lambda) = \frac{\ell}{3}\int_0^\lambda \frac{d\tilde\lambda}{\tilde\lambda}\left[\frac{\delta X(\tilde\lambda)}{X_0(\tilde\lambda)}\delta A(\tilde\lambda) - \frac{4}{3}\int_0^{\tilde\lambda}\delta X\right] e^{\int_0^{\tilde\lambda}\frac{B_0(\tilde\lambda)}{X_0(\tilde\lambda)}}. \tag{H.58}$$

The last term is subleading in the limit $\lambda \to 0$, so we neglect it for the moment. The second termcan be computed from (H.24) and one finds,

$$\delta A(\lambda) = -\frac{9}{4}G_0 e^{-\frac{4}{b_0\lambda}}(b_0\lambda)^{-4b-2} + \cdots \tag{H.59}$$

Finally the first term follows from (7.9). All in all, one finds,

$$\delta r(\lambda) = \frac{9}{4\Lambda}g_0 e^{-\frac{5}{b_0\lambda}}(b_0\lambda)^{-5b-2} + \cdots \tag{H.60}$$

where we also used the definition of Λ in (H.44). Now, $\delta\lambda$ follows from (H.55) as,

$$\delta\lambda = D_0(\lambda)\delta r(\lambda) = \frac{9G_0}{4b_0}(\Lambda\ell)^4 e^{-\frac{4}{b_0\lambda}}(b_0\lambda)^{-4b}, \tag{H.61}$$

which yields

$$\delta\Phi(r) = \frac{\delta\lambda}{\lambda_0} = \frac{9}{4}G_0(\Lambda\ell)^4(r/\ell)^4\log(r\Lambda). \tag{H.62}$$

This is the correct coefficient that produces the mathching of the conformal anomaly in section 4.

One can also compute $\delta b(r)$ in the r-frame, from the expressions that we obtained above in the λ-frame. By definition,

$$\delta b(r) = b(r) - b_0(r) = b(r) - b_0(r_0) - \left.\frac{db_0}{dr}\right|_{r_0}\delta r = b_0(\lambda)\delta A(\lambda) - \frac{dB_0}{d\lambda}d_0(\lambda)\delta r(\lambda), \tag{H.63}$$

where $\delta A(\lambda)$ and $\delta r(\lambda)$ are given by (H.60) and (H.59) above. We see that the leading terms cancel each other out, and one has to take into account the subleading terms in (H.60) and (H.59). This is a straightforward but lengthy computation and best carried out by a symbolical evaluation program. We shall only present the result here:

$$\delta b(r) = \frac{2}{5}G_0(\Lambda\ell)^4(r/\ell)^4. \tag{H.64}$$

This is the result in the r-frame. In the u-frame, the coefficient becomes $\frac{1}{2}G_0$.

H.8 Higher order terms in the near horizon expansion

Demanding regularity at the horizon determines the higher terms in the expansion of (7.21) and (7.22). One finds,

$$X_1 = \frac{3}{16}\left(\frac{V''(\Phi_h)}{V(\Phi_h)} - \frac{V'(\Phi_h)^2}{V(\Phi_h)^2}\right), \qquad Y_1 = \frac{9}{64}\left(\frac{V''(\Phi_h)}{V(\Phi_h)} - 2\frac{V'(\Phi_h)^2}{V(\Phi_h)^2}\right) - 1. \tag{H.65}$$

JHEP05(2009)033

H.9 Derivation of eq. (7.26)

Here, we compute temperature in the scalar variables. By definition, T is given by $4\pi T = |\dot{f}(r_h)| = |f\frac{dg}{dA}\frac{dA}{du}\frac{du}{dr}|$. Using the definition of Y in (7.1), eqs. (H.1), (H.3), (7.5), (7.4) and $du/dr = \exp(A)$ we obtain,

$$T = \frac{Y(\lambda_h)}{\pi\ell} e^{A_0 - \int_{\lambda_0}^{\lambda_h} \frac{d\lambda}{\lambda}\frac{1}{X}} e^{\frac{4}{3}\int_{\lambda_0}^{\lambda_h}\frac{d\lambda}{\lambda}\frac{1+Y-X^2}{X}}. \tag{H.66}$$

Now, using Y equation of motion (7.3) we see that the integrand in the last exponential is a total derivative and can easily be integrated. One finds,

$$T = \frac{Y(\lambda_0)}{\pi\ell} e^{A_0 - \int_{\lambda_0}^{\lambda_h}\frac{d\lambda}{\lambda}\frac{1}{X}}. \tag{H.67}$$

Using the UV asymptotics of Y in (7.8) and (7.4) with $b = \exp(A)$ one identifies the r.h.s. of (H.67) as,

$$T = \frac{\mathbf{Y_0}}{\pi b^3(\lambda_h)}[\ell^{-1} e^{4A_0 - \frac{4}{b_0\lambda_0}}(b_0\lambda_0)^{-4b}]. \tag{H.68}$$

The expression in the square brackets defines Λ, see (2.18). Thus, one finally obtains eq. (7.26).

H.10 Integral representation for the free energy and the energy

Here, we provide further formulas regarding the integral representation of the free energy in section 5.2.3. For the big BH one has,

$$\mathcal{F}_B(\lambda_h) = -4\pi M^3 V_3 \int_\infty^{\lambda_h} b^3(\tilde{\lambda}_h)\frac{dT}{d\tilde{\lambda}_h}d\tilde{\lambda}_h, \qquad \lambda_h < \lambda_{\min}. \tag{H.69}$$

Note that the two branches are combined in the integral, as $b(\lambda_h)$ is a single valued in the entire range $\lambda_h \in \{\lambda_0, \infty\}$. One can also put this equation in various useful forms. For example, one can write it in terms of the $\mathbf{Y_0}(\lambda_h)$ function. For this purpose, we make use of the relation between T and $\mathbf{Y_0}$ in (7.26). Use this in (H.69), carry out the integral and note that $\mathbf{Y_0}(\infty) = 0$ to get:

$$\mathcal{F}_B(\lambda_h) = \Lambda^4 (M\ell)^3 V_3 \left(12\int_\infty^{\lambda_h} \mathbf{Y_0}(\tilde{\lambda}_h)\frac{dA}{d\tilde{\lambda}_h}d\tilde{\lambda}_h - 4\mathbf{Y_0}(\lambda_h)\right). \tag{H.70}$$

Comparison of this equation with (7.29) reveals an alternative expression for the energy density:

$$\rho(\lambda_h) = \Lambda^4 (M\ell)^3 12\int_\infty^{\lambda_h} \mathbf{Y_0}(\tilde{\lambda}_h)\frac{dA}{d\tilde{\lambda}_h}d\tilde{\lambda}_h \tag{H.71}$$

I High T asymptotics

We can determine how the various quantities we described above approach their ideal gas values for large-T, by studying the next-to-leading order corrections to the AdS black-hole. To leading order $\mathbf{Y_0}$ in (7.10) is determined by the AdS black-hole:

$$\mathbf{Y_0} = \pi\frac{T}{\Lambda}\frac{1}{(r_h\Lambda)^3}, \qquad T = \frac{1}{\pi r_h}. \tag{I.1}$$

JHEP05(2009)033

The subleading corrections to the AdS scale factor, close to the boundary, is presented in section (5.1). From (7.8) and (3.10), one arrives at the following expression:

$$\mathbf{Y_0}(T) = \tilde{T}^4 \left[1 - \frac{4}{3}\frac{1}{\log(\tilde{T})} - \frac{16}{9}\, b\, \frac{\log(\log(\tilde{T}))}{\log^2(\tilde{T})} + \cdots\right], \qquad \tilde{T} \equiv \pi\frac{T}{\Lambda}, \tag{I.2}$$

Let us first compute how $(\rho - 3P)/T^4$ approaches to 0 at high-T. This determines the high-T asymptotics of the gluon condensate. It follows from (I.2) and integration by parts in (7.10) that,

$$\frac{\rho - 3p}{T^4} \to \frac{4\pi^2}{135}\left[\frac{1}{\log^2\left(\frac{T}{T_c}\right)} + 8\, b\, \frac{\log\left(\log\left(\frac{T}{T_c}\right)\right)}{\log^3\left(\frac{T}{T_c}\right)} + \cdots\right] \tag{I.3}$$

This computation can easily be extended to the large-T asymptotics of p, ρ and s. We find:

$$\frac{p}{T^4} = \frac{\pi^2}{45} - \frac{4\pi^2}{135}\frac{1}{\log\left(\frac{T}{T_c}\right)} - \frac{16b}{135}\frac{\log\left(\log\left(\frac{T}{T_c}\right)\right)}{\log^2\left(\frac{T}{T_c}\right)} + \cdots \tag{I.4}$$

$$\frac{s}{T^3} = \frac{4\pi^2}{45} - \frac{16\pi^2}{135}\frac{1}{\log\left(\frac{T}{T_c}\right)} - \frac{64\pi^2 b}{135}\frac{\log\left(\log\left(\frac{T}{T_c}\right)\right)}{\log^2\left(\frac{T}{T_c}\right)} + \cdots \tag{I.5}$$

$$\frac{\rho}{T^4} = \frac{3\pi^2}{45} - \frac{4\pi^2}{45}\frac{1}{\log\left(\frac{T}{T_c}\right)} - \frac{16\pi^2 b}{45}\frac{\log\left(\log\left(\frac{T}{T_c}\right)\right)}{\log^2\left(\frac{T}{T_c}\right)} + \cdots \tag{I.6}$$

We note that the pressure, entropy density and the energy density approach their ideal gas limits *from below* as they should.

It is also useful to derive the high-T asymptotics of the speed of sound. It is obtained from eqs. (I.2) and (7.33):

$$\frac{1}{c_s^2} - 3 = \frac{4}{3}\frac{1}{\log^2\left(\frac{T}{T_c}\right)} + \frac{32b}{9}\frac{\log\left(\log\left(\frac{T}{T_c}\right)\right)}{\log^3\left(\frac{T}{T_c}\right)} + \cdots \tag{I.7}$$

We note that the speed of sound approaches to its ideal gas value 1/3 also *from below* as it should.

We remark that, all of these expressions are completely independent of the parameters of our theory *and* any modification to the dilaton potential. It follows directly from demanding an asymptotically AdS solution dual to the UV of the field theory. Moreover, the coefficients of the first terms are even independent of the parameters of the gauge theory, i.e. the β-function coefficients. Thus, we expect this form hold universally for any large-N_c gauge theory that exhibits logarithmic running in the UV.

J Analytic solutions

One can easily obtain analytic solutions to the system, by restricting to the fixed points of (7.2) and (7.3). One obvious fixed point of (7.3) is $Y = 0$. This takes us back to the

JHEP05(2009)033

zero-T analysis which was studied in [28]. In the following we always consider the case $Y \neq 0$. We present our solutions in the domain-wall coordinate system, see section A.2. They can easily be converted into the conformal frame using (H.4).

J.1 Analytic solutions: zero potential

Another obvious fixed point of the system is $X = const.$, $Y = const$ and $1 + Y - X^2 = 0$. From (7.6), we see that this corresponds to vanishing dilaton potential, thus it is not very interesting for our purposes regarding holography. Nevertheless, it produces the following interesting analytic solution.

It is straightforward to solve (H.1), (H.2) and (H.3). One finds, for the dilaton:

$$\lambda = e^{\Phi} = \left(C_1 - 4X^2 \frac{u}{\ell}\right)^{\frac{3}{4X}} . \tag{J.1}$$

Then the metric can be found as,

$$ds^2 = \left(C_1 - 4X^2 \frac{u}{\ell}\right)^{\frac{1}{2X^2}} \left(dx_i dx^i - \left(C_1 - 4X^2 \frac{u}{\ell}\right)^{\frac{X^2-1}{X^2}} dt^2 \right) + \left(C_1 - 4X^2 \frac{u}{\ell}\right)^{\frac{1-X^2}{X^2}} du^2. \tag{J.2}$$

There is a curvature singularity at,

$$\frac{u_0}{\ell} = \frac{C_1}{4X^2}, \tag{J.3}$$

where the dilaton blows up and the metric shrinks to a point (for $X^2 < 1$) or a line (for $X^2 > 1$). Note that $X < 0$ in all of our solutions.

In order to understand the physics of this solution, one has to distinguish these two cases. For $X^2 > 1$ the same point u_0 coincides with the event horizon. Therefore there is a curvature singularity at the event horizon $u_h = u_0$ where the geometry shrinks to a point. We note also that $Y > 0$ in this case. Therefore, from (H.3) we see that g (or f) is monotonically decreasing. It decreases from 1 at the boundary to 0 at the horizon.

In the other case, $X^2 < 1$, there is no event horizon. There is a curvature singularity at u_0, where the geometry shrinks to a line. Also in this case g is monotonically increasing.

J.2 Analytic solutions: exponential potential

A less obvious fixed point of (7.2) is when $X = const.$ and the dilaton potential is exponential:

$$V = V_0(1 - X^2)\lambda^{-\frac{8}{3}X}. \tag{J.4}$$

The proportionality constant will become clear below.

Also in this case one can find the most general analytic solution to the system. This case is of more interest because of the following reasons. We find below that in this case Y does not need to be constant or zero and it can be a function of Φ. However, as (J.4) does not depend on Y, we find that it is a moduli of the exponential potential. This fact will allow us to obtain both thermal gas solutions and the black-hole solutions to the same potential. Moreover, we note from [28] that the leading IR behavior of the dilaton potential,

JHEP05(2009)033

in most of the confining theories is an exponential. Since the confinement-deconfinement phase transition is expected to take place in the IR of the theory, (J.4) can be taken a first approximation to understand the finite temperature dynamics of the interesting confining theories.

One first solves (7.3) to obtain Y as,

$$Y = \frac{C_2(1-X^2)}{\lambda^\alpha - C_2}, \tag{J.5}$$

where $C_2 \geq 0$ and we defined,

$$\alpha = \frac{4(1-X^2)}{3X}. \tag{J.6}$$

Note that for a monotonically decreasing g we need $Y < 0$. As we also require $Y \to 0$ near the boundary, where $\lambda \to 0$, one should take $X^2 < 1$, hence $\alpha < 0$. We stress that, this case covers the rest of the physically interesting, constant X solutions, as the physical solution in the previous subsection covered the range $X^2 > 1$.

As we demonstrate below, the solution (J.5) describes a black-hole for $C_2 > 0$ and a thermal gas for $C_2 = 0$. To check that indeed Y is a moduli of (J.4), one inserts (J.5) in (7.6) and finds (J.4) after nice cancelations.

Both for the black-hole and the thermal gas, one finds the same λ behavior for the dilaton:

$$\lambda = e^{\Phi} = \left(C_1 - 4X^2 \frac{u}{\ell}\right)^{\frac{3}{4X}}, \tag{J.7}$$

and the scale factor,

$$e^A = e^{A_0} \lambda^{\frac{1}{3X}}. \tag{J.8}$$

We note that these are the same as in the previous subsection, as they follow directly from the fact that X is constant.

One finds the location of the horizon by solving for f from (7.5):

$$f = e^g = 1 - C_2 \lambda^{-\alpha}. \tag{J.9}$$

We find that indeed $f \to 1$ on the boundary, $(\lambda \to 0)$ as $\alpha < 0$. There is an event horizon located at (using (J.7)),

$$\lambda_h = C_2^{\frac{1}{\alpha}} \qquad i.e. \qquad \frac{u_h}{\ell} = \frac{C_1}{4X^2} - \frac{C_2^{\frac{X^2}{1-X^2}}}{4X^2}. \tag{J.10}$$

The curvature singularity is located at $\lambda = \infty$ i.e. ,

$$\frac{u_0}{\ell} = \frac{C_1}{4X^2}. \tag{J.11}$$

We note that $u_h < u_0$ and indeed there is a well-behaved black-hole solution to the system. The metric of the black-hole is given by,

$$\begin{aligned} ds^2 = {} & e^{2A_0} \left(C_1 - 4X^2 \frac{u}{\ell}\right)^{\frac{1}{2X^2}} \left\{ dx_i dx^i - \left(1 - C_2 (C_1 - 4X^2 \frac{u}{\ell})^{\frac{1-X^2}{X^2}}\right) dt^2 \right\} \\ & + \left(1 - C_2 (C_1 - 4X^2 \frac{u}{\ell})^{\frac{1-X^2}{X^2}}\right)^{-1} du^2. \end{aligned} \tag{J.12}$$

JHEP05(2009)033

The temperature of the black-hole is determined by requiring regularity of the Euclidean continuation at u_h:

$$\beta = \frac{1}{T} = \frac{4\pi}{|f'(u_h)|e^{A(u_h)}}. \tag{J.13}$$

One finds,

$$\beta = \pi\ell \frac{e^{-A_0} C_2^{\frac{\frac{1}{4}-X^2}{1-X^2}}}{1-X^2}. \tag{J.14}$$

The physically most interesting case corresponds to the value $X = -1/2$, see [28]. Very interestingly, in this case the temperature is only given by the integration constant A_0:

$$\beta = \frac{1}{T} = \frac{4\pi\ell}{3e^{A_0}}. \tag{J.15}$$

Otherwise the temperature is determined by the combination of A_0 and C_2, namely the string tension and the location of the event horizon.

The thermal gas solution is found by setting $C_2 = 0$ in (J.5), hence $f = 1$. The dilaton is given again by (J.7) and the metric is,

$$ds^2 = e^{2A_0}\left(C_1 - 4X^2\frac{u}{\ell}\right)^{\frac{1}{2X^2}}\left\{dx_i dx^i + dt^2\right\} + du^2. \tag{J.16}$$

Here we required the same integration constant for A as the black-hole solution (J.12). This is because they should have the same asymptotics at the boundary. Euclidean time is compactified with circumference, $\bar{\beta}$. We note that there is a curvature singularity ar u_0 that is given by (J.11). It is the same locus as the curvature singularity of the black-hole solution — that is cloaked behind the event horizon — resides.

Computation of the energy of the solutions. Here we prove that the analytic solutions describe above do not demonstrate a Hawking-Page transition. Hence they are not interesting for holographic purposes. The action is given by (2.1). One finds that the trace of the intrinsic curvature is given by,

$$K = \frac{\sqrt{f}}{2}(8A' + g') \tag{J.17}$$

in the domain-wall coordinate system. Thus, the boundary contribution to the action becomes,

$$S_{\rm bnd} = -M^3 V_3 \beta \left\{e^{g+4A}(8A' + g')\right\}_{u_b}, \tag{J.18}$$

where u_b denotes the regulated boundary of the geometry infinitesimally close to $-\infty$.

The bulk contribution to the action, evaluated on the solution can be simplified as,

$$\begin{aligned} S_{\rm bulk} &= 2M^3 V_3 \beta \int_{u_b}^{u_s} du \frac{d}{du}\left(f e^{4A} A'\right) \\ &= 2M^3 V_3 \beta \left\{f(u_s)e^{4A(u_s)}A'(u_s) - f(u_b)e^{4A(u_b)}A'(u_b)\right\}. \end{aligned} \tag{J.19}$$

Here u_s denotes u_0 or u_h depending on which appears first. Thus, for the black-hole solution $u_s = u_h$, whereas for the thermal gas $u_s = u_0$.

JHEP05(2009)033

The first term in (J.19) deserves attention. Clearly it vanishes for the black-hole, as $f(u_h) = 0$ by definition. However, it is not a priori clear that it also vanishes for the thermal gas. A straightforward computation using (J.8), (J.7) and,

$$A' = -\frac{1}{\ell}\lambda^{-\frac{4X}{3}} \tag{J.20}$$

shows that it indeed vanishes for our physically interesting case $X^2 < 1$. Therefore, one obtains the following total expression for the action from (J.18) and (J.19) by dropping the first term in (J.19):

$$S = -2M^3V_3\beta e^{g(u_b)+4A(u_b)}\left(5A'(u_b) + \frac{1}{2}g'(u_b)\right). \tag{J.21}$$

In order to compare the energies of the black-hole and the thermal gas geometries, we fix the UV asymptotics of the thermal gas geometry by requiring the same circumference for the Euclidean time at u_b:

$$\bar{\beta} = \beta\sqrt{f(u_b)}. \tag{J.22}$$

Now, it is straightforward to compute the energy of the geometries. For the black-hole (J.12), one finds:

$$S_{BH} = -2M^3V_3\left(\frac{\beta}{\ell}\right)e^{4A_0}\left(C_2(3+2X^2) - 5\lambda_b^\alpha\right). \tag{J.23}$$

Here λ_b is the value of the dilaton on the regulated boundary u_b. As $\alpha < 0$ and $\lambda \to 0$ near the boundary, it is a divergent piece that should be regulated.

For the thermal gas one finds, using (J.22),

$$S_{TG} = -10M^3V_3\left(\frac{\beta}{\ell}\right)e^{4A_0}\left(\frac{C_2}{2} - \lambda_b^\alpha\right). \tag{J.24}$$

We note that the divergent terms in (J.23) and (J.24) cancels in the difference and one finds,

$$S_{BH} - S_{TG} = -2M^3V_3\left(\frac{\beta}{\ell}\right)e^{4A_0}C_2\left(3X^2 + \frac{1}{2}\right). \tag{J.25}$$

We note from (J.14) that the temperature is given by,

$$e^{A_0} = \frac{\pi T\ell}{1-X^2}C_2^{\frac{\frac{1}{4}-X^2}{1-X^2}}. \tag{J.26}$$

As (J.25) is always negative, we observe that the BH solution always minimizes the action, hence if it exist it is the dominant solution. Therefore, there is no phase transition in this geometry.

JHEP05(2009)033

References

[1] J.M. Maldacena, *The large-N limit of superconformal field theories and supergravity*, *Adv. Theor. Math. Phys.* **2** (1998) 231 [*Int. J. Theor. Phys.* **38** (1999) 1113] [hep-th/9711200] [SPIRES].

[2] E. Witten, *Anti-de Sitter space and holography*, *Adv. Theor. Math. Phys.* **2** (1998) 253 [hep-th/9802150] [SPIRES].

[3] S.S. Gubser, I.R. Klebanov and A.M. Polyakov, *Gauge theory correlators from non-critical string theory*, *Phys. Lett.* **B 428** (1998) 105 [hep-th/9802109] [SPIRES].

[4] E. Witten, *Anti-de Sitter space, thermal phase transition and confinement in gauge theories*, *Adv. Theor. Math. Phys.* **2** (1998) 505 [hep-th/9803131] [SPIRES].

[5] J.M. Maldacena and C. Núñez, *Towards the large-N limit of pure $N = 1$ super Yang-Mills*, *Phys. Rev. Lett.* **86** (2001) 588 [hep-th/0008001] [SPIRES];
I.R. Klebanov and M.J. Strassler, *Supergravity and a confining gauge theory: duality cascades and χSB-resolution of naked singularities*, *JHEP* **08** (2000) 052 [hep-th/0007191] [SPIRES].

[6] S.W. Hawking, C.J. Hunter and M. Taylor, *Rotation and the AdS/CFT correspondence*, *Phys. Rev.* **D 59** (1999) 064005 [hep-th/9811056] [SPIRES];
A. Chamblin, R. Emparan, C.V. Johnson and R.C. Myers, *Charged AdS black holes and catastrophic holography*, *Phys. Rev.* **D 60** (1999) 064018 [hep-th/9902170] [SPIRES];
M. Cvetič and S.S. Gubser, *Phases of R-charged black holes, spinning branes and strongly coupled gauge theories*, *JHEP* **04** (1999) 024 [hep-th/9902195] [SPIRES];
T. Harmark and N.A. Obers, *Thermodynamics of spinning branes and their dual field theories*, *JHEP* **01** (2000) 008 [hep-th/9910036] [SPIRES];
D. Mateos, R.C. Myers and R.M. Thomson, *Holographic phase transitions with fundamental matter*, *Phys. Rev. Lett.* **97** (2006) 091601 [hep-th/0605046] [SPIRES]; *Thermodynamics of the brane*, *JHEP* **05** (2007) 067 [hep-th/0701132] [SPIRES].

[7] O. Aharony, J. Sonnenschein and S. Yankielowicz, *A holographic model of deconfinement and chiral symmetry restoration*, *Annals Phys.* **322** (2007) 1420 [hep-th/0604161] [SPIRES].

[8] C.P. Herzog, *A holographic prediction of the deconfinement temperature*, *Phys. Rev. Lett.* **98** (2007) 091601 [hep-th/0608151] [SPIRES].

[9] N. Evans and E. Threlfall, *The thermal phase transition in a QCD-like holographic model*, *Phys. Rev.* **D 78** (2008) 105020 [arXiv:0805.0956] [SPIRES].

[10] J. Babington, J. Erdmenger, N.J. Evans, Z. Guralnik and I. Kirsch, *Chiral symmetry breaking and pions in non-supersymmetric gauge/gravity duals*, *Phys. Rev.* **D 69** (2004) 066007 [hep-th/0306018] [SPIRES].

[11] T. Sakai and S. Sugimoto, *Low energy hadron physics in holographic QCD*, *Prog. Theor. Phys.* **113** (2005) 843 [hep-th/0412141] [SPIRES].

[12] S. Kuperstein and J. Sonnenschein, *Non-critical supergravity ($d > 1$) and holography*, *JHEP* **07** (2004) 049 [hep-th/0403254] [SPIRES]; *Non-critical, near extremal AdS_6 background as a holographic laboratory of four dimensional YM theory*, *JHEP* **11** (2004) 026 [hep-th/0411009] [SPIRES];
I.R. Klebanov and J.M. Maldacena, *Superconformal gauge theories and non-critical superstrings*, *Int. J. Mod. Phys.* **A 19** (2004) 5003 [hep-th/0409133] [SPIRES];
F. Bigazzi, R. Casero, A.L. Cotrone, E. Kiritsis and A. Paredes, *Non-critical holography and*

JHEP05(2009)033

four-dimensional CFT's with fundamentals, *JHEP* **10** (2005) 012 [hep-th/0505140] [SPIRES];
R. Casero, A. Paredes and J. Sonnenschein, *Fundamental matter, meson spectroscopy and non-critical string/gauge duality*, *JHEP* **01** (2006) 127 [hep-th/0510110] [SPIRES];
A. Paredes, *On unquenched $N = 2$ holographic flavor*, *JHEP* **12** (2006) 032 [hep-th/0610270] [SPIRES];
C. Csáki and M. Reece, *Toward a systematic holographic QCD: a braneless approach*, *JHEP* **05** (2007) 062 [hep-ph/0608266] [SPIRES].

[13] J. Polchinski and M.J. Strassler, *Hard scattering and gauge/string duality*, *Phys. Rev. Lett.* **88** (2002) 031601 [hep-th/0109174] [SPIRES]; *Hard scattering and gauge/string duality*, *Phys. Rev. Lett.* **88** (2002) 031601 [hep-th/0109174] [SPIRES].

[14] J. Erlich, E. Katz, D.T. Son and M.A. Stephanov, *QCD and a Holographic Model of Hadrons*, *Phys. Rev. Lett.* **95** (2005) 261602 [hep-ph/0501128] [SPIRES];
L. Da Rold and A. Pomarol, *Chiral symmetry breaking from five dimensional spaces*, *Nucl. Phys.* **B 721** (2005) 79 [hep-ph/0501218] [SPIRES].

[15] C.A. Ballon Bayona, H. Boschi-Filho, N.R.F. Braga and L.A. Pando Zayas, *On a holographic model for confinement/deconfinement*, *Phys. Rev.* **D 77** (2008) 046002 [arXiv:0705.1529] [SPIRES].

[16] A. Karch, E. Katz, D.T. Son and M.A. Stephanov, *Linear confinement and AdS/QCD*, *Phys. Rev.* **D 74** (2006) 015005 [hep-ph/0602229] [SPIRES].

[17] O. Andreev, *Some thermodynamic aspects of pure glue, fuzzy bags and gauge/string duality*, *Phys. Rev.* **D 76** (2007) 087702 [arXiv:706.3120] [SPIRES].

[18] K. Kajantie, T. Tahkokallio and J.T. Yee, *Thermodynamics of AdS/QCD*, *JHEP* **01** (2007) 019 [hep-ph/0609254] [SPIRES].

[19] STAR collaboration, J. Adams et al., *Experimental and theoretical challenges in the search for the quark gluon plasma: the STAR collaboration's critical assessment of the evidence from RHIC collisions*, *Nucl. Phys.* **A 757** (2005) 102 [nucl-ex/0501009] [SPIRES];
B.B. Back et al., *The PHOBOS perspective on discoveries at RHIC*, *Nucl. Phys.* **A 757** (2005) 28 [nucl-ex/0410022] [SPIRES];
BRAHMS collaboration, I. Arsene et al., *Quark gluon plasma an color glass condensate at RHIC? The perspective from the BRAHMS experiment*, *Nucl. Phys.* **A 757** (2005) 1 [nucl-ex/0410020] [SPIRES];
PHENIX collaboration, K. Adcox et al., *Formation of dense partonic matter in relativistic nucleus nucleus collisions at RHIC: experimental evaluation by the PHENIX collaboration*, *Nucl. Phys.* **A 757** (2005) 184 [nucl-ex/0410003] [SPIRES].

[20] M. Luzum and P. Romatschke, *Conformal relativistic viscous hydrodynamics: applications to RHIC results at $\sqrt{s_{NN}} = 200\,GeV$*, *Phys. Rev.* **C 78** (2008) 034915 [arXiv:0804.4015] [SPIRES].

[21] G. Policastro, D.T. Son and A.O. Starinets, *The shear viscosity of strongly coupled $N = 4$ supersymmetric Yang-Mills plasma*, *Phys. Rev. Lett.* **87** (2001) 081601 [hep-th/0104066] [SPIRES];
P. Kovtun, D.T. Son and A.O. Starinets, *Viscosity in strongly interacting quantum field theories from black hole physics*, *Phys. Rev. Lett.* **94** (2005) 111601 [hep-th/0405231] [SPIRES].

JHEP05(2009)033

[22] E. Shuryak, *Physics of strongly coupled quark-gluon plasma*, *Prog. Part. Nucl. Phys.* **62** (2009) 48 [arXiv:0807.3033] [SPIRES];
D.T. Son and A.O. Starinets, *Viscosity, black holes and quantum field theory*, *Ann. Rev. Nucl. Part. Sci.* **57** (2007) 95 [arXiv:0704.0240] [SPIRES];
M. Natsuume, *String theory and quark-gluon plasma*, hep-ph/0701201 [SPIRES].

[23] F. Karsch, D. Kharzeev and K. Tuchin, *Universal properties of bulk viscosity near the QCD phase transition*, *Phys. Lett.* **B 663** (2008) 217 [arXiv:0711.0914] [SPIRES].

[24] H.B. Meyer, *A calculation of the bulk viscosity in* SU(3) *gluodynamics*, *Phys. Rev. Lett.* **100** (2008) 162001 [arXiv:0710.3717] [SPIRES]; *Energy-momentum tensor correlators and viscosity*, arXiv:0809.5202 [SPIRES].

[25] C.P. Herzog, A. Karch, P. Kovtun, C. Kozcaz and L.G. Yaffe, *Energy loss of a heavy quark moving through $N = 4$ supersymmetric Yang-Mills plasma*, *JHEP* **07** (2006) 013 [hep-th/0605158] [SPIRES].

[26] H. Liu, K. Rajagopal and U.A. Wiedemann, *Calculating the jet quenching parameter from AdS/CFT*, *Phys. Rev. Lett.* **97** (2006) 182301 [hep-ph/0605178] [SPIRES].

[27] S.S. Gubser, *Drag force in AdS/CFT*, *Phys. Rev.* **D 74** (2006) 126005 [hep-th/0605182] [SPIRES].

[28] U. Gürsoy and E. Kiritsis, *Exploring improved holographic theories for QCD: part I*, *JHEP* **02** (2008) 032 [arXiv:0707.1324] [SPIRES];
U. Gürsoy, E. Kiritsis and F. Nitti, *Exploring improved holographic theories for QCD: part II*, *JHEP* **02** (2008) 019 [arXiv:0707.1349] [SPIRES].

[29] S.S. Gubser, *Curvature singularities: The good, the bad, and the naked*, *Adv. Theor. Math. Phys.* **4** (2000) 679 [hep-th/0002160] [SPIRES].

[30] U. Gürsoy, E. Kiritsis, L. Mazzanti and F. Nitti, *Deconfinement and gluon plasma dynamics in improved holographic QCD*, *Phys. Rev. Lett.* **101** (2008) 181601 [arXiv:0804.0899] [SPIRES].

[31] S.S. Gubser and A. Nellore, *Mimicking the QCD equation of state with a dual black hole*, *Phys. Rev.* **D 78** (2008) 086007 [arXiv:0804.0434] [SPIRES].

[32] G. Boyd et al., *Thermodynamics of* SU(3) *lattice gauge theory*, *Nucl. Phys.* **B 469** (1996) 419 [hep-lat/9602007] [SPIRES].

[33] B. Lucini, M. Teper and U. Wenger, *Properties of the deconfining phase transition in SU(N) gauge theories*, *JHEP* **02** (2005) 033 [hep-lat/0502003] [SPIRES].

[34] U. Gursoy, E. Kiritsis, G Michalogeorgiakis and F. Nitti, *Bulk viscosity and jet quenching in improved holograpgic QCD*, in preparation.

[35] H.A. Chamblin and H.S. Reall, *Dynamic dilatonic domain walls*, *Nucl. Phys.* **B 562** (1999) 133 [hep-th/9903225] [SPIRES];
T. Hertog and K. Maeda, *Stability and thermodynamics of AdS black holes with scalar hair*, *Phys. Rev.* **D 71** (2005) 024001 [hep-th/0409314] [SPIRES].

[36] U. Gursoy, E. Kiritsis, L. Mazzanti and F. Nitti, *Improved holographic Yang-Mills at finite temperature: comparison with data*, arXiv:0903.2859 [SPIRES].

[37] T. Hertog, *Towards a novel no-hair theorem for black-holes*, *Phys. Rev.* **D 74** (2006) 084008 [gr-qc/0608075] [SPIRES].

JHEP05(2009)033

[38] S.W. Hawking and D.N. Page, *Thermodynamics of black holes in Anti-de Sitter space*, *Commun. Math. Phys.* **87** (1983) 577 [SPIRES].

[39] P.K. Townsend, *Positive energy and the scalar potential in higher dimensional (super)gravity theories*, *Phys. Lett.* **B 148** (1984) 55 [SPIRES].

[40] K. Skenderis and P.K. Townsend, *Gravitational stability and renormalization-group flow*, *Phys. Lett.* **B 468** (1999) 46 [hep-th/9909070] [SPIRES];
O. DeWolfe, D.Z. Freedman, S.S. Gubser and A. Karch, *Modeling the fifth dimension with scalars and gravity*, *Phys. Rev.* **D 62** (2000) 046008 [hep-th/9909134] [SPIRES].

[41] E. Vicari and H. Panagopoulos, *Theta dependence of* SU(N) *gauge theories in the presence of a topological term*, *Phys. Rept.* **470** (2009) 93 [arXiv:0803.1593] [SPIRES].

[42] A. Kehagias and K. Sfetsos, *On running couplings in gauge theories from type-IIB supergravity*, *Phys. Lett.* **B 454** (1999) 270 [hep-th/9902125] [SPIRES].

[43] S.S. Gubser, *Dilaton-driven confinement*, hep-th/9902155 [SPIRES].

[44] Y. Kinar, E. Schreiber and J. Sonnenschein, *Q anti-Q potential from strings in curved spacetime: classical results*, *Nucl. Phys.* **B 566** (2000) 103 [hep-th/9811192] [SPIRES].

[45] M. Bianchi, D.Z. Freedman and K. Skenderis, *Holographic renormalization*, *Nucl. Phys.* **B 631** (2002) 159 [hep-th/0112119] [SPIRES];
I. Papadimitriou and K. Skenderis, *Thermodynamics of asymptotically locally AdS spacetimes*, *JHEP* **08** (2005) 004 [hep-th/0505190] [SPIRES].

[46] S.W. Hawking and G.T. Horowitz, *The gravitational hamiltonian, action, entropy and surface terms*, *Class. Quant. Grav.* **13** (1996) 1487 [gr-qc/9501014] [SPIRES].

[47] I.R. Klebanov and E. Witten, *AdS/CFT correspondence and symmetry breaking*, *Nucl. Phys.* **B 556** (1999) 89 [hep-th/9905104] [SPIRES].

[48] S.S. Gubser, I.R. Klebanov and A.W. Peet, *Entropy and temperature of black* 3*-branes*, *Phys. Rev.* **D 54** (1996) 3915 [hep-th/9602135] [SPIRES].

[49] U. Gursoy and I. Papadimitriou, *Holographic renormalization and correlation functions in log-corrected asymptotically AdS spaces*, to appear.

[50] A. Buchel and J.T. Liu, *Universality of the shear viscosity in supergravity*, *Phys. Rev. Lett.* **93** (2004) 090602 [hep-th/0311175] [SPIRES].

[51] D. Anninos and G. Pastras, *Thermodynamics of the Maxwell-Gauss-Bonnet Anti-de Sitter black hole with higher derivative gauge corrections*, arXiv:0807.3478 [SPIRES].

JHEP05(2009)033